Energetic Neutral Atoms

SHIELD Summer School

Maher A. Dayeh
(Southwest Research Institute)

Boston University, 05 June 2025

Outline

- **Energetic Neutral Atoms**
  - Definition
  - Production mechanisms
  - Presence in the Heliosphere

Outline

- **Energetic Neutral Atoms**
  - Definition
  - Production mechanisms
  - Presence in the Heliosphere

- **ENA Detection Techniques**
  - Basic particle detection methods
  - ENA imaging
  - Examples from past and current missions

Outline

- **Energetic Neutral Atoms**
  - Definition
  - Production mechanisms
  - Presence in the Heliosphere

- **ENA Detection Techniques**
  - Basic particle detection methods
  - ENA imaging
  - Examples from past and current missions

- **IBEX Observations**
  - IBEX design and payload
  - Major discoveries
  - ENA measurements over a full solar cycle
  - Magnetospheric ENA by IBEX

Review resources: Gruntman et al. 1997; Wurz et al. 2000; Brandt et al. 2005

Energetic Neutral Atoms - formation

$$\text{Ion}_{energetic} + \text{Neutral}_{cold} \rightarrow \text{ENA}_{energetic} + \text{Ion}_{cold}$$

Examples:

$$H^+ + H \rightarrow H + H^+$$

$$H^+ + O \rightarrow H + O^+$$

- Charge exchange happens over large internuclear distances, thus reserving energy and momentum for the most part

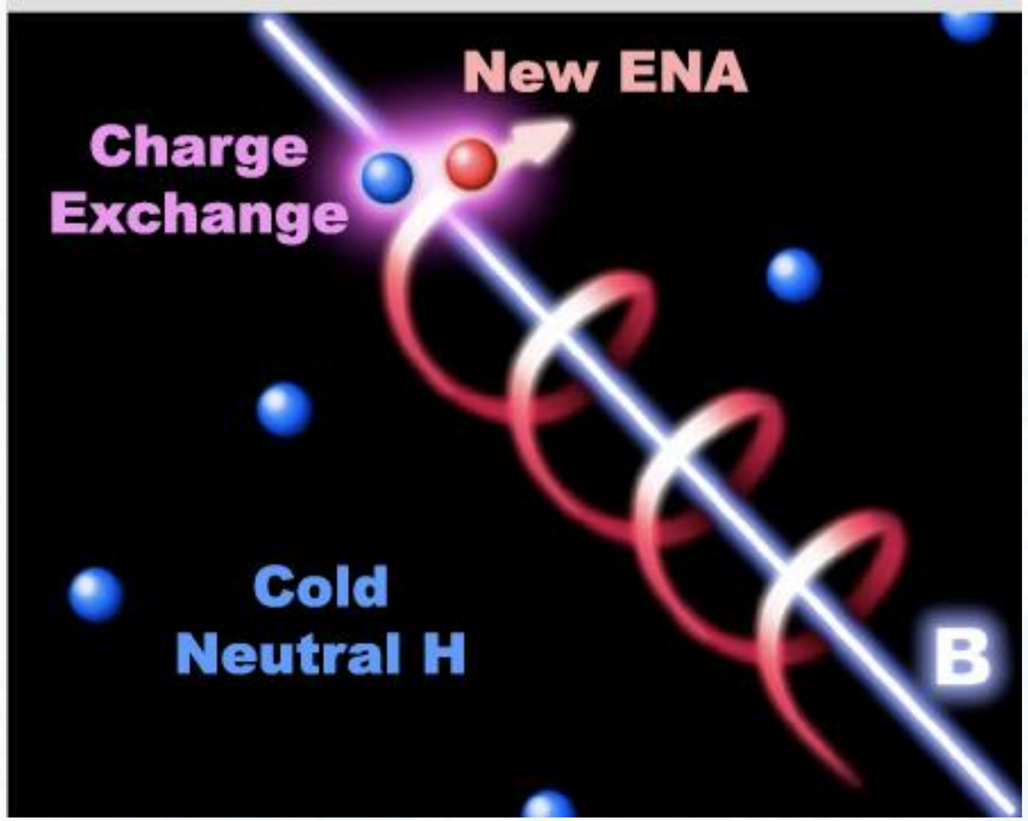

Bransden & McDowell 1992; Goldstein & McComas 2018

Energetic Neutral Atoms - formation

$$\text{Ion}_{energetic} + \text{Neutral}_{cold} \rightarrow \text{ENA}_{energetic} + \text{Ion}_{cold}$$

- The probability that a given charge exchange process will occur in a collision is expressed as a reaction **cross-section**.

This reaction occurs at random and produced ENAs exit the plasma population in all directions.

The Charge-Exchange cross-section imposes a major constraint on ENA production and ultimately measurement!

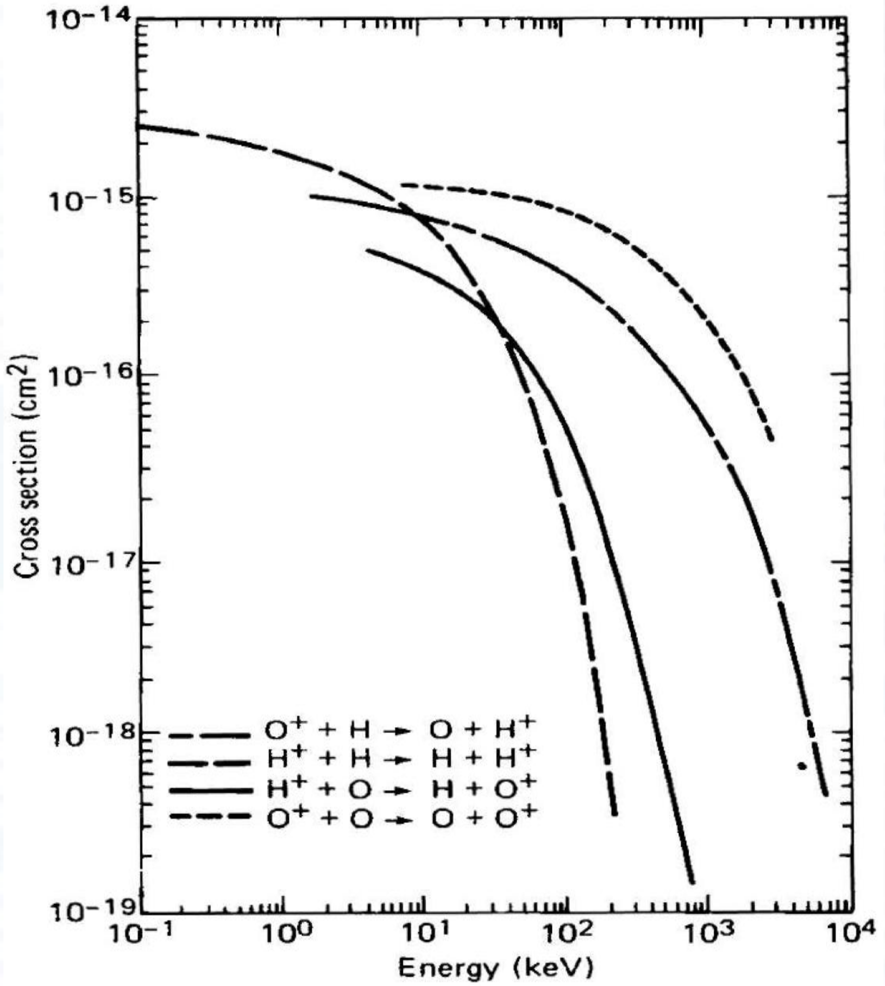

Wurz 2000

Energetic Neutral Atoms as plasma probes

$$\text{Ion}_{\text{energetic}} + \text{Neutral}_{\text{cold}} \rightarrow \text{ENA}_{\text{energetic}} + \text{Ion}_{\text{cold}}$$

- The probability that a given charge exchange process will occur in a collision is expressed as a reaction **cross-section**.
- ENAs travel to large distances (large!) unaffected by E & M fields, conserving their parent ions' properties.
- ENA imaging is thus a powerful tool to probe plasma regions in space.

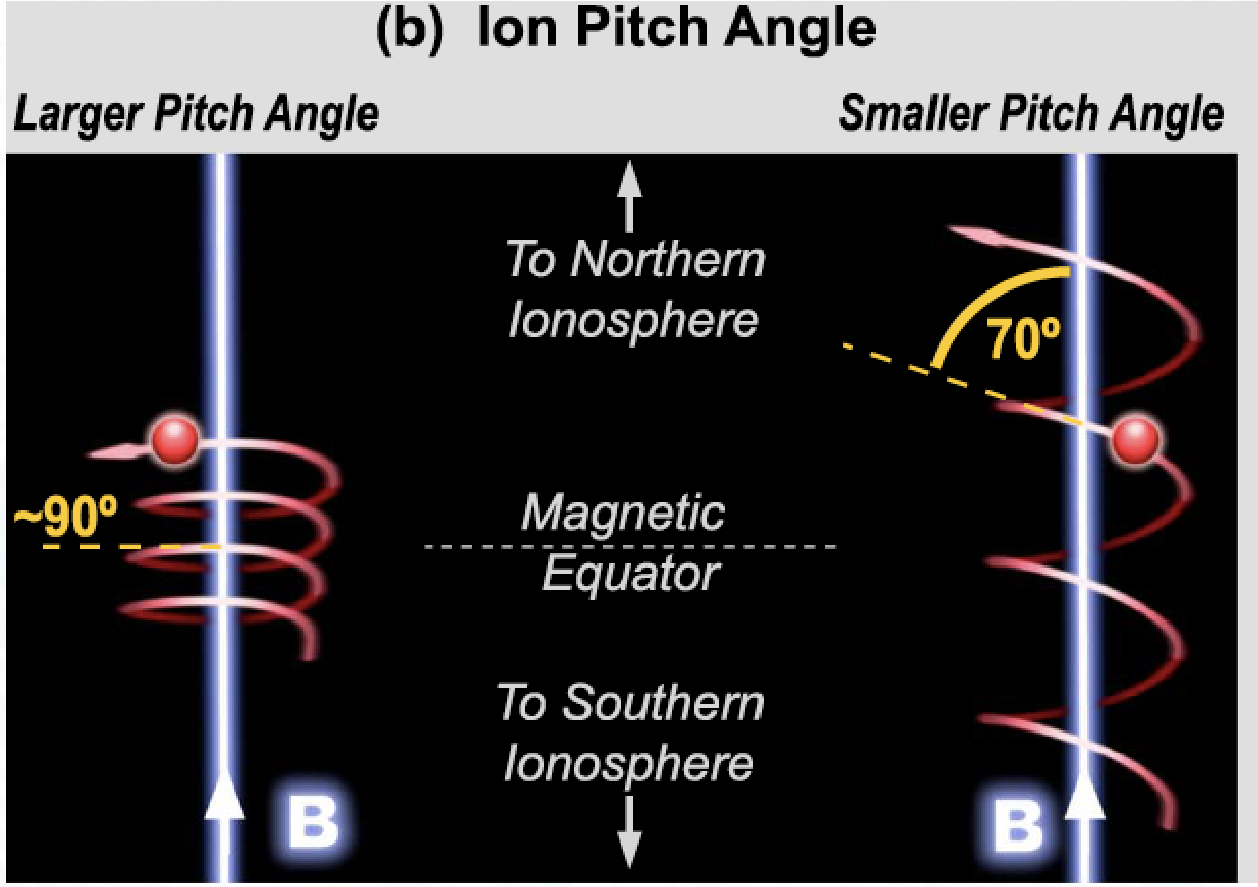

Goldstein & McComas 2018

Energetic Neutral Atoms as plasma probes

$$\text{Ion}_{\text{energetic}} + \text{Neutral}_{\text{cold}} \rightarrow \text{ENA}_{\text{energetic}} + \text{Ion}_{\text{cold}}$$

- The probability that a given charge exchange process will occur in a collision is expressed as a reaction **cross-section**.

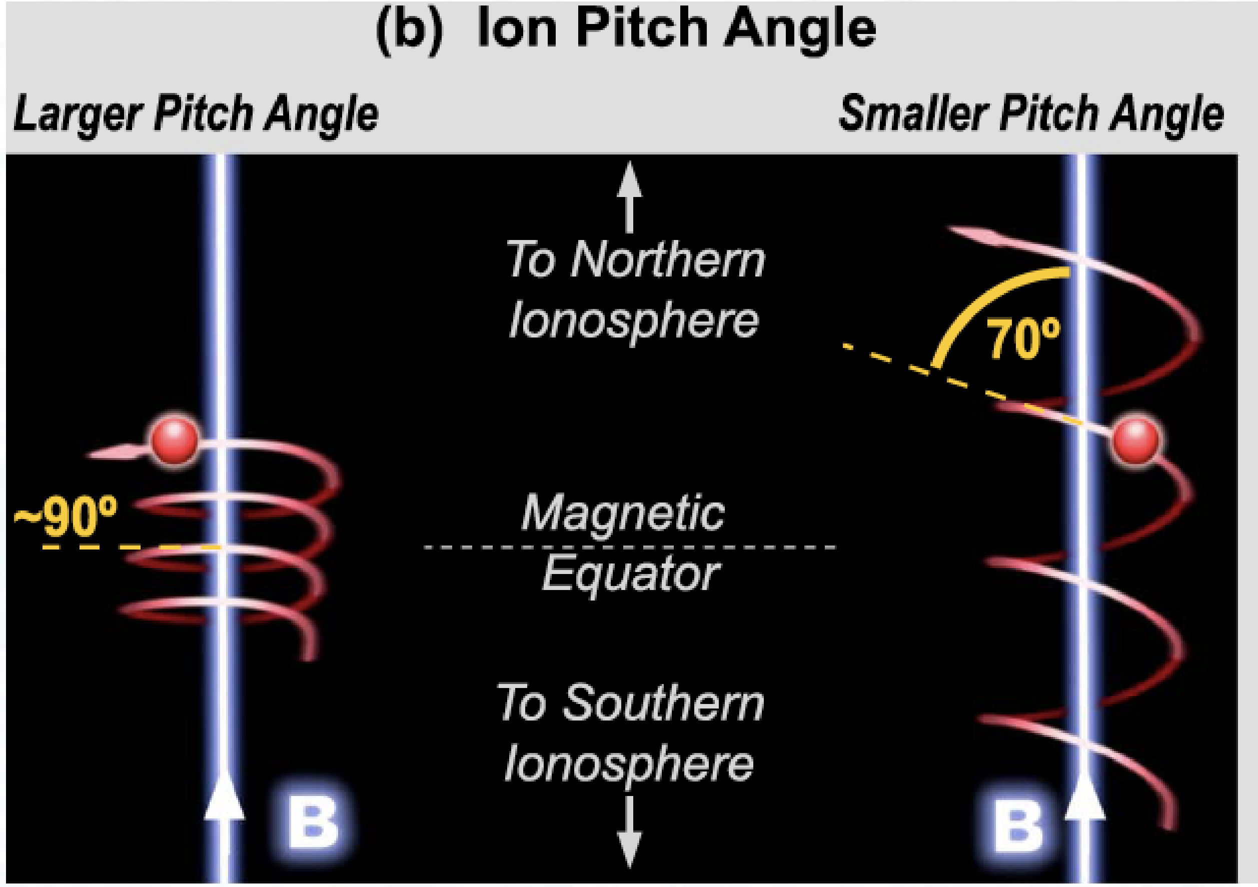

- Pitch angle plays an important role:
  - Affects ChX probability (e.g., different densities parallel vs across B)
  - Creates anisotropic ENA emission patterns (e.g., scattering)
  - Affects interpretation of source distributions (escaping vs trapping along field lines

Goldstein & McComas 2018

Energetic Neutral Atoms as plasma probes

$$\text{Ion}_{energetic} + \text{Neutral}_{cold} \rightarrow \text{ENA}_{energetic} + \text{Ion}_{cold}$$

- The probability that a given charge exchange process will occur in a collision is expressed as a reaction **cross-section**.

This reaction occurs at random and produced ENAs exit the plasma population in all directions.

Unidirectional flux for species i along a line of sight is given as:

$$f_i(E) = \sum_k \sigma_{ik}(E) \int j_i(E,l) n_k(l) dl$$

$n_k(l)$: density of component k of the neutral gas
$J_i(E,l)$: directional ion flux along the line of sight at each point i for species i
$\sigma_{ik}(E)$: charge-exchange cross section for species i

Energetic Neutral Atoms – energy range

Thermal low medium high

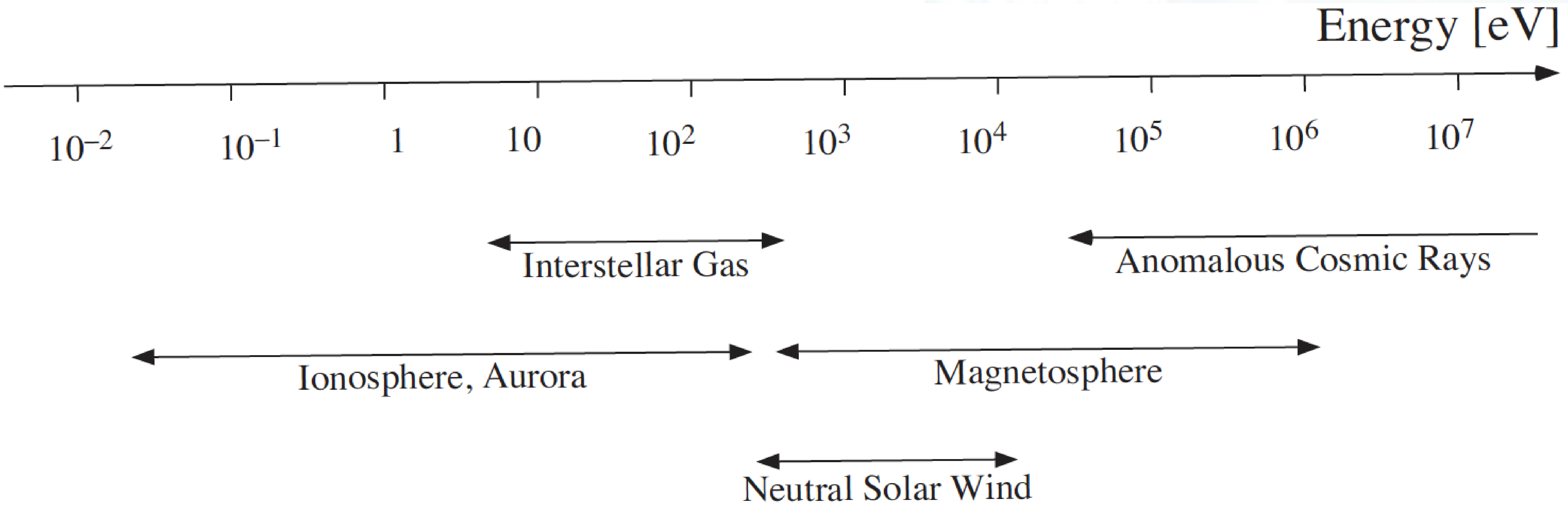

- No single particle analyzer can cover the entire energy interval from about 10 eV to beyond 1 MeV.
- These energy ranges depend on the plasma being examined.

neutral population ← → ion population

Wurz 2000

Energetic Neutral Atoms - Sources

- Magnetospheric ENAs
  - The terrestrial magnetosphere efficiently traps charged particles.
  - The ionospheric and solar wind plasmas leak and fill the magnetosphere with ions and electrons

The magnetosphere is very dynamic and is populated with energetic particles with different distributions and energy ranges.

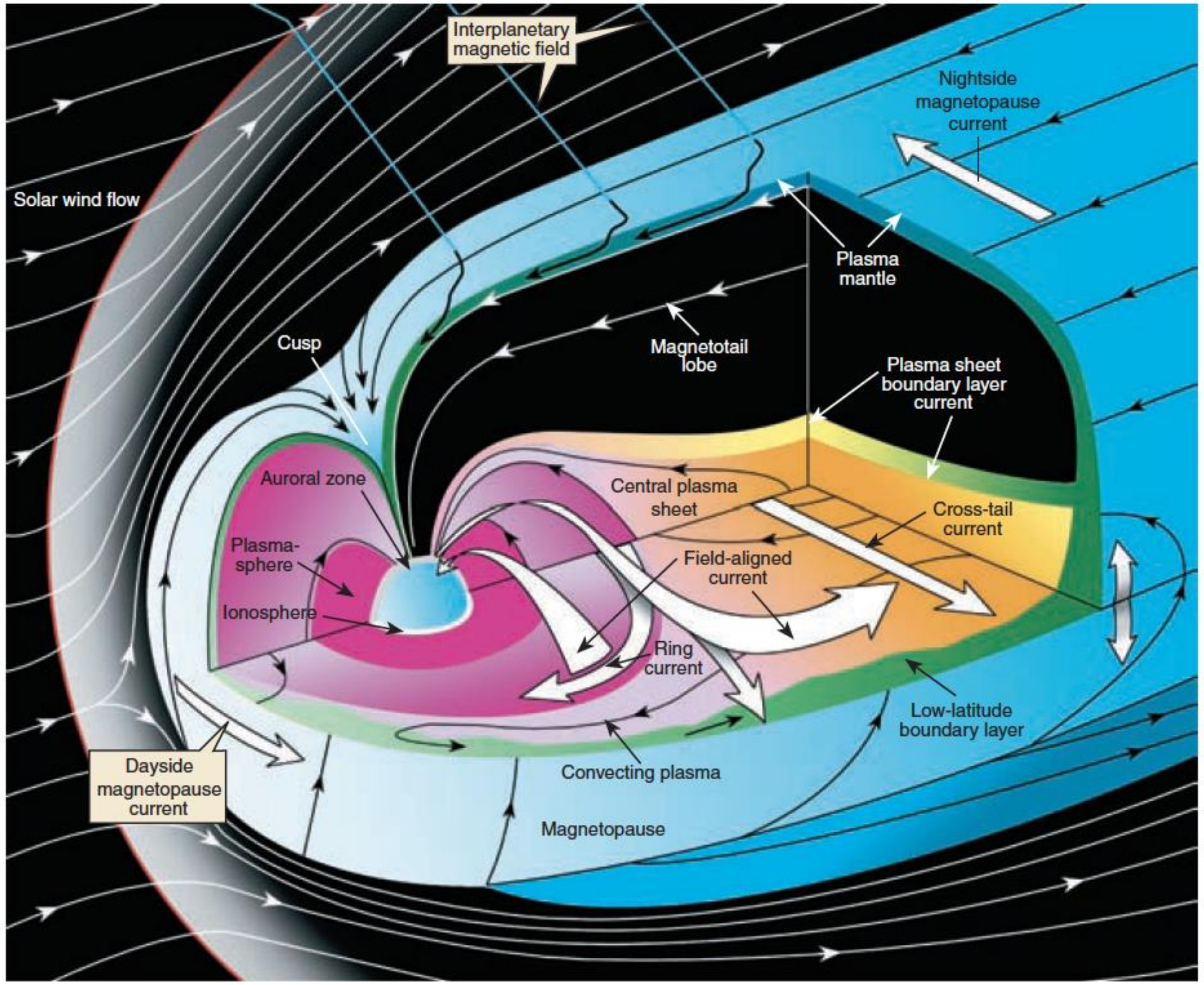

The structure of the terrestrial magnetosphere

Brandt et al. 2005

Energetic Neutral Atoms - Sources

- Magnetospheric ENAs
  - The terrestrial magnetosphere efficiently traps charged particles.
  - The ionospheric and solar wind plasmas leak and fill the magnetosphere with ions and electrons

The Exosphere provides neutral collision partners for ENA production. The Geocorona extends beyond that and can be seen by UV.

The H distribution is spherically symmetric close to the Earth. Abundant background neutral gas can be found in the magnetospheres of other planets as well.

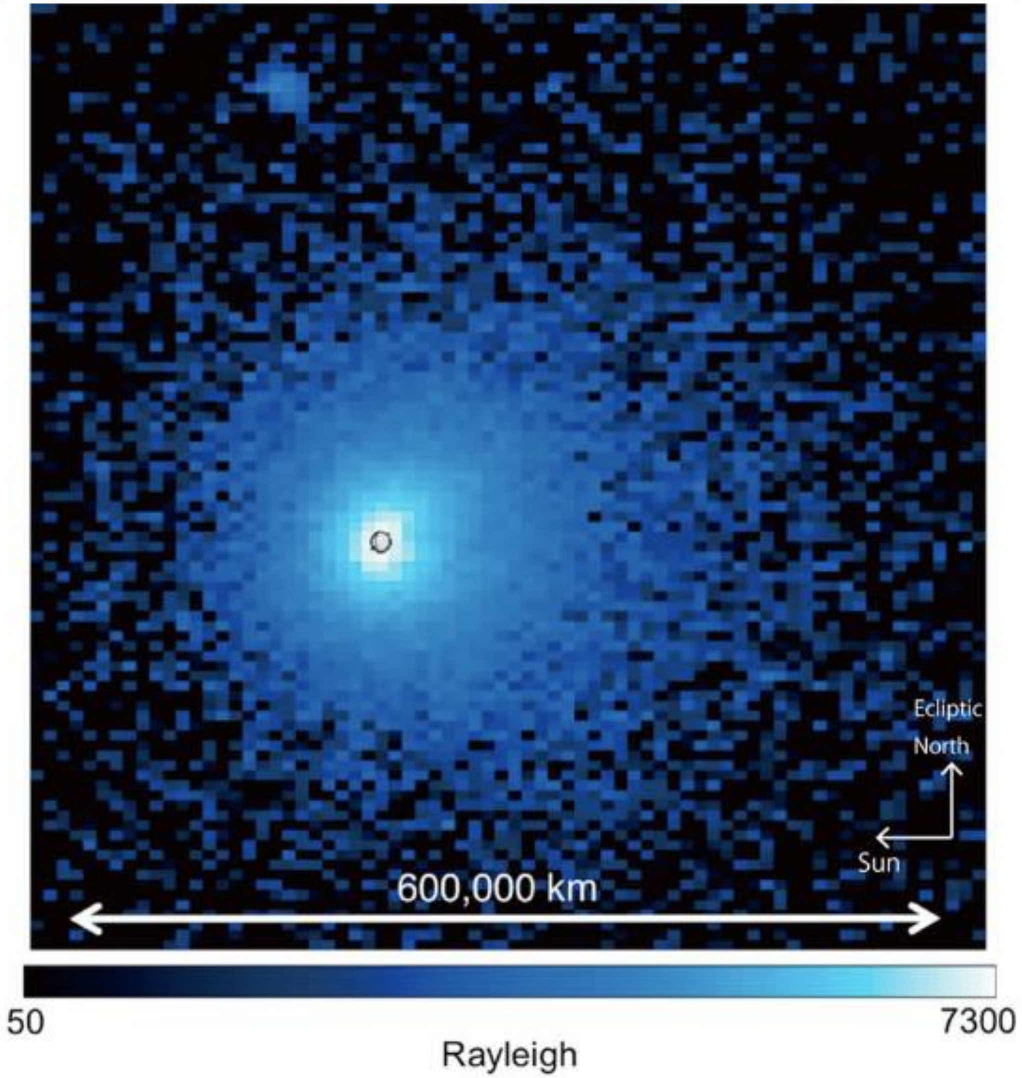

Kameda et al. 2017

Energetic Neutral Atoms - Sources

- Magnetospheric ENAs

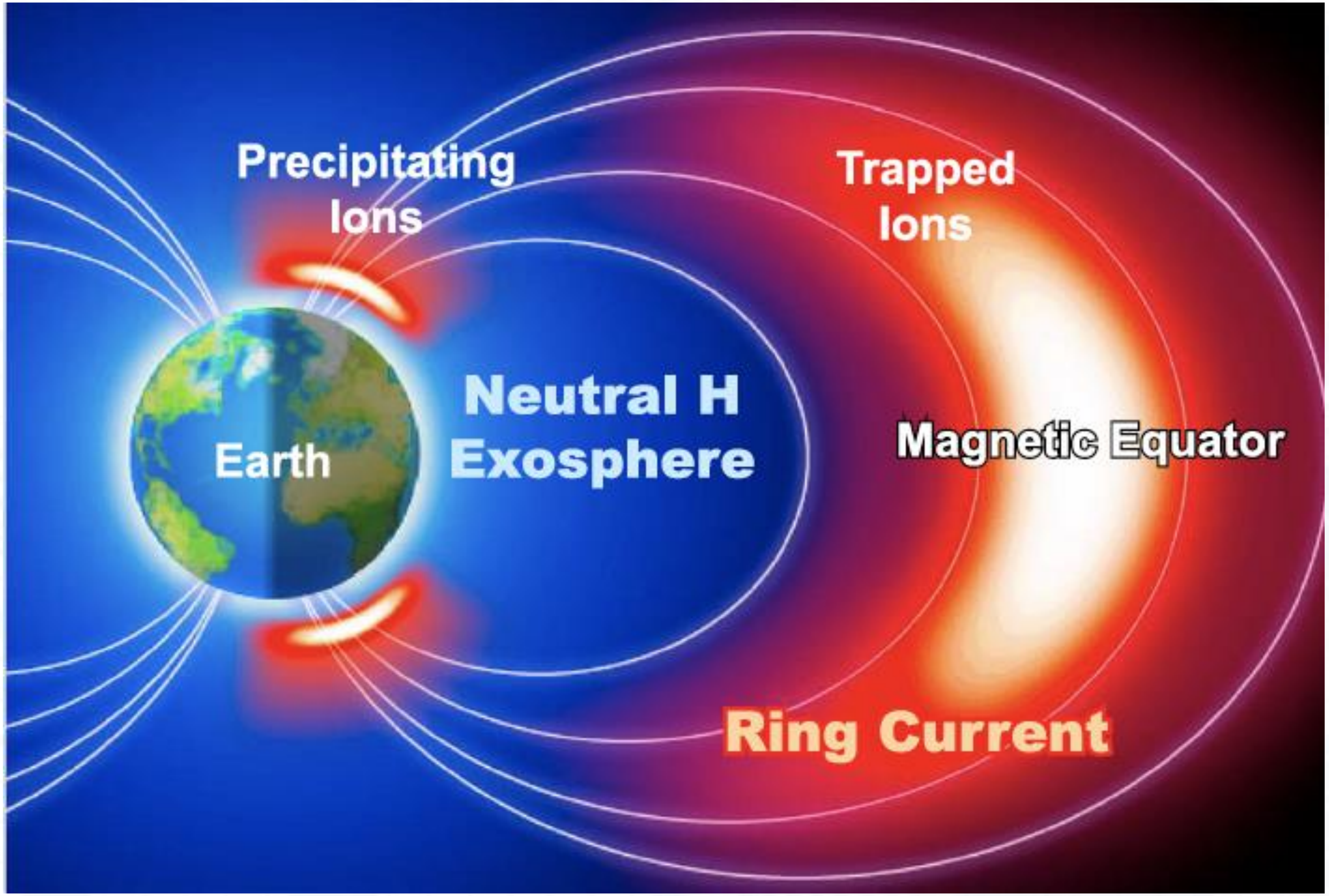

Goldstein & McComas 2018

Energetic Neutral Atoms - Sources

- Magnetospheric ENAs

(1) Observations from IMP-7 & -8 of particles coming from the direction of Earth. (Krimigis et al. 1975)
(2) Detection of neutral atoms precipitating onto Earth's upper atmosphere. (Moritz et al. 1972)

Evidence grew that ENAs are being observed and not ions. (Hovestadt & Scholer 1976)

Roelof et al. 1987, utilizing the 3-D capability of ISEE-1/MEPI, constructed the first ENA image.

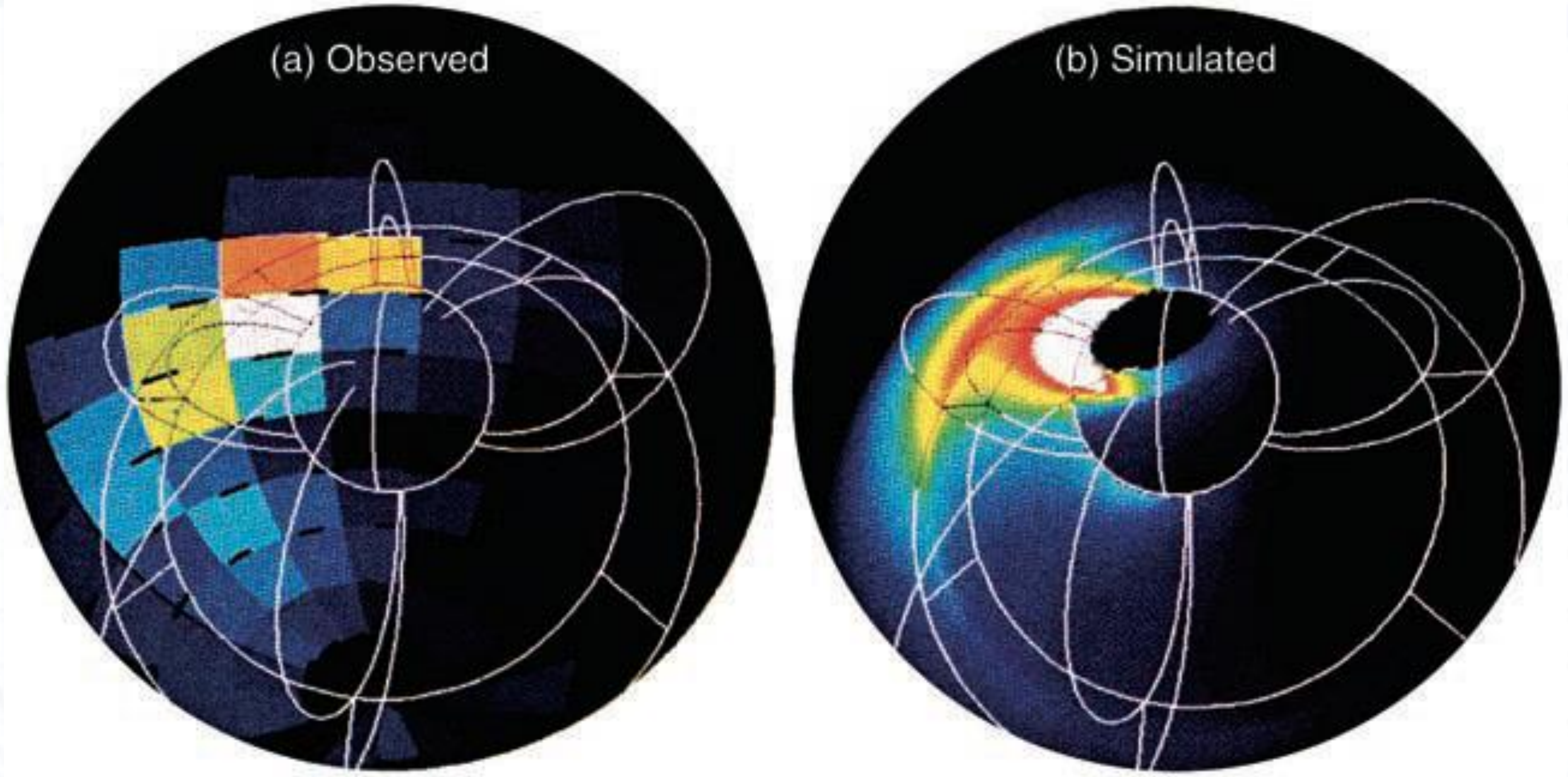

First ENA image constructed from data obtained by the MEPI detector onboard ISEE-1. (b) Simulated image using a parametric ring current and exospheric model.

Structure of the Heliosphere

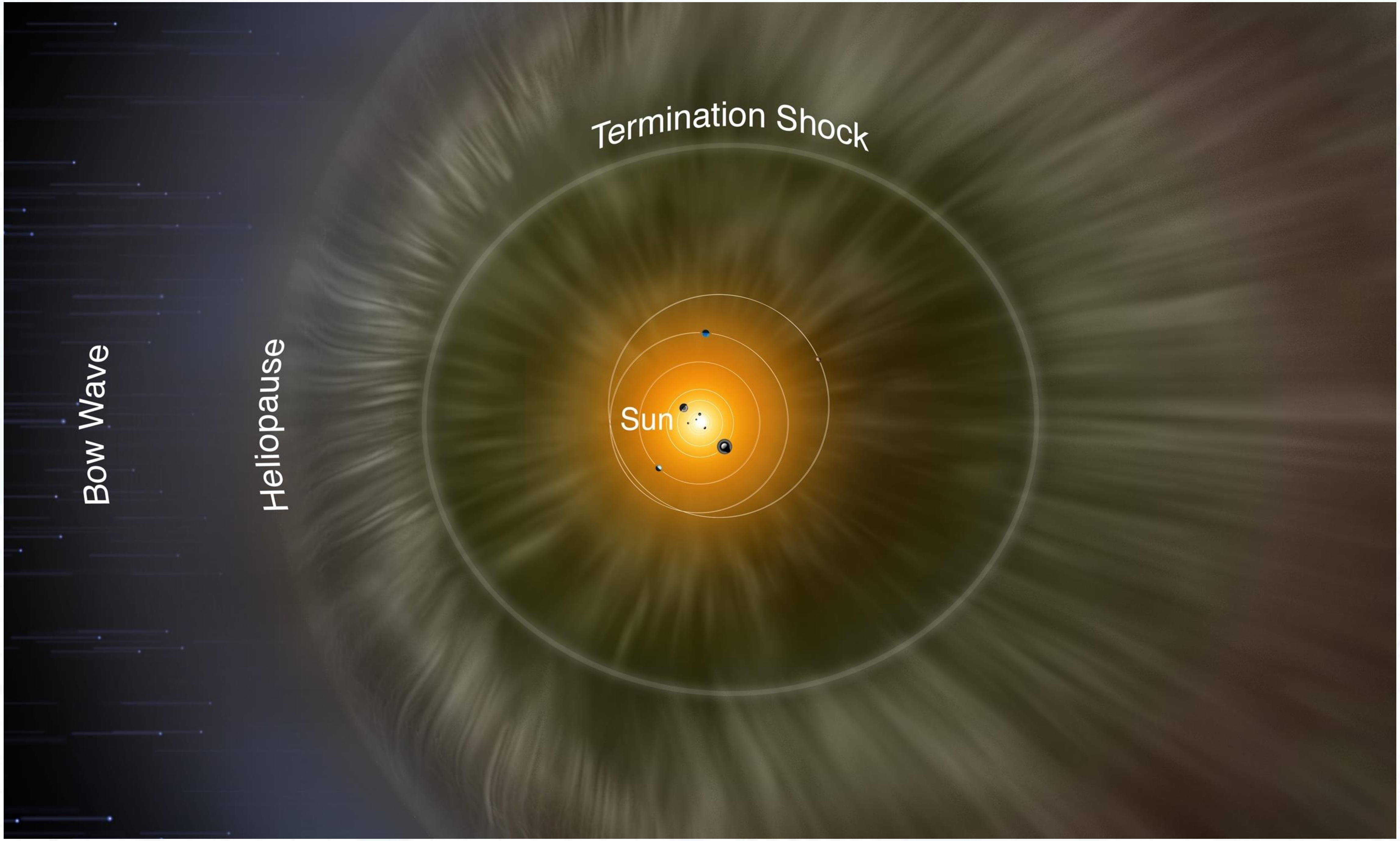

Structure of the Heliosphere

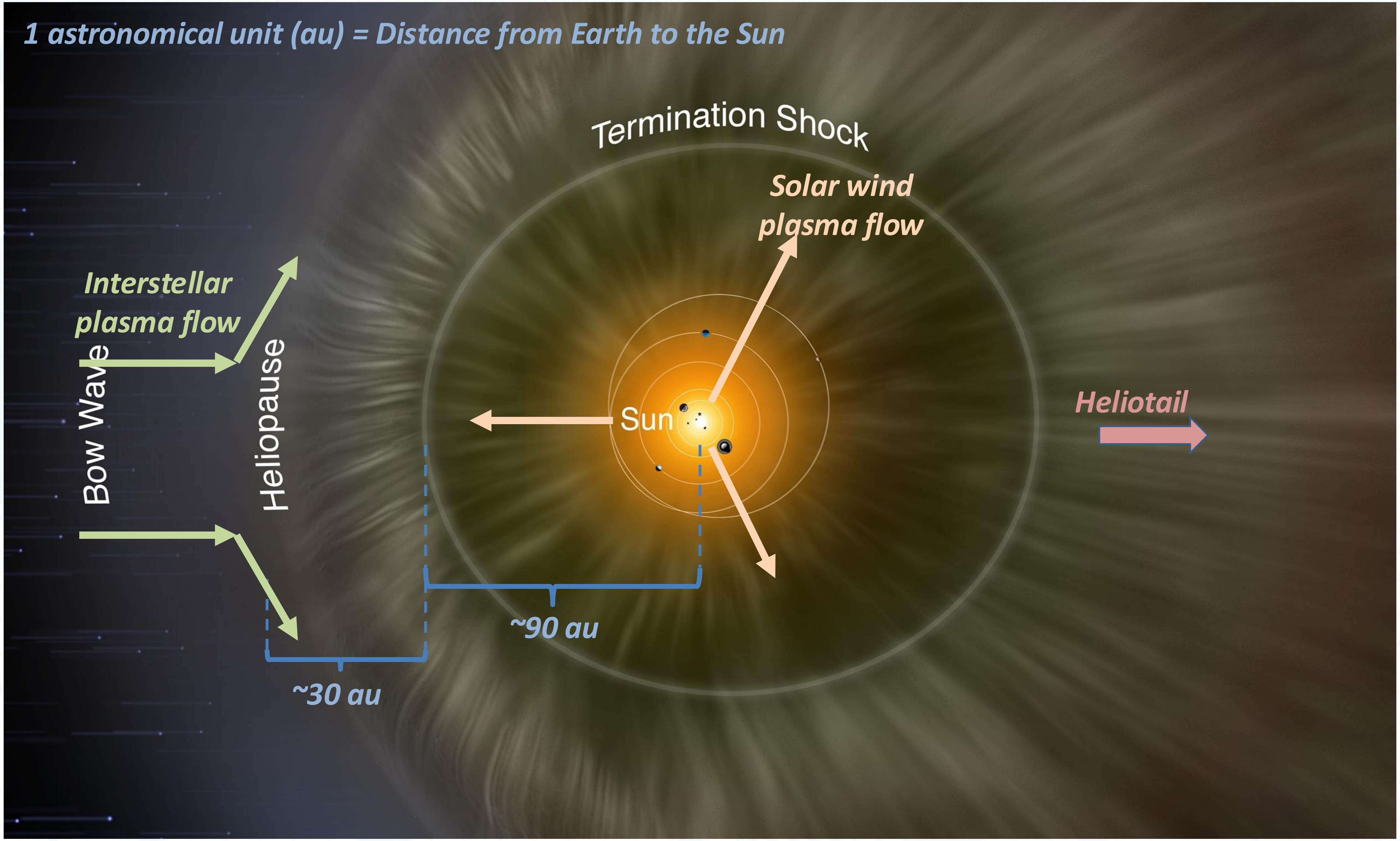

Neutrals in Space - Heliosphere

- Background neutrals - Interstellar gas (ISG)
  - Neutral interstellar gas serves as a background gas for ENAs producing charge-exchange collisions in the heliosphere
  - Different interstellar species would have different fluxes and velocity distribution functions at the same observation point (due to differences in ionization rates)
  - Direct detection of ENA fluxes of interstellar helium atoms accelerated by the solar gravitation was demonstrated (no mass details) for the first time by the GAS experiment on the Ulysses spacecraft. Later nicely measured by IBEX

Neutrals in Space - Heliosphere

- Background neutrals - Neutral solar wind (NSW) flux

  - This neutral solar wind is born in charge exchange between the solar wind ions and interplanetary neutrals

  - The NSW atoms move in the anti-sunward direction with approximately a solar wind velocity

  - Small component of the solar wind near 1 au, but increases further away from the Sun

Neutrals in Space - Heliosphere

- Charge-exchange is a ubiquitous process occurring throughout the heliosphere. Ion sources for the ENA production

- Pickup Ions (PUIs): PUIs are charged particles that originate from neutral atoms drifting into the heliosphere. When these neutral particles encounter the solar wind, they get ionized and become PUIs, energized by the motional SW electric field. As PUIs traverse through the heliosphere, they can undergo charge exchange with ambient charged plasma. The PUI becomes neutralized, and an ENA is formed.

- Possible component: Anomalous Cosmic Rays (ACRs): ACRs are high-energy charged particles, primarily protons and helium nuclei, that originate from the interstellar medium and are accelerated at the termination shock. When ACRs interact with the ambient plasma, they can also undergo charge exchange and neutralize, resulting in the creation of an ENA.

Neutrals in Space - Heliosphere

- ENAs are also produced in Solar transients.

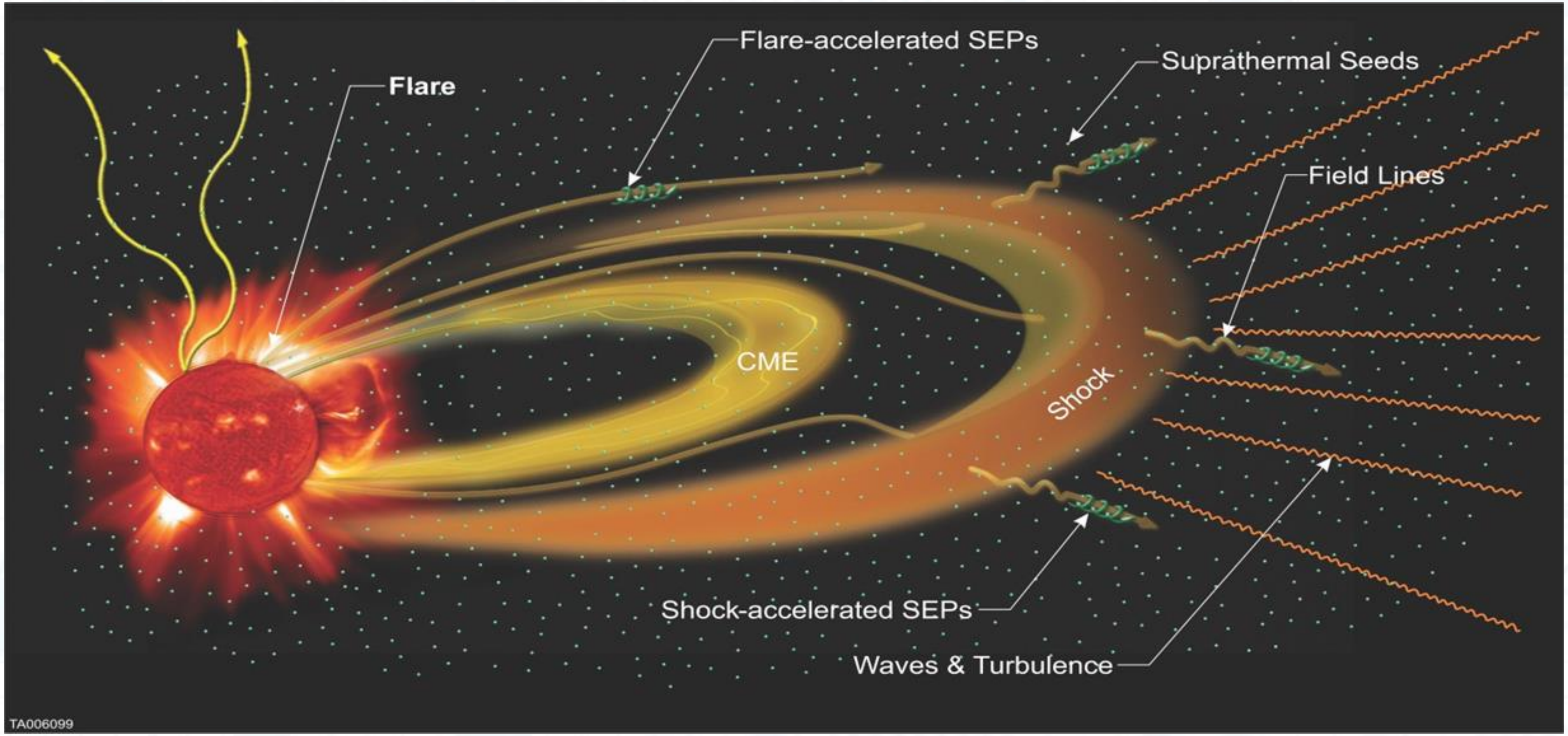

Dayeh et al. 2017

Neutrals in Space - Heliosphere

- ENAs are also produced in Solar transients.

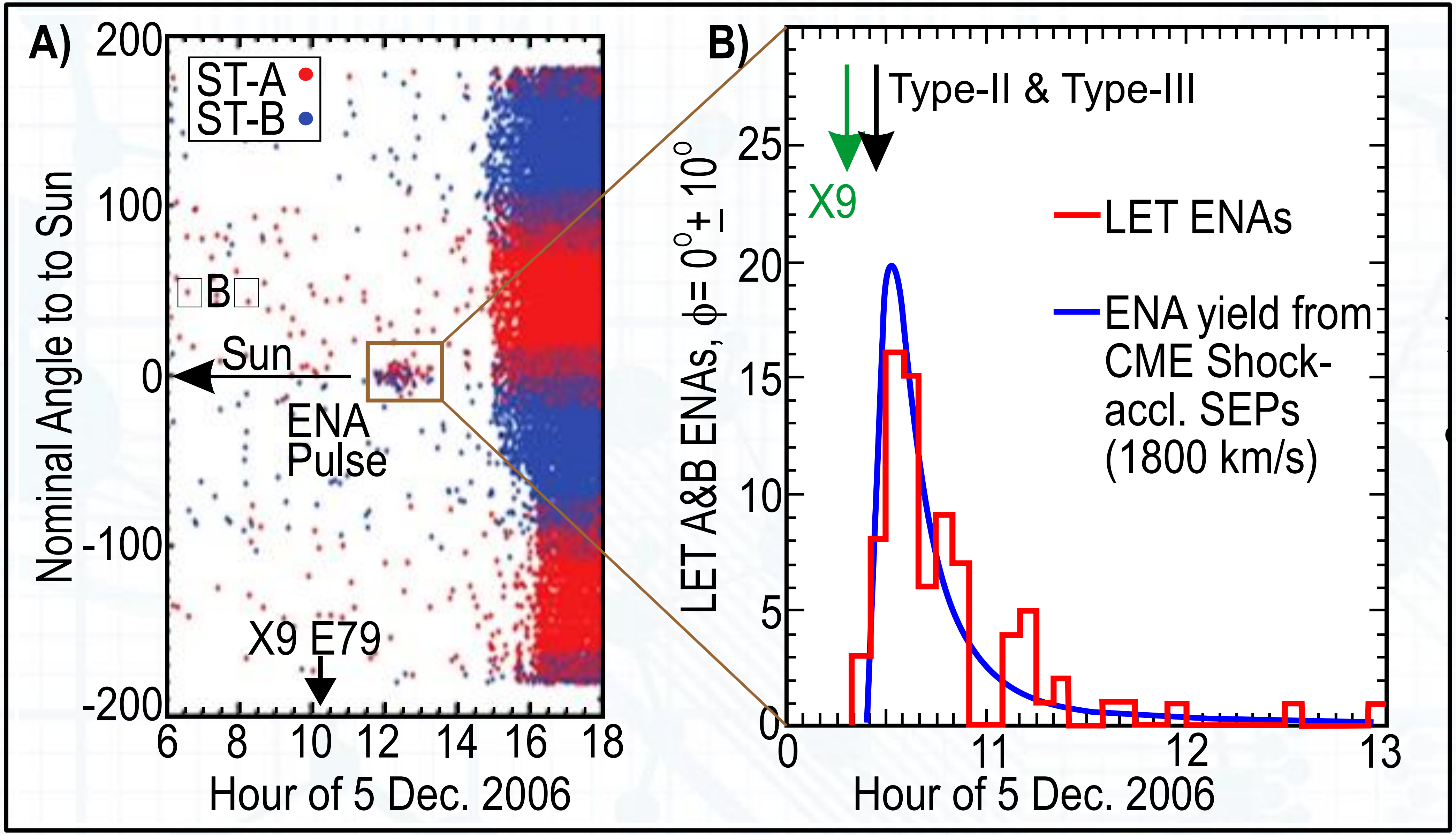

Mewaldt et al. 2009

Break I

ENA Instrumentation

ENA Detection- Requirements

- Requirements of a working instrument:

  - Detect ENA properties (mass, energy, incidence direction) with sufficient resolution and over a good dynamic energy range.

  - Background suppression
    Charged particles
    Penetrating radiation
    UV and EUV photons

  All these background sources are often far more intense than the ENA flux.

ENA Detection- Requirements

Background suppression

Charged particles - Mitigation

Deflect with electric or/and magnetic fields. Typically, Electric fields using a Collimator.

A collimator defines the instrument field-of-view and comprises two closely-spaced metallic plates (designs differ). High voltage of alternate polarity on both plates creates an E-field, such as:

$$E/q = \frac{1}{4}U\left(\frac{L_E}{2D}\right)^2$$

(U: applied potential; LE: Length of plates; D: Separation distance)

Particles with lower E/q are deflected.

At higher energies, this becomes a potential problem.

ENA Detection- Requirements

Background suppression

Charged particles - Mitigation

Warning!

Deflecting ions is not enough – need to ensure they do not scatter back as neutralized atoms into the core detector system. Roughening the plates to reduce scattering often helps.

Based on numerous experiments to date, simulations and theoretical predictions do not fully reproduce scattering inside the detector.

Best practice is to test the instrument under different conditions.

ENA Detection- Requirements

Background suppression

Rejection of Penetrating Particles - Mitigation

Above ~ 1MeV/n particles can enter the walls of the instrument and cause false signals, among numerous other problems.
Passive protection and optimized planning of launching and orbit selection (avoiding the radiation belts) help, but that is limited.

Cosmic Rays and solar transients become the main problem. Active anti-coincidence shielding around the detector is a viable solution.

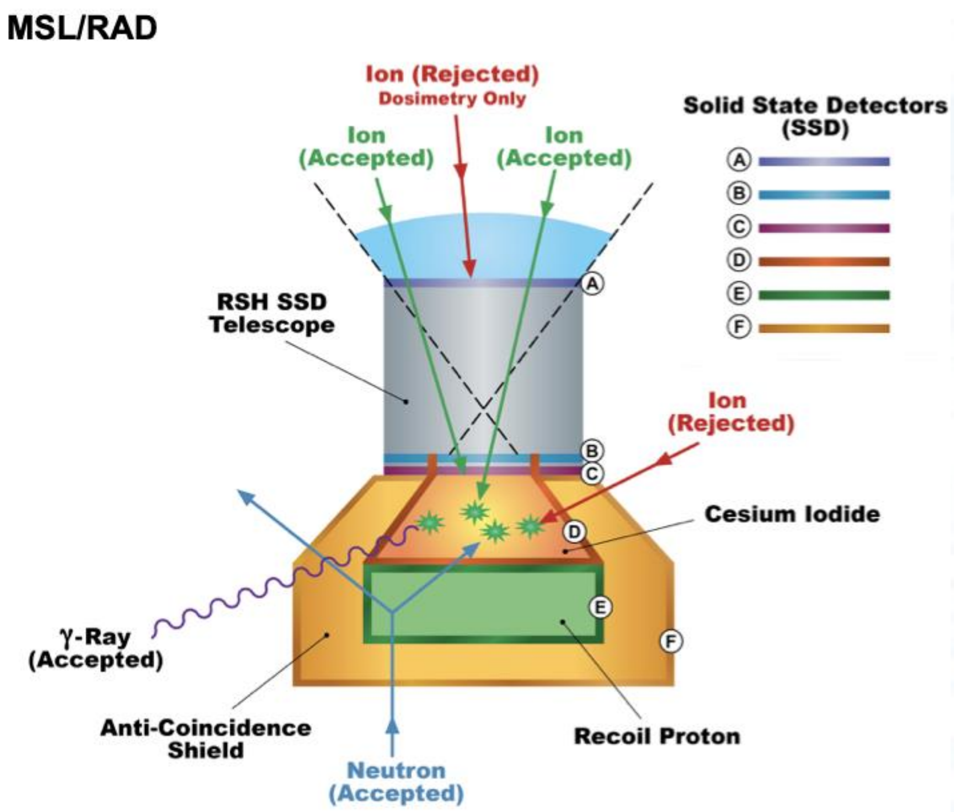

Fig. 1: The RAD instrument measures energetic particles using silicon detectors (A, B, C), a CsI scintillator (D) and plastic scintillators (E, F). Charged particles are measured with (D, E) in coincidence with (A, B, C). Neutral particles are measured with (D, E) in anticoincidence with (B, C, F) [Hassler et al., 2012].

ENA Detection- Requirements

SHIELD

Background suppression

Photons - Mitigation

Ultraviolet (UV/Extreme UV) and ENAs often present in the same region as ENAs.
UV/EUV create large background count rates in ENA detectors, either directly or indirectly (photons create photoelectrons inside the instrument). What to do?!

- Using a multi-parameter measurement for ENA registration reduces the readings arising from UV photons.
- Block UV using thin foils. This affects the dynamics range of the detection.

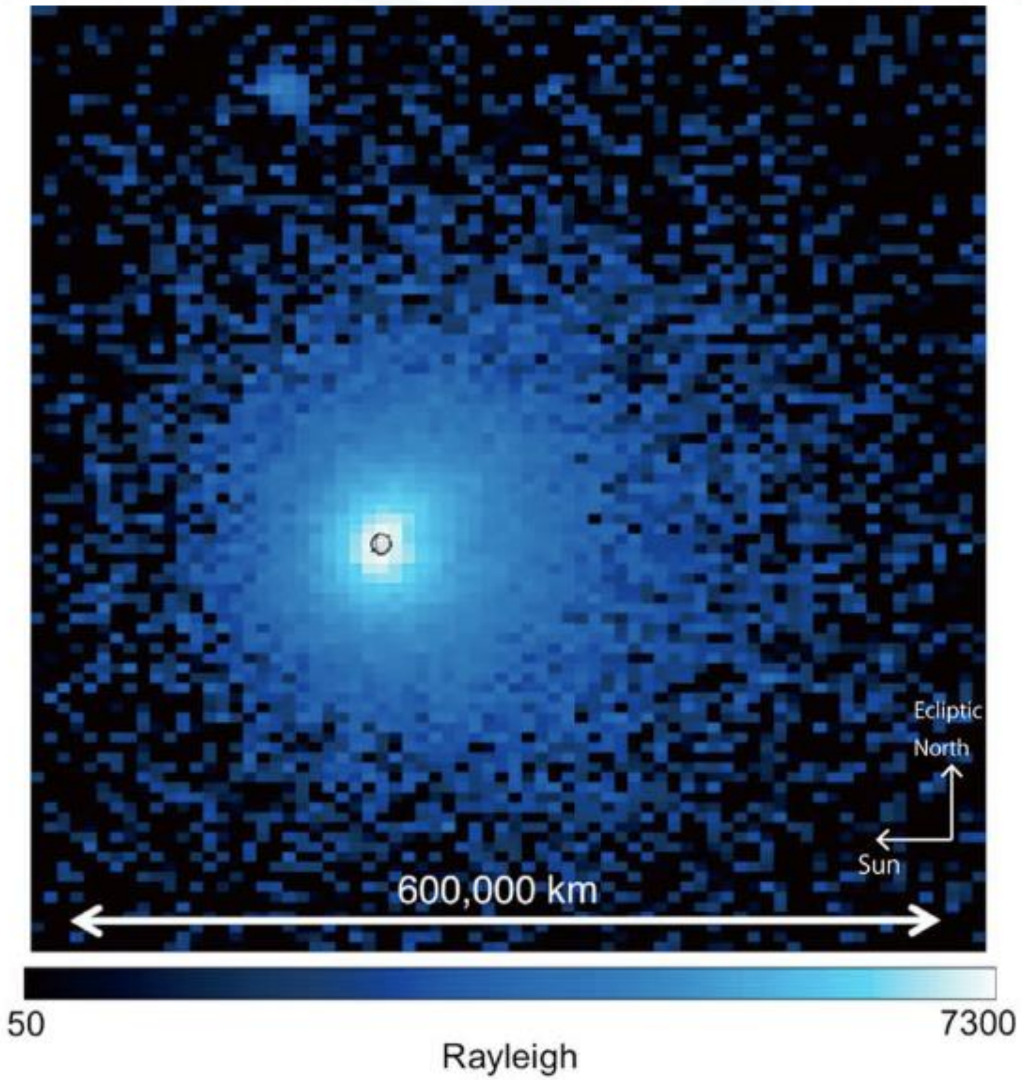

Kameda et al. 2017

ENA Detection- Basics

- Imaging detectors Basics

  - **Micro Channel Plates:**

  A MCP is a two-dimensional array of several million channels of 5–20 μm diameter, which have a semiconducting surface coating inside the channel (e.g., Wiza, 1979; Fraser, 1989). Particles impinging on the channel wall create secondary electrons that get accelerated by an electric potential along the channel, which leads to charge multiplication. Typically, two MCPs are used in series to obtain amplifications on the order of 10^6.

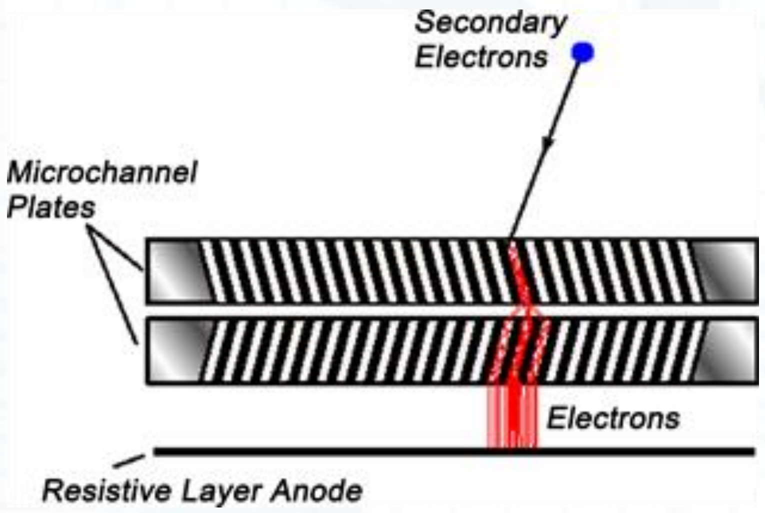

ENA Detection- Basics

- Imaging detectors Basics

  - **Solid State Detectors:**

  An energetic particle penetrates a SSD and loses most of its energy in creating electron-hole pairs. In silicon it takes 3.62 eV to create such an electron-hole pair at room temperature.

  By applying an electric field across the SSD, the created charge carriers drift to contacts of opposite polarity. By measuring the total collected charge collected on one contact one can determine the energy deposited by the particle.

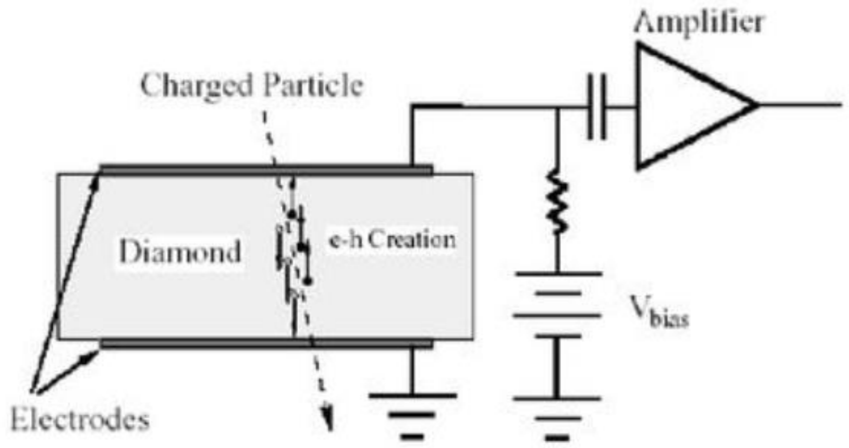

ENA Detection- Basics

- Imaging detectors Basics

  - **Foils:**
    * Ultrathin foils play an exceptionally important role in ENA instrumentation
    * Stripping passing ENAs
    * Producing secondary electrons

  - **Conversion surfaces:**
    * Convert neutrals to negative ions
    * Only work for very low energies (below ~1 keV)

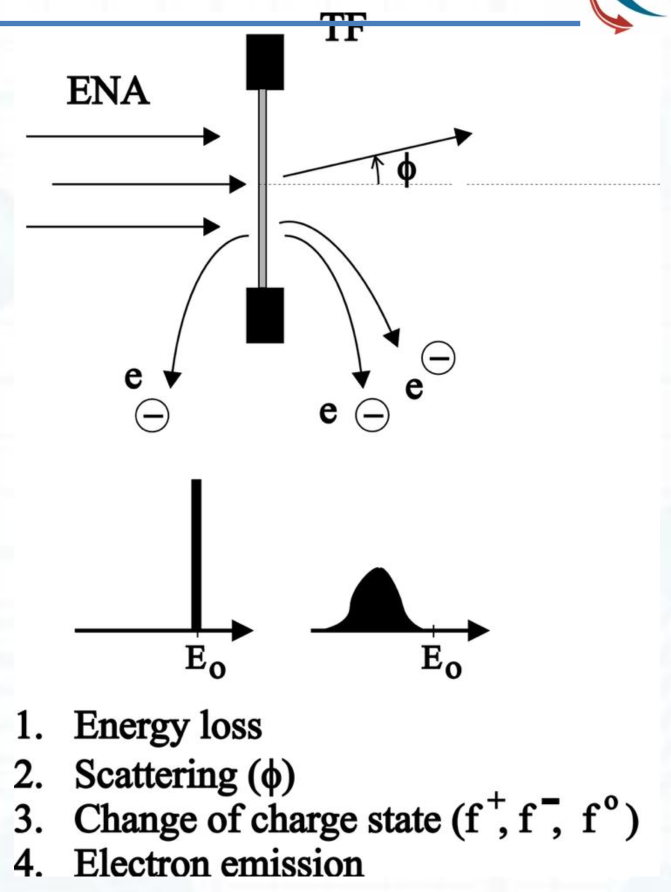

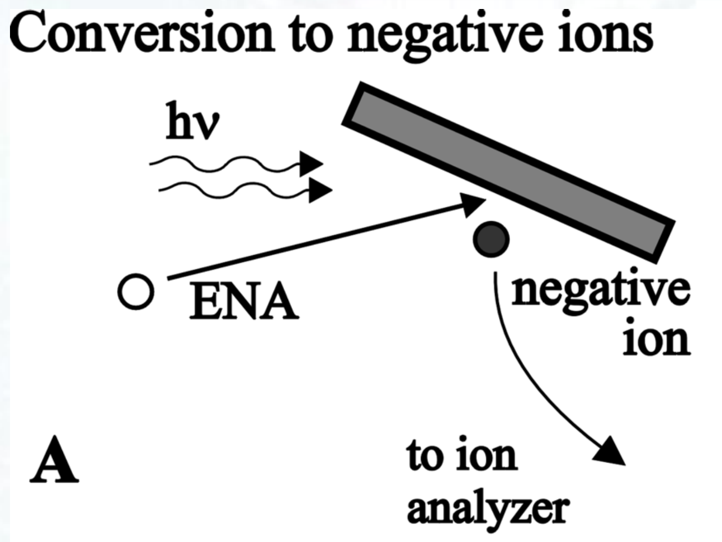

Gruntman 1997

ENA Detection- Basics

- Imaging detectors Basics

  - **Time of Flight spectrometer system:**
    * start-foil (carbon foil),
    * free path for the particles
    * secondary electron extraction optics
    * Two start and stop MCP detectors

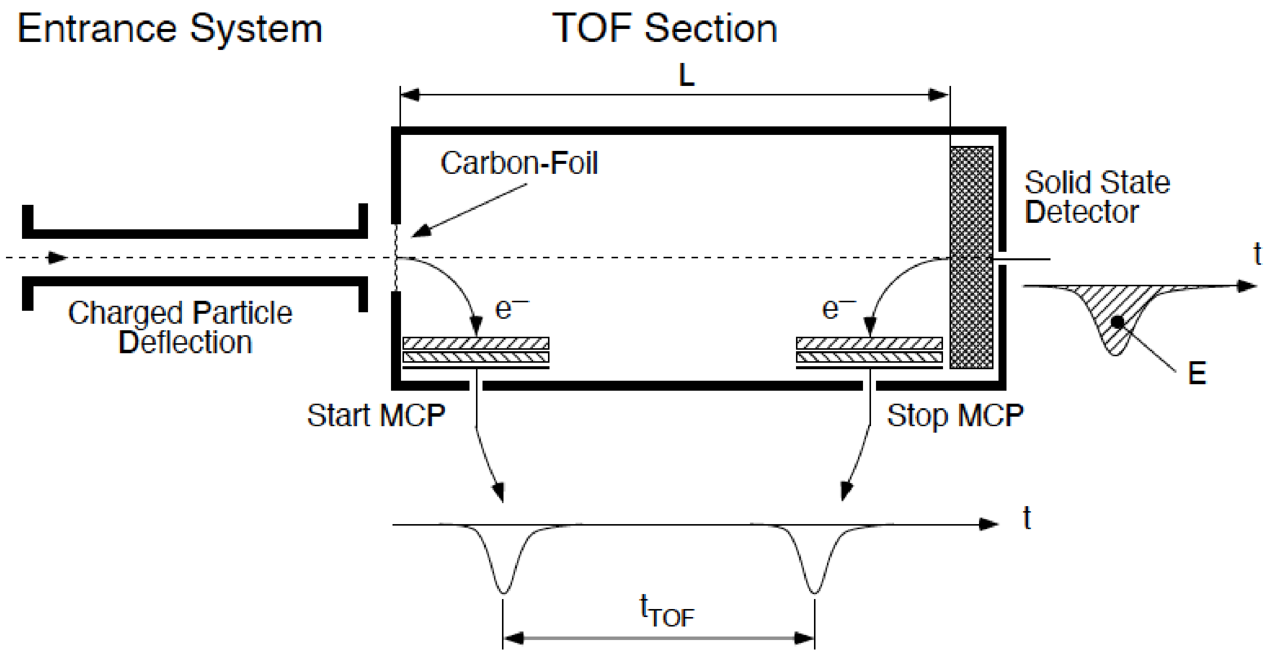

TOF → particle velocity
SSD → Energy

Helpful hint: By setting a window of allowed TOFs, one can discriminate against particles being too energetic, light (electrons), or photons.

Wurz 2000

ENA Detection- Examples

- IMAGE mission (magnetosphere)

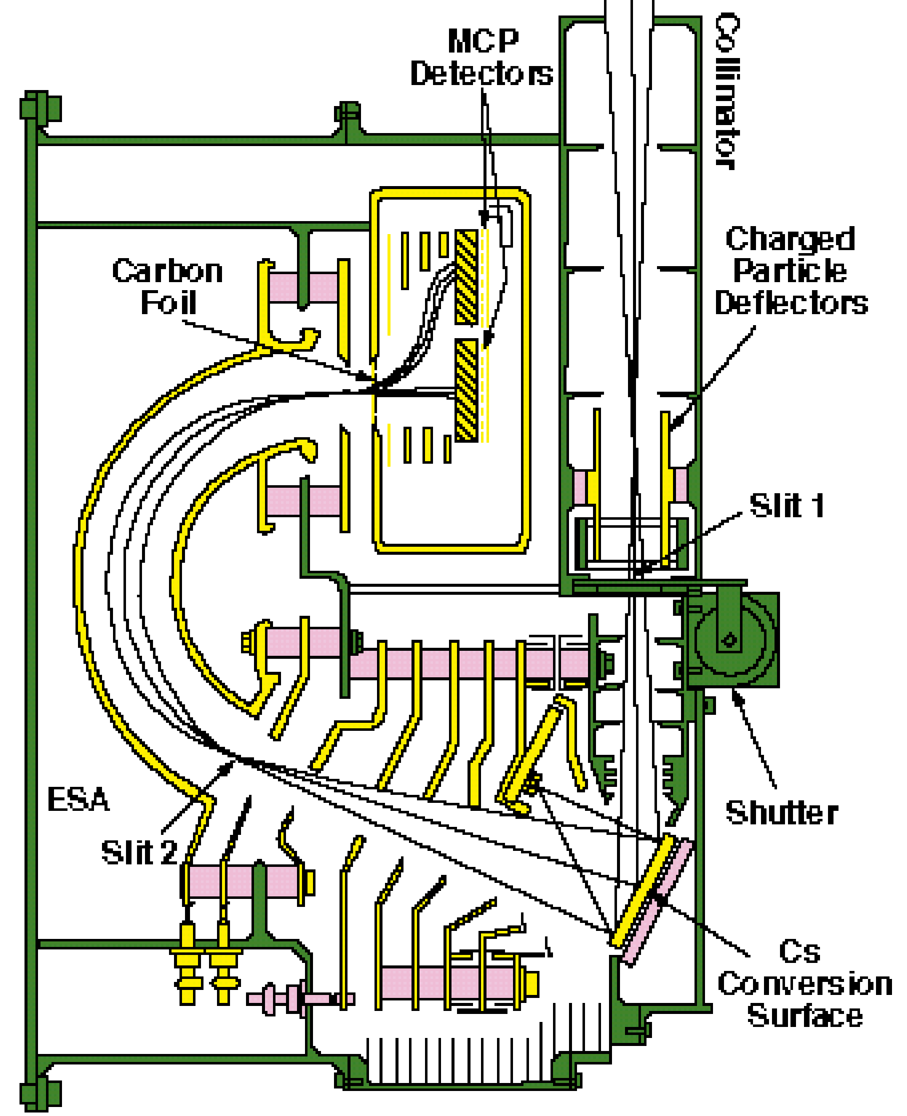

IMAGE/LENA (0.01-0.3 keV)

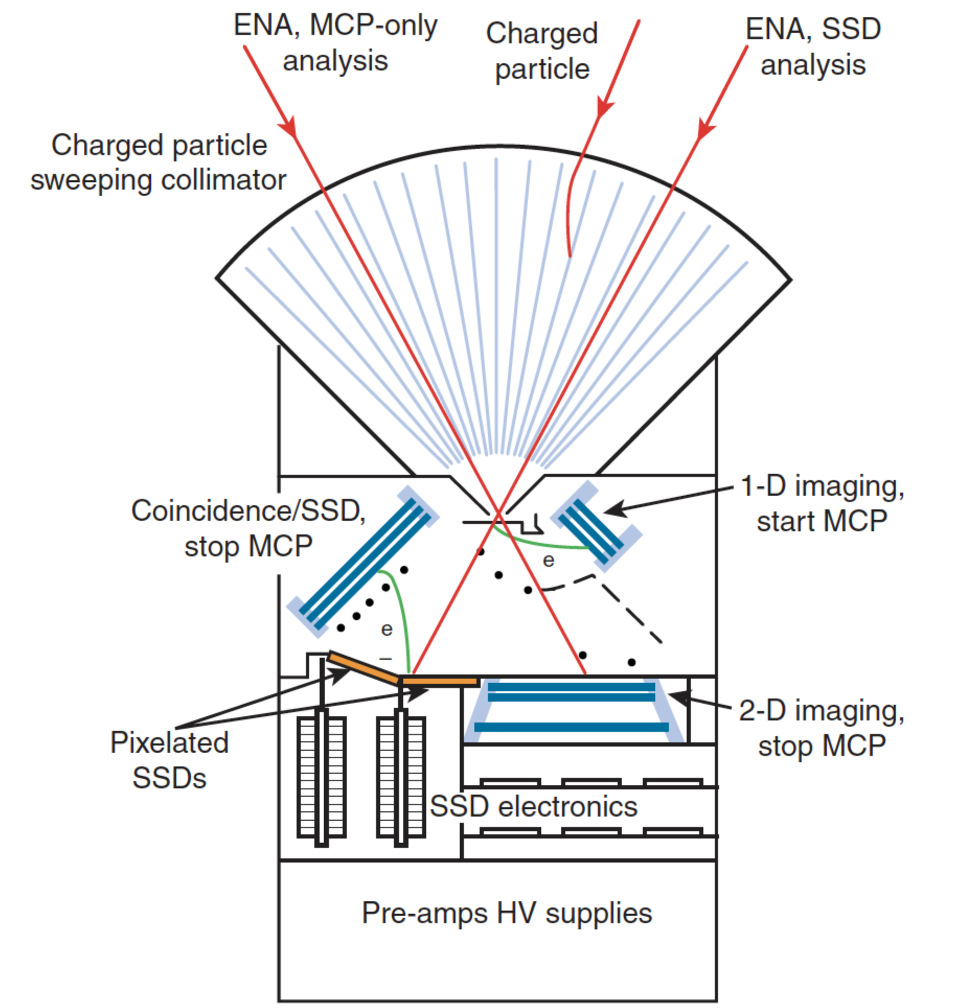

IMAGE/HENA (10-200 keV)

Burch et al. 2000

ENA Detection- Examples

- IBEX mission (Heliosphere)

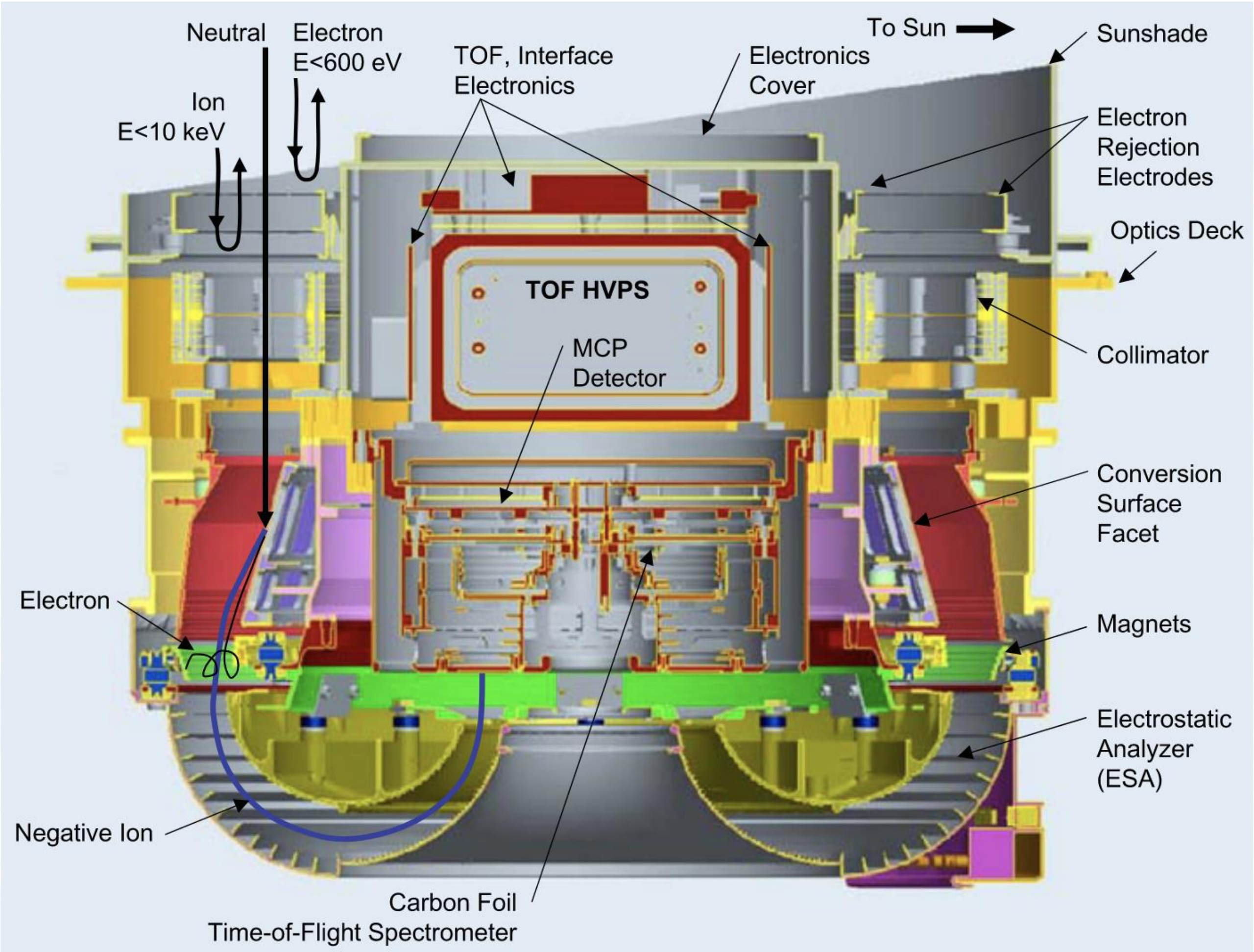

IBEX-Lo (~0.1-2 keV)

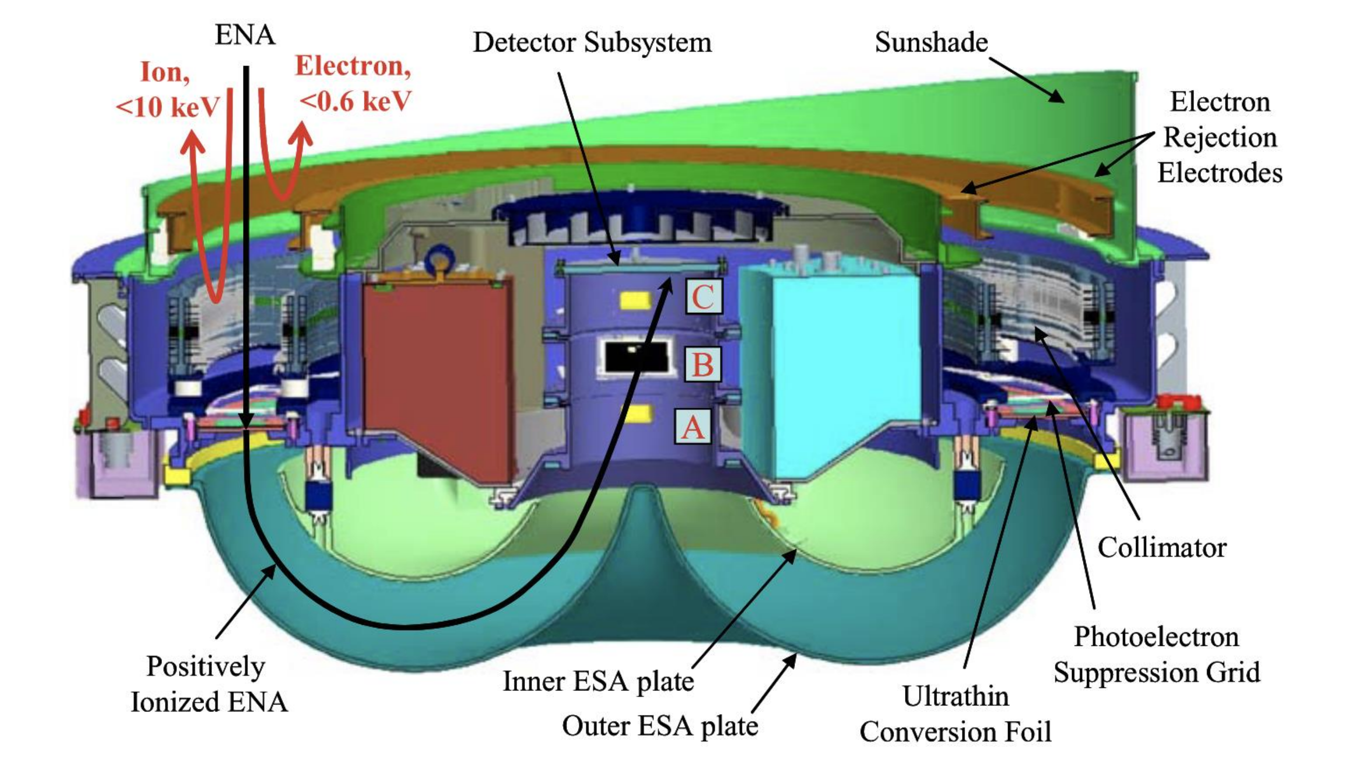

IBEX-Hi (~0.5-6 keV)

McComas et al. 2009

ENA Instrumentation

Same detection concept

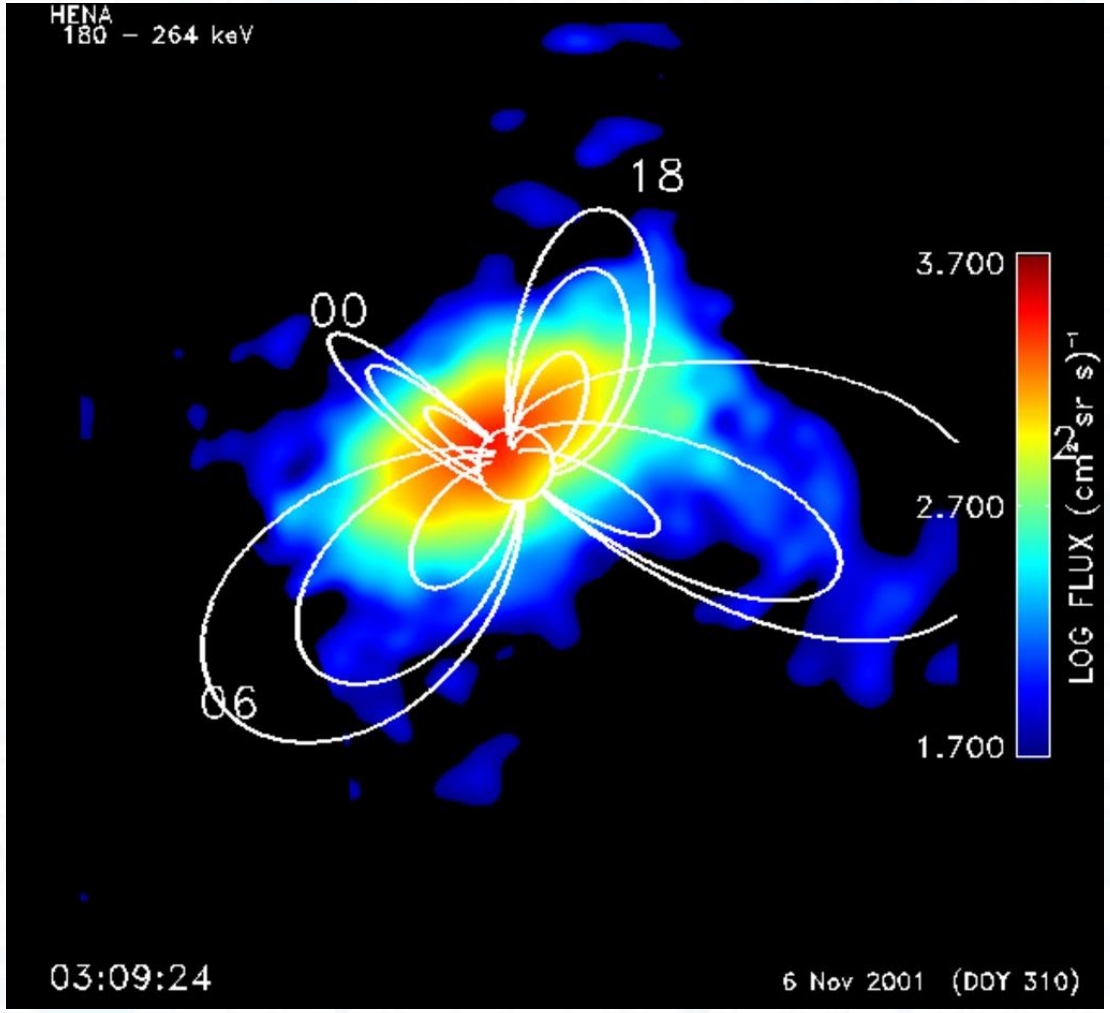

HENA image of magnetospheric Oxygen
Fuselier et al. 2002

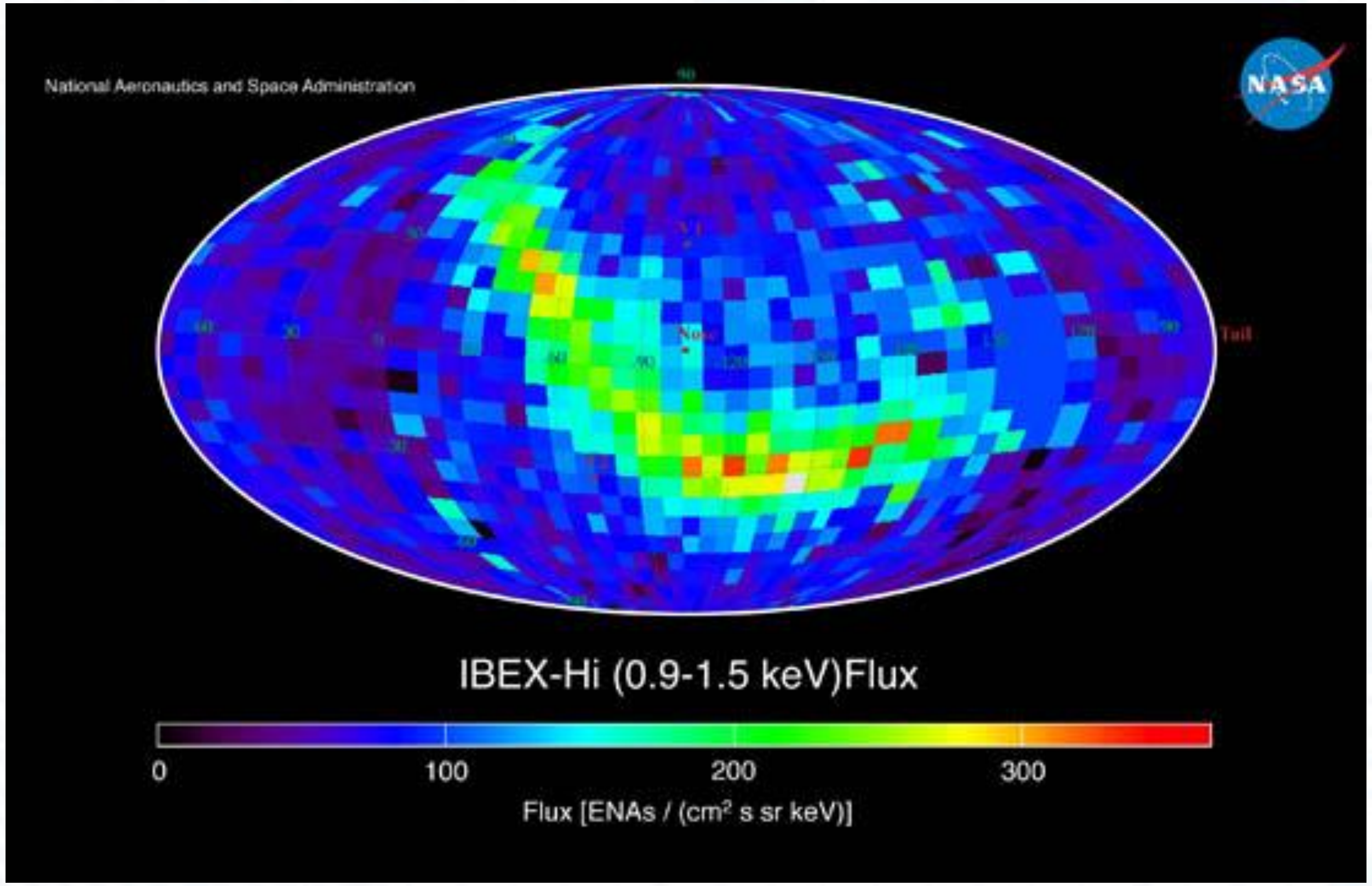

IBEX-Hi image of Heliospheric ENAs
McComas et al. 2009

Break II

IBEX ENA measurements

The Interstellar Boundary Explorer (IBEX)

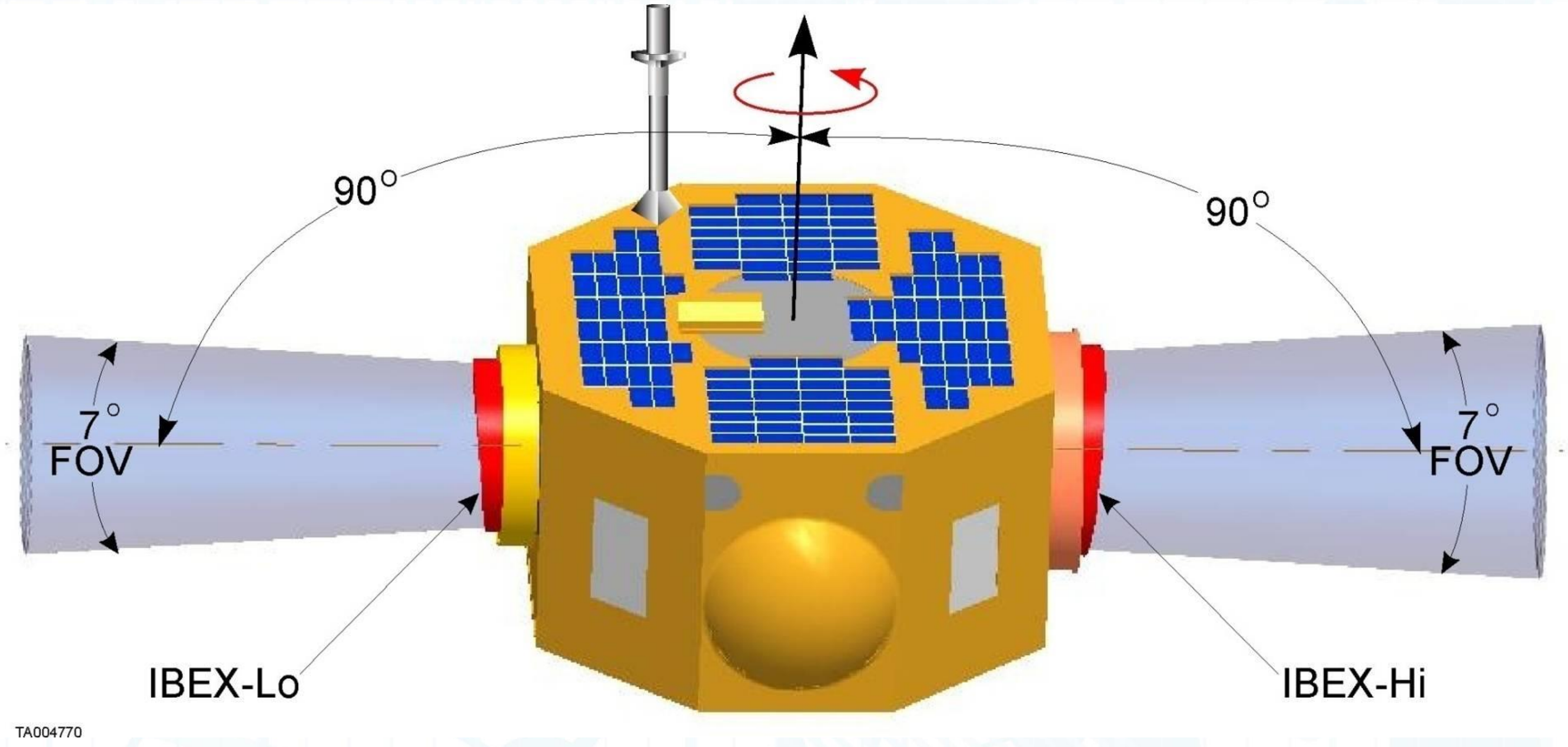

- Two huge aperture, single pixel ENA cameras
  - IBEX-Lo (~10 eV to 2 keV)
  - IBEX-Hi (~300 eV to 6 keV)

The Interstellar Boundary Explorer (IBEX)

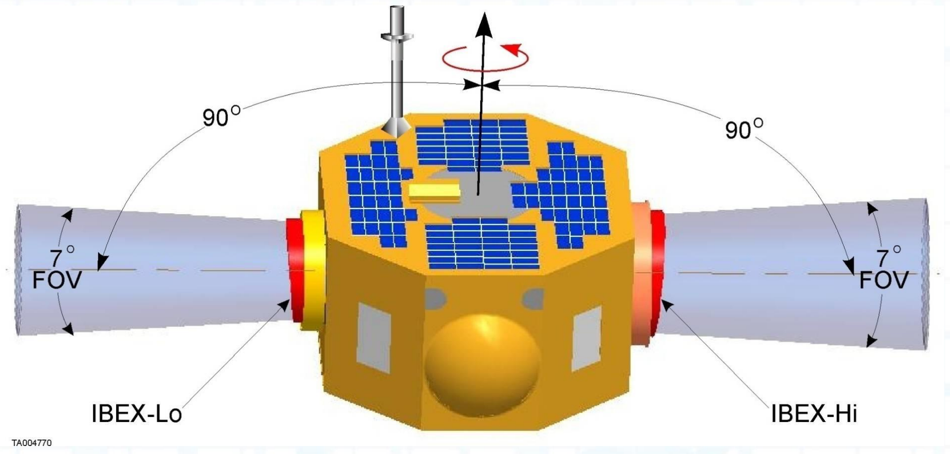

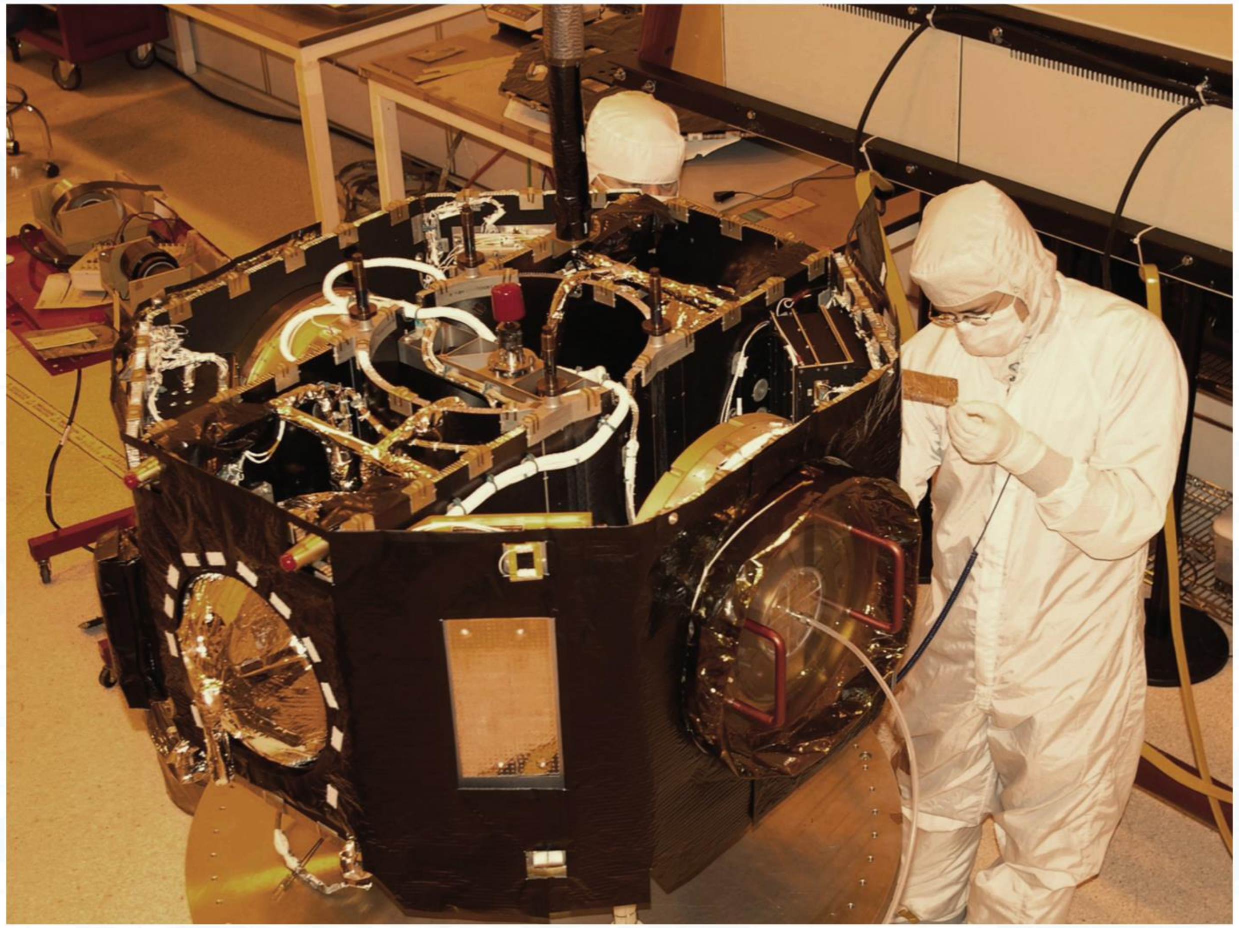

- Two huge aperture, single pixel ENA cameras
  - IBEX-Lo (~10 eV to 2 keV)
  - IBEX-Hi (~300 eV to 6 keV)

Creating All-sky maps

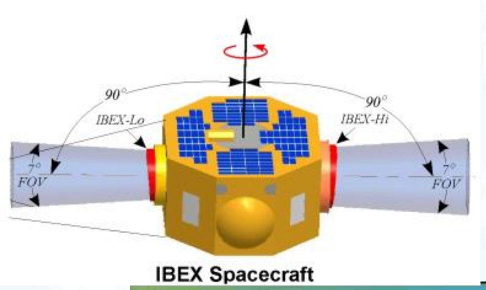

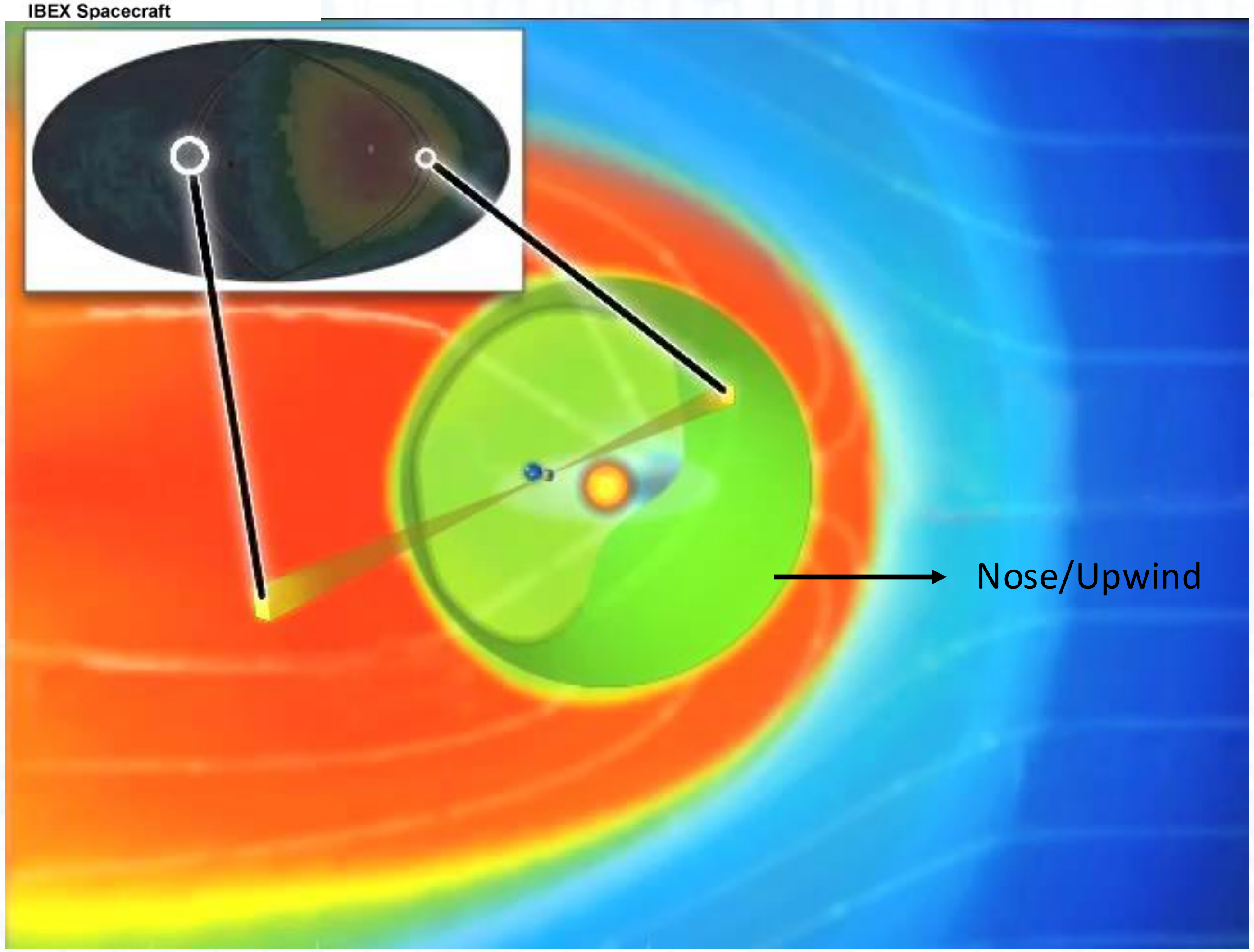

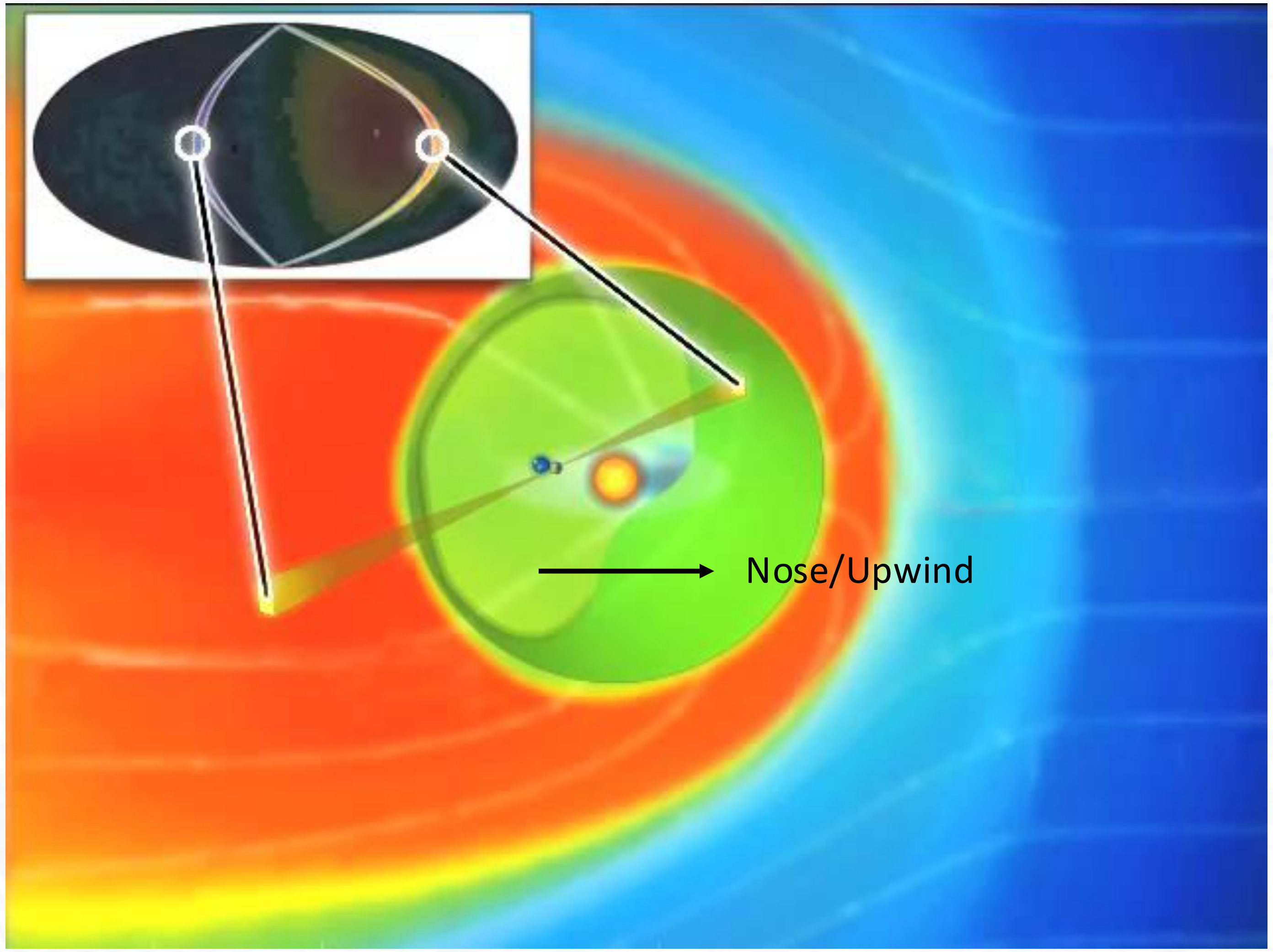

Credit: IBEX Team/SwRI

What did we expect?

- Models predict enhanced ENA fluxes from the nose-ward (plot center) and tail-ward (left/right) directions

- Most models assume largest ~keV ENA contribution from suprathermal ions in the IHS

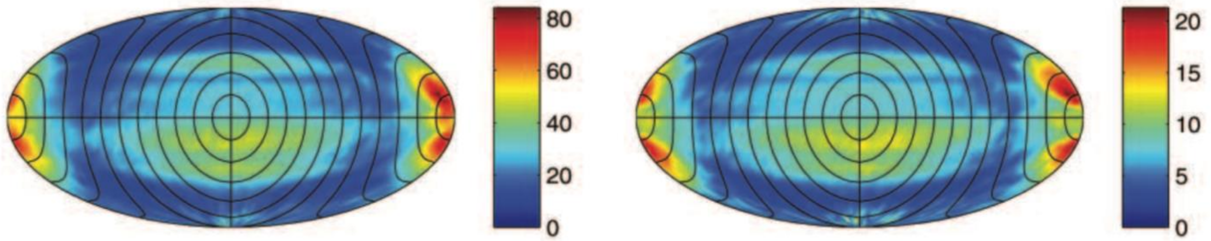

1000 ± 100 eV 2400 ± 200 eV

Heerikhuisen et al. (2008, ApJ)

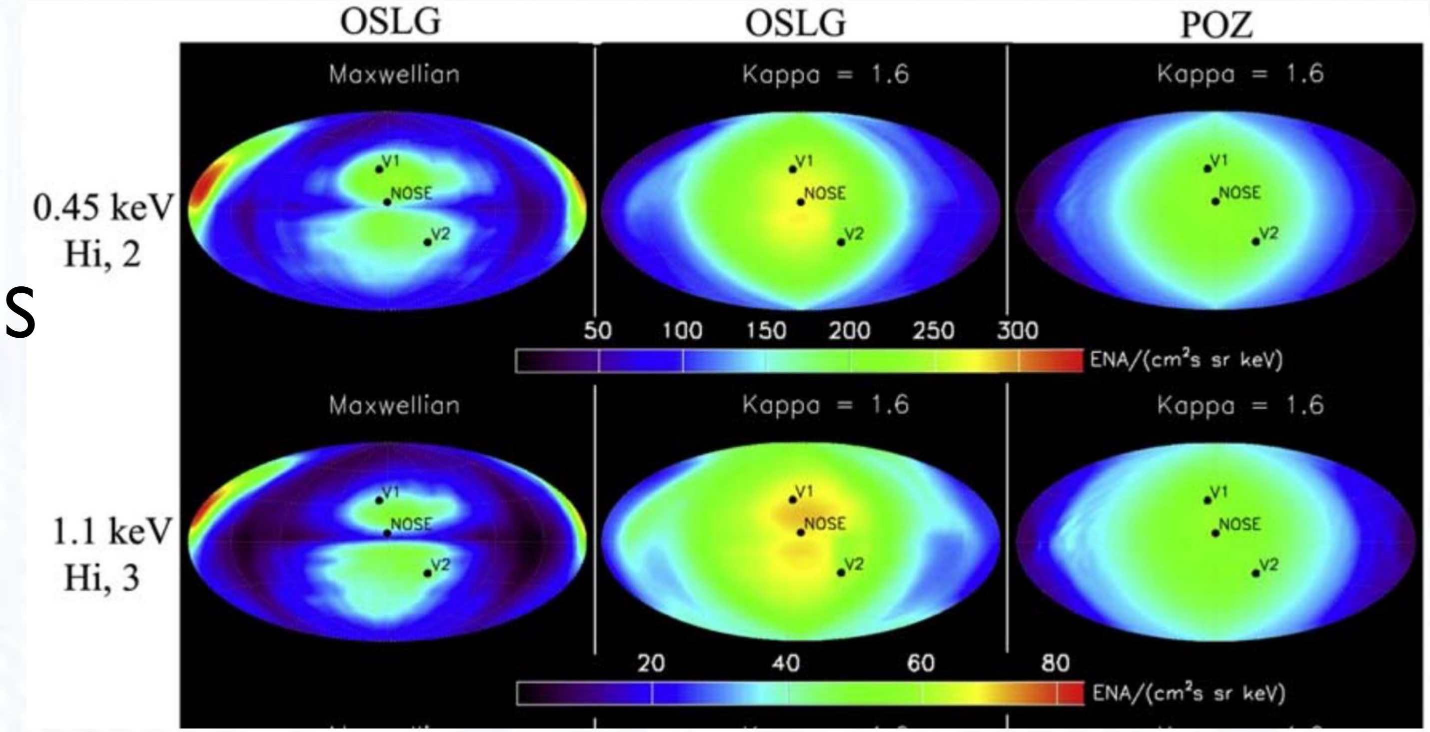

Prested et al. (2008, JGR)

What IBEX measured…

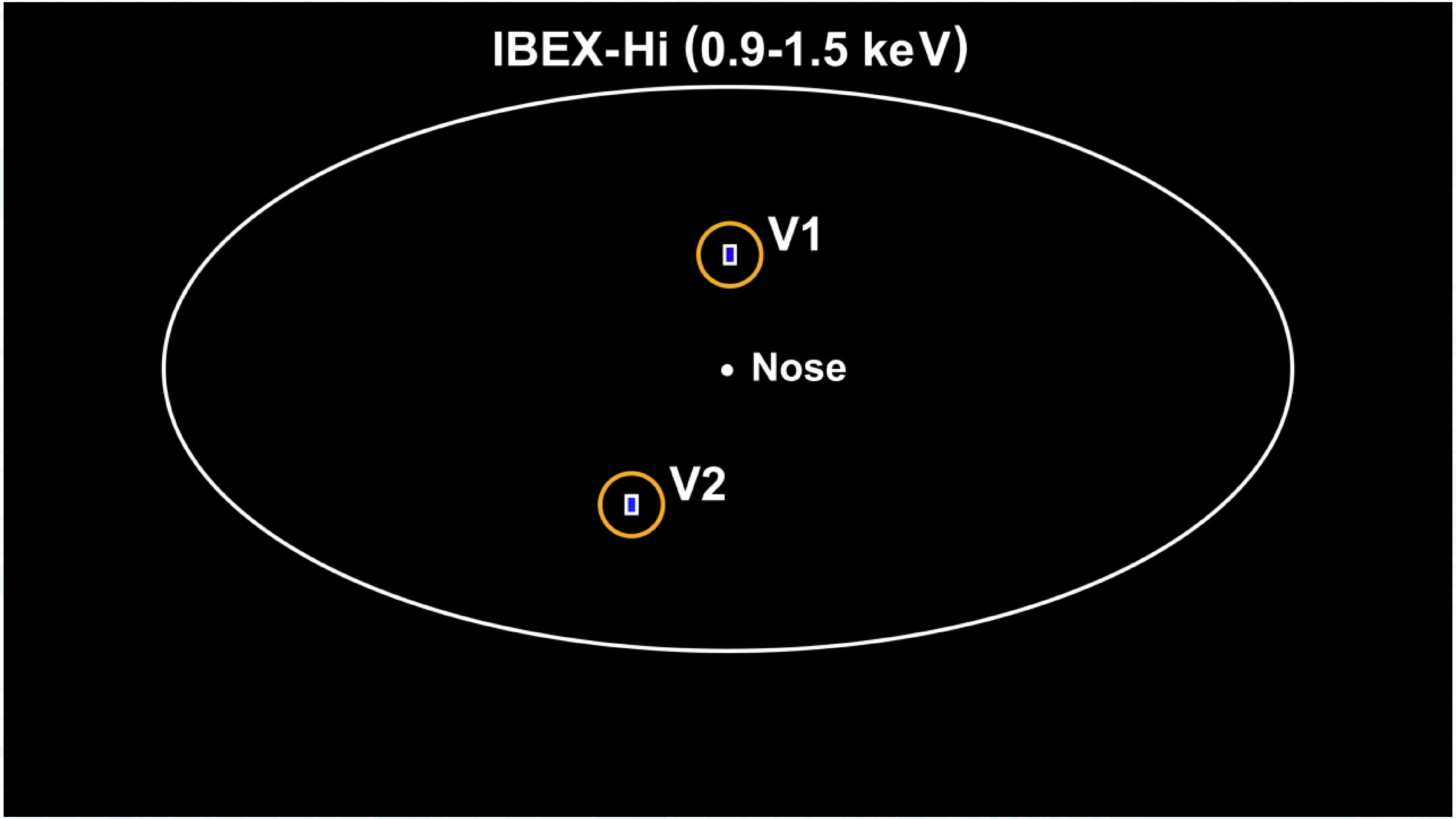

What IBEX measured…

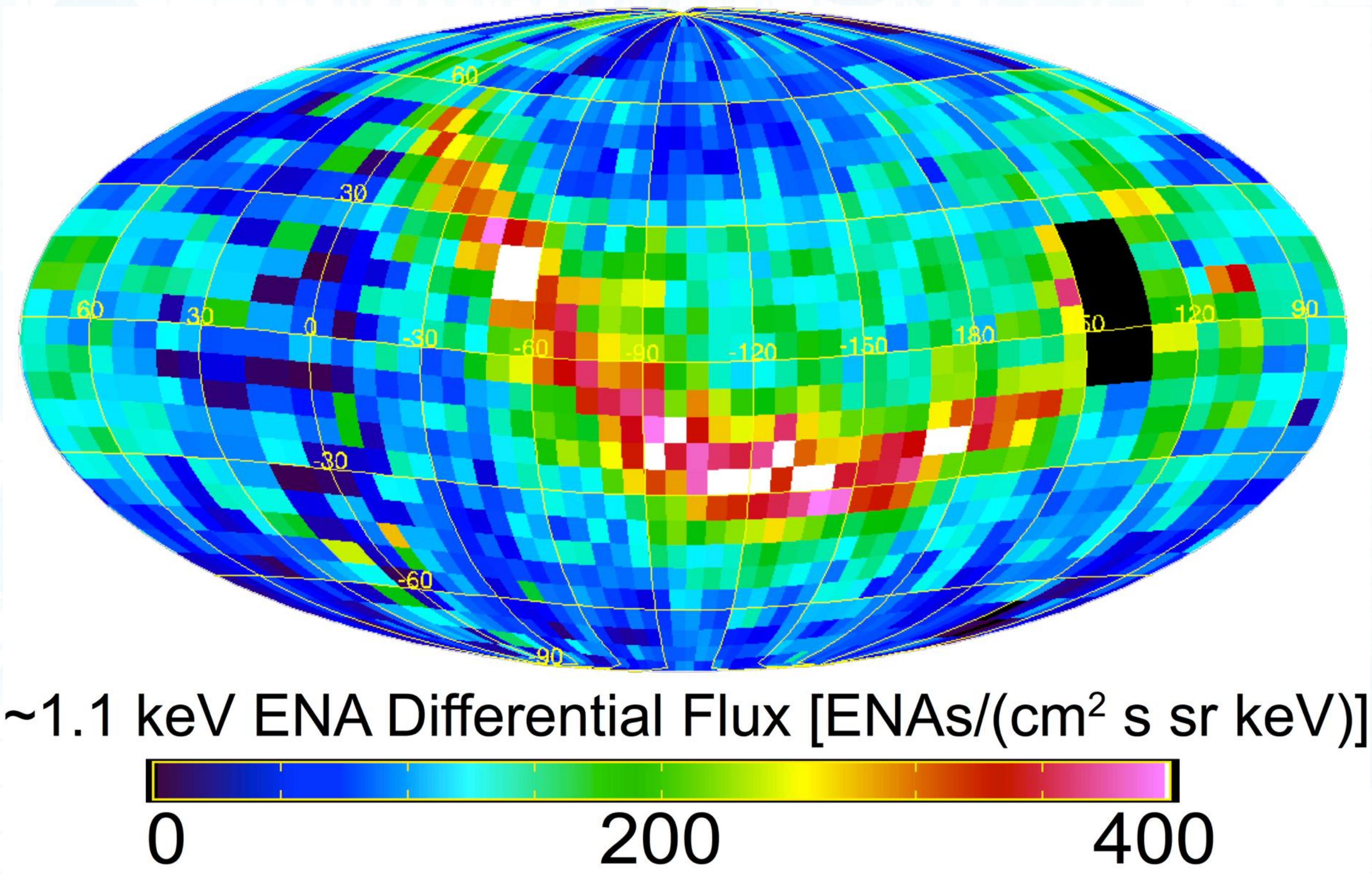

First IBEX observations

"Ribbon" completely unexpected, but realized to be connected to the local ISMF:

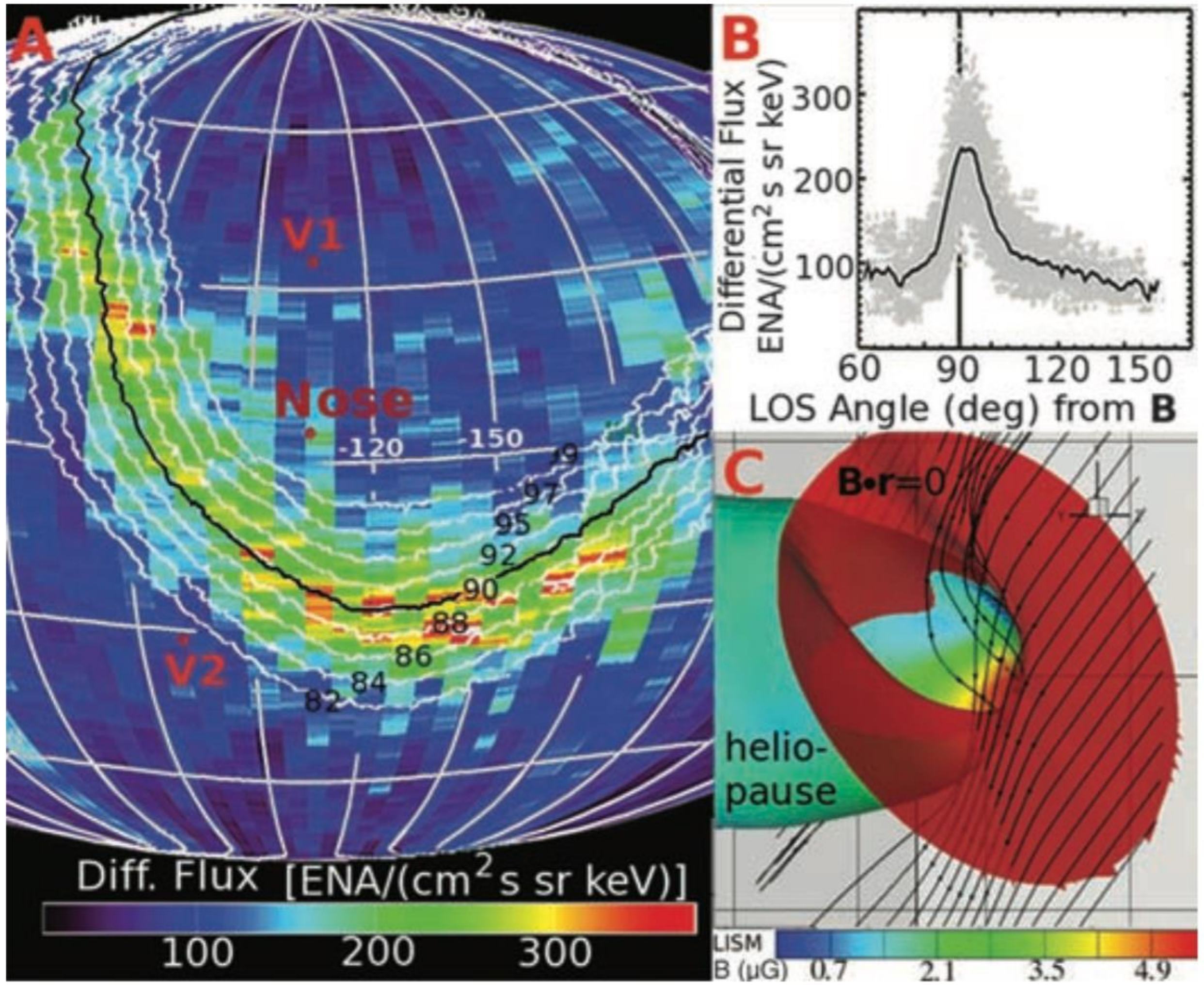

Schwadron et al. (2009, Sci)

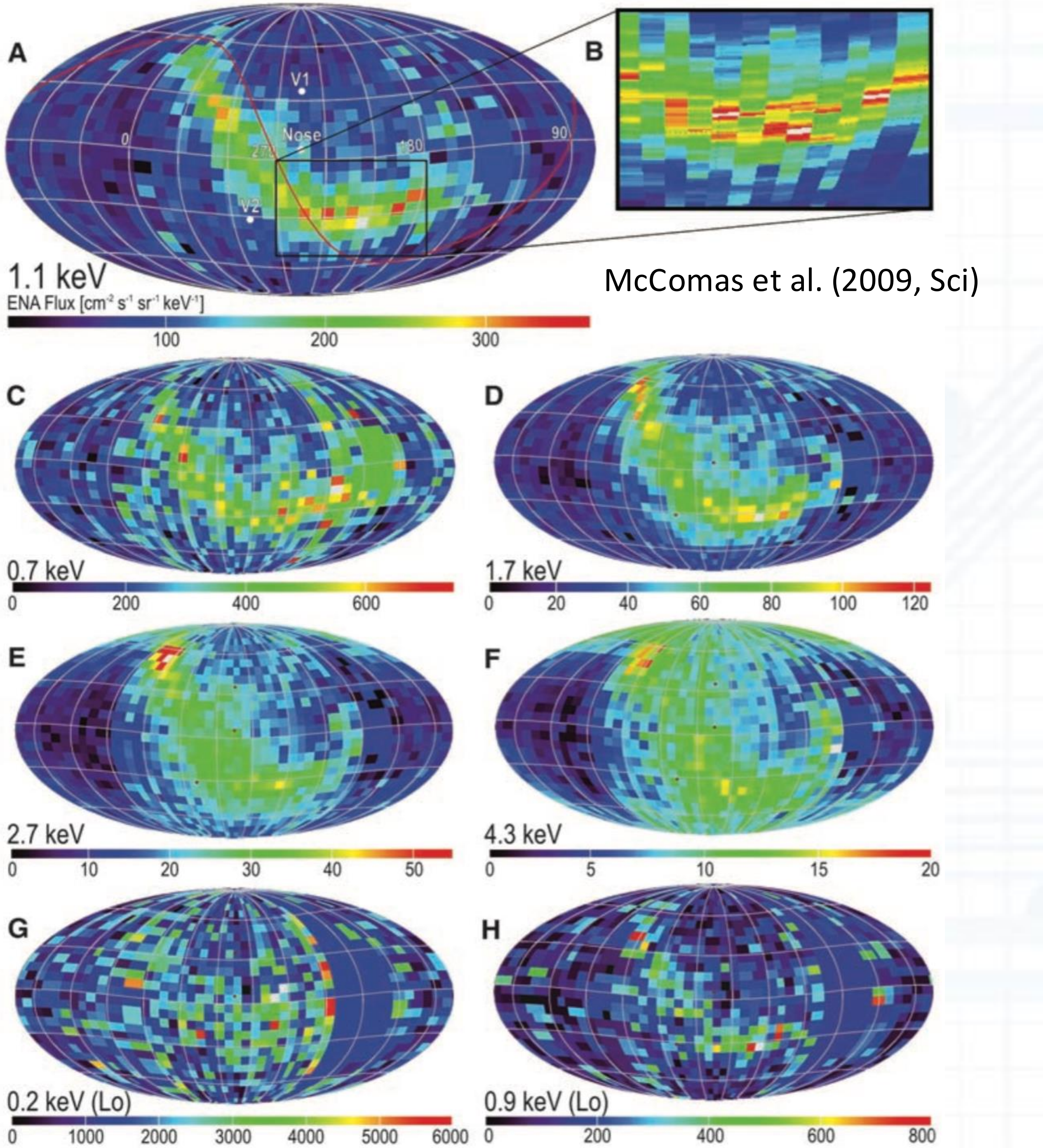

McComas et al. (2009, Sci)

First all-sky maps produced/published in 2009

First IBEX observations

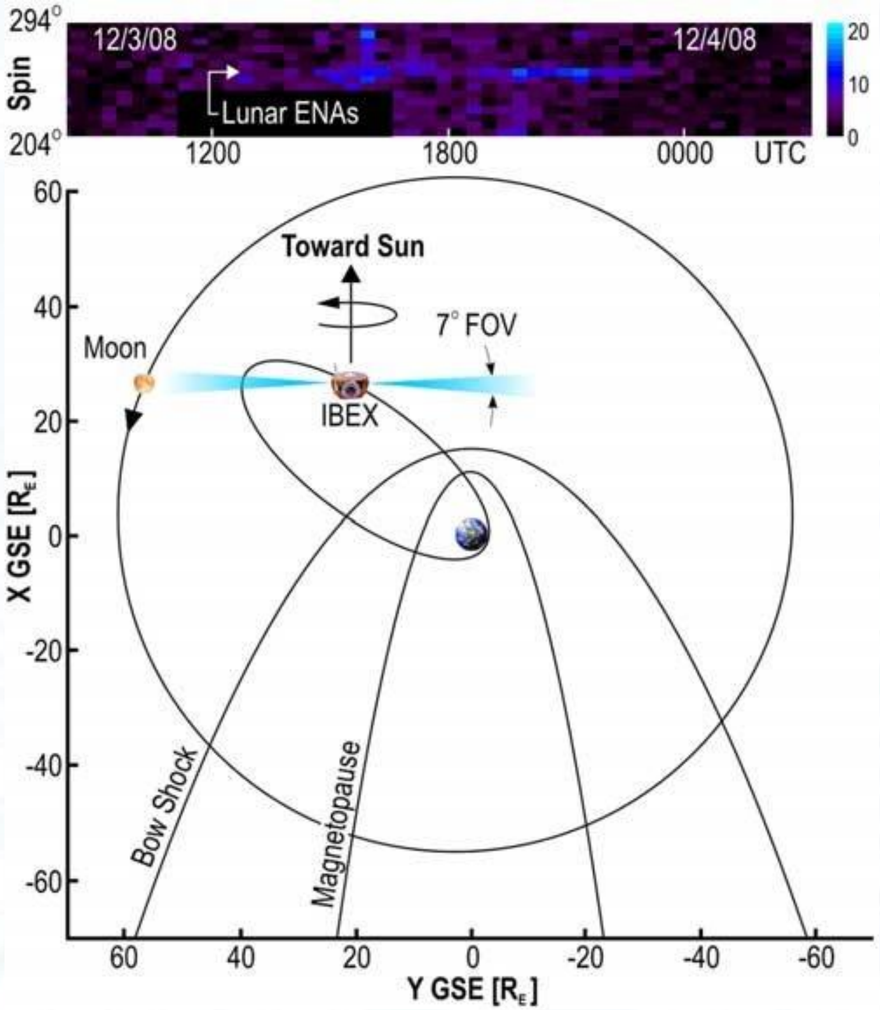

First detection of lunar ENAs (McComas et al. 2009)

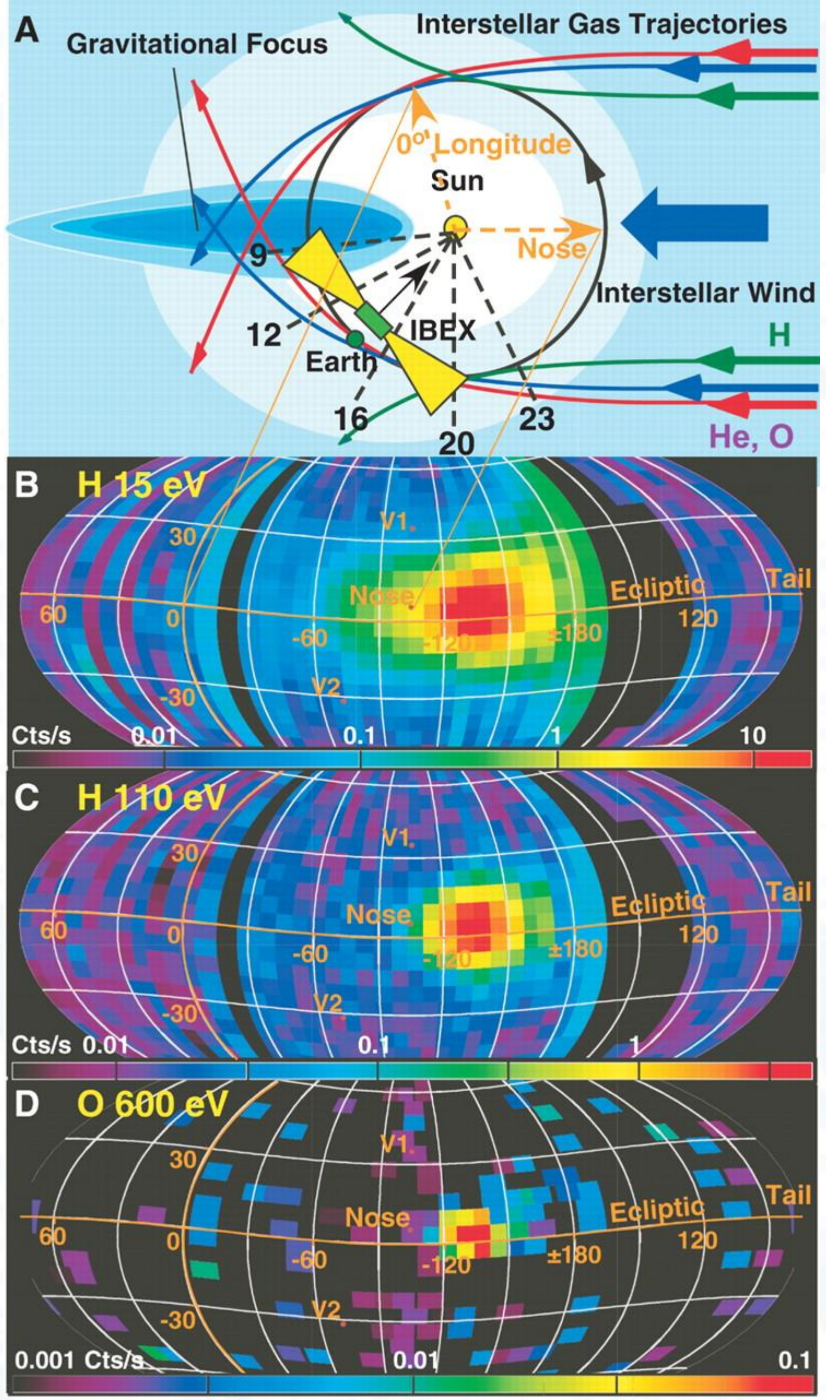

First IBEX observation of interstellar gas. (Mobius et al. 2009)

A remarkable mission!

13 November 2009 Issue

McComas et al., Science, 2009

Over 50 Major "Firsts" & Discoveries

IBEX observations cover:

- Global Heliosphere
- Local Interstellar Medium
- Terrestrial Magnetosphere
- Moon

IBEX Ribbon	
Discovery of an enhanced ENA Ribbon flux and its connection to the interstellar magnetic field (see review by McComas	McComas et al. (2009c)
	Fuselier et al. (2009a) Funsten et al. (2009b) Schwadron et al. (2009)
	McComas et al. (2012c)
re and secondary ENA	McComas et al. (2014a)
	McComas et al. (2010)
bon and ISN flow	Schwadron et al. (2015b)
ource	Swaczyna et al. (2016a)
	Swaczyna et al. (2016b)
	McComas et al. (2009c) Schwadron et al. (2009)
on to decreasing solar	McComas et al. (2010)
	Reisenfeld et al. (2012, 2016) McComas et al. (2012c)
	Dayeh et al. (2011) Desai et al. (2015)
stellar magnetic	Schwadron et al. (2011a)
	McComas et al. (2013b)
ager directions	Wu et al. (2010) Desai et al. (2014) Zank et al. (2010) Zirnstein et al. (2014)
	Livadiotis et al. (2011) Livadiotis & McComas (2013)
eliosheath observed by	Schwadron et al. (2014c)
	McComas & Schwadron (2014)
eliotail, where they	McComas et al. (2014a)
power law	Desai et al. (2015) Dayeh et al. (2012)
TS/IHS geometry, PUI	Schwadron et al. (2014c)
	McComas & Schwadron (2014) Zirnstein et al. (2016a)
	Fuselier et al. (2014) Galli et al. (2016)
	Reisenfeld et al. (2016)
for generating heliotail	Zirnstein et al. (2017)
ted to the B–V plane of	Cairns & Fuselier (2017)

Interstellar Medium	
First direct observations of interstellar hydrogen, deuterium, oxygen, and neon	Möbius et al. (2009) Bochsler et al. (2012) Rodríguez Moreno et al. (2013)
Discovery of secondary population of He (the "warm breeze")	Kubiak et al. (2014)
First connection of LISM environment from *IBEX* to TeV cosmic rays	Schwadron et al. (2014a)
Discovery that the heliosphere might have a bow wave ahead of it instead of a bow shock	McComas et al. (2012a) Zank et al. (2013)
First precise estimate of interstellar field strength as well as direction	Zirnstein et al. (2016b)
Refined ISN He flow direction, temperature, and speed	McComas et al. (2015b) Schwadron et al. (2015a) Bzowski et al. (2015)
VLISM is warmer than previously expected	McComas et al. (2015a) Möbius et al. (2015b)
Co-planarity of ISN He, H, He Warm Breeze, the *IBEX* Ribbon center, and the interstellar magnetic field deduced from the Ribbon	ApJ Supp. Series (2015) Kubiak et al. (2016) Zirnstein et al. (2016b)
Determination of the local gas Ne/O ratio from neutral flow observations	Bochsler et al. (2012) Park et al. (2014)
Confirmation of He and O secondary component possibly from the VLISM	Park et al. (2016)
First quantitative derivation of ISN O properties; evidence for significant processing in the VLISM	Schwadron et al. (2016a)
First direct sampling of ISN H and its evolution during the solar cycle	Saul et al. (2012, 2013)
Independent derivation of solar radiation pressure from ISN H observations revealed to be greater than that inferred from solar Lyα flux data	Katushkina et al. (2015)
Possible IS dust filament in the VLISM and correlation with LISM inflow direction	Frisch et al. (2015)
First derivation of IS flow longitude from symmetry of IS PUI cutoff at 1 au and connection to *IBEX* measurements	Möbius et al. (2015c)
Terrestrial Magnetosphere	
First imaging of Earth's subsolar magnetopause	Fuselier et al. (2010)
First imaging of dynamic magnetotail and possible disconnection event	McComas et al. (2011b)
First images of magnetospheric cusps and their asymmetry	Petrinec et al. (2011)
First characterization of dayside magnetosheath using ENAs	Ogasawara et al. (2013)
First combined mission ENA imaging to provide direct timing of plasma transfer from dayside compression to magnetospheric ring current	McComas et al. (2012b)
Motion of terrestrial plasma sheet dominated by seasonal and diurnal motion of Earth's dipole tilt	Dayeh et al. (2015)
First imaging of development of cold terrestrial plasma sheet during period of northward IMF and its reversal	Fuselier et al. (2015)
Evidence for suprathermal ion acceleration by diffusive shock acceleration at Earth's bow shock, shocked SW in subsolar magnetopause	Ogasawara et al. (2015)
Moon	
First measurement of neutralized and backscattered solar wind from the Moon	McComas et al. (2009b)
Discovery of lunar ENA albedo on solar wind speed and Mach number	Funsten et al. (2013a) Allegrini et al. (2013)
Space Mission Capabilities	
First use of additional Solid Rocket Motor on Pegasus LV and spacecraft propulsion to achieve very high altitude orbit	McComas et al. (2009a) Scherrer et al. (2009)
Space Mission Capabilities	
Discovery and first use of long-term stable lunar synchronous orbit	McComas et al. (2011a)

McComas et al., ApJS, 2017

Two distinct ENA populations

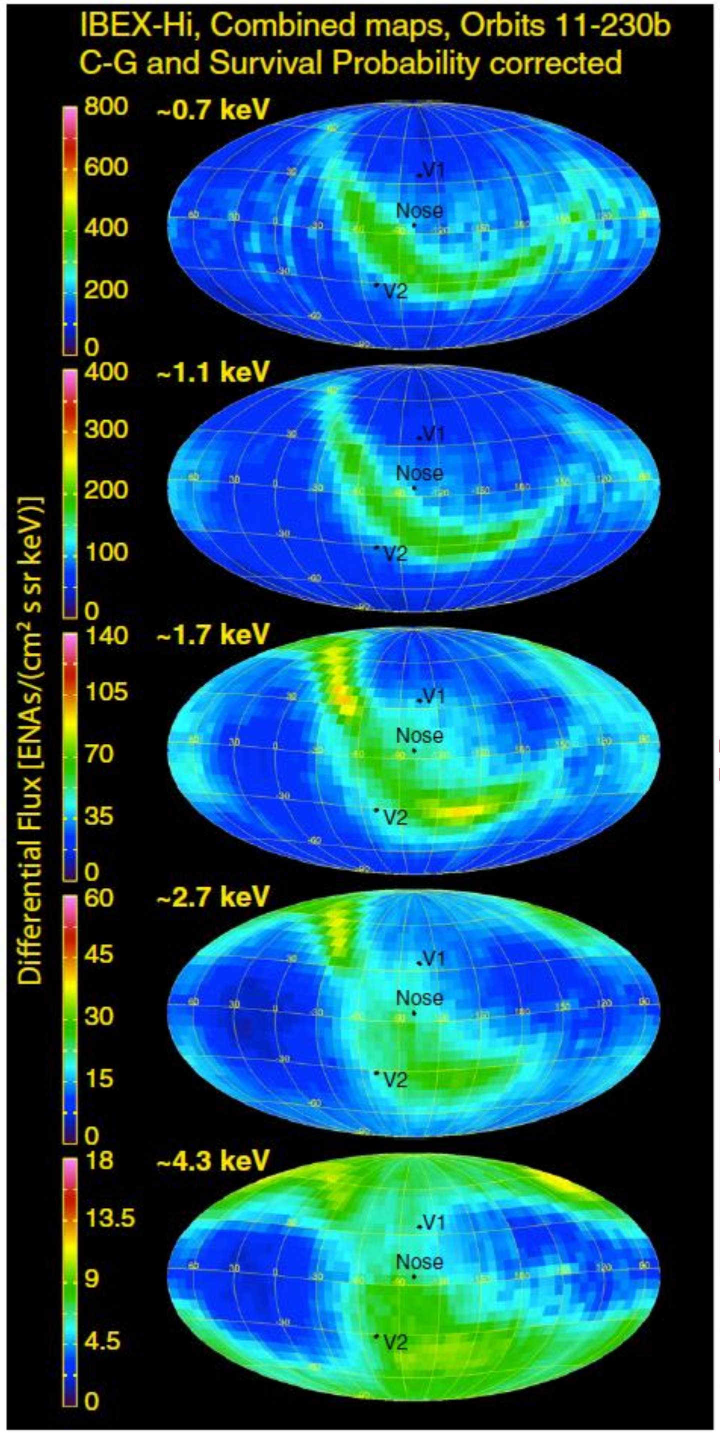

McComas et al. (2014, ApJS)

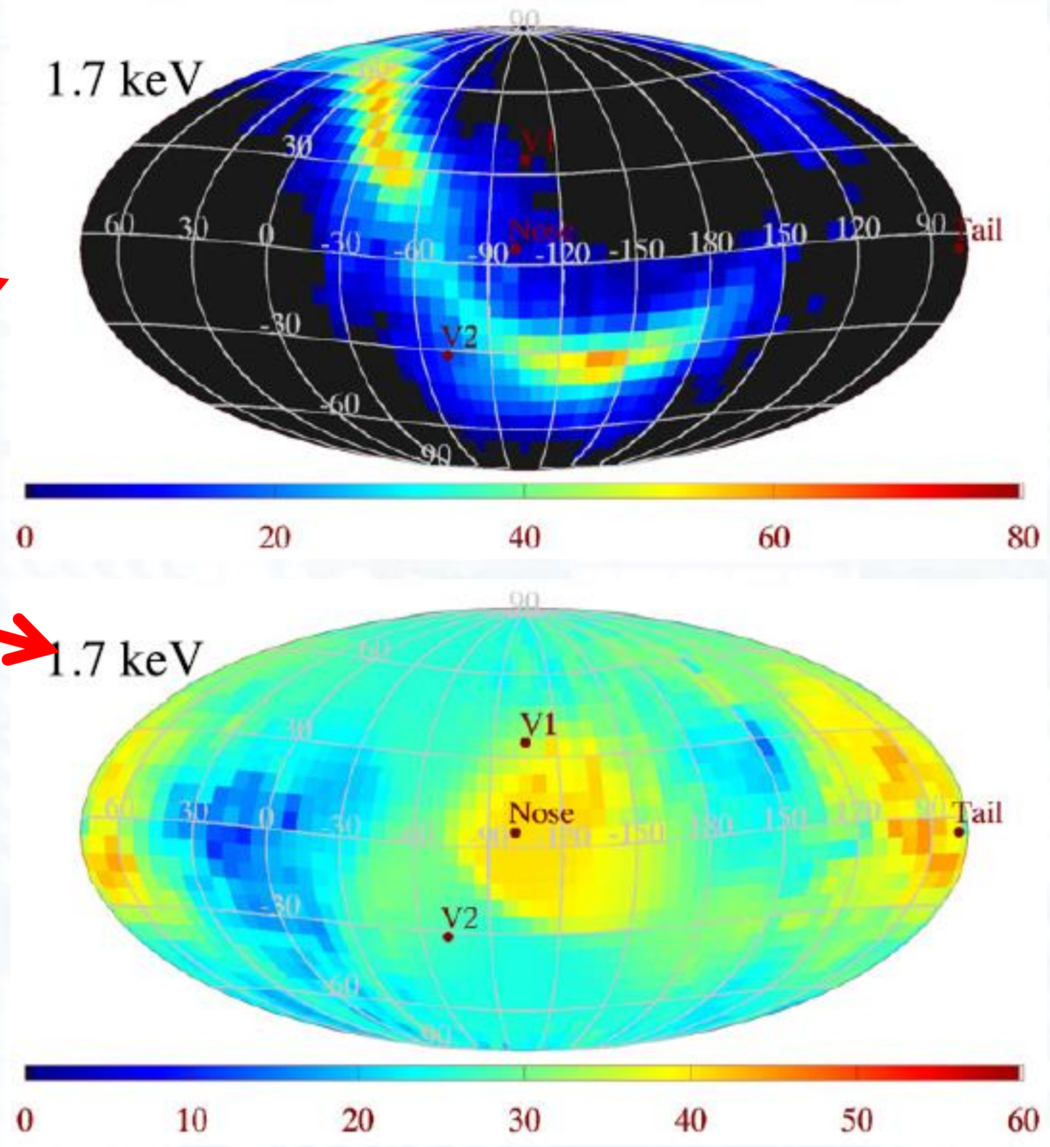

Ribbon

Globally distributed flux (GDF)

Schwadron et al. (2014, ApJS)

Possible Ribbon mechanisms

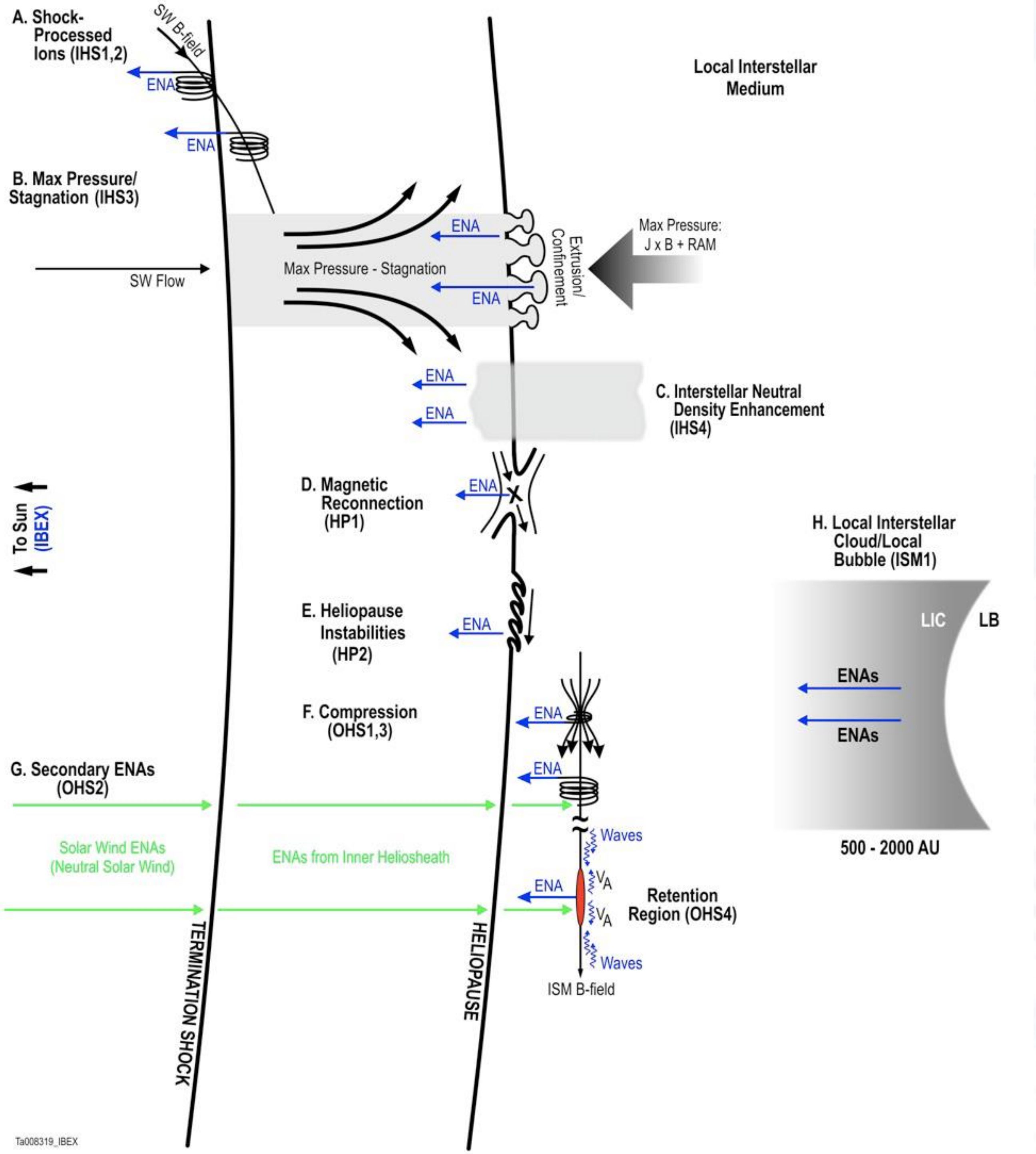

Model / Scenario	Strength[1]	Weakness
	Inner Heliosheath	
IHS 1: Shock-processed PUIs / ACRs	Produces ring of enhanced 1 keV ENA emissions resembling Ribbon. Relative intensities of ring and global emissions consistent with observations.	Ordering of Ribbon by draped ISMF not explained. Uses idealized symmetric TS/HP geometry.
IHS 2: Specularly reflected SW ions/PUIs	Explains enhancement of Ribbon emissions vis-à-vis globally distributed flux in terms of well-established shock-physical processes.	Ribbon's ordering by ISMF not explicitly addressed. Uses ad hoc TS/HP geometry. LOS path length for global emissions not consistent with estimates of IHS thickness. Ring-beam distribution of Ribbon ENA source may not be stable (cf. OHS 2).
IHS 3: Stagnation Region	Region of enhanced IHS plasma density to balance external JxB force may explain Ribbon's ordering by ISMF and enhanced intensity vis-à-vis global flux. Possible HP extrusions may explain fine structure.	Does not predict different energy spectra for the Ribbon and global flux. MHD models including external JxB force do not find enhanced pressure. Stagnation scenario still requires some missing non-MHD physics.
IHS 4: H-wave	Predicts ring-like emission feature ordered by ISMF. Accounts for broadening of Ribbon at higher energies.	To satisfy B•r=0, assumes that normal of H-wave phase front is not significantly tilted from ISMF direction. Difference between Ribbon and global flux energy spectra not satisfactorily explained.
	Heliopause	
HP 1: Magnetic Reconnection	Potentially accounts for Ribbon's ordering by ISMF. May explain Ribbon fine structure.	Likely to produce multiple distributed source regions instead of continuous Ribbon owing to alternating IMF polarity.
HP 2: K-H & R-T Instabilities	May explain Ribbon fine structure.	Does not explain Ribbon's shape and position and may not provide large enough structures for factor of 2 enhanced flux.
	Outer Heliosheath	
OHS 1: ISMF Compression	Produces Ribbon ordered by draped ISMF as a result of conservation of first adiabatic invariant / increased density in compressed field region. (Cf. OHS 3)	Assumes unspecified suprathermal source in OHS.
OHS 2: Secondary ENAs	Produces narrow Ribbon ordered by draped ISMF. Can reproduce observed ordering of ENA energies by heliographic latitude.	PUI ring-beam distribution must remain stable against pitch-angle scattering long enough for re-neutralization to occur.
OHS 3: Magnetic Mirror	Produces Ribbon-like structure ordered by draped ISMF from PUIs transported along ISMF to regions of increased B (magnetic mirror points). (Cf. OHS 1)	Assumes no pitch-angle scattering in OHS as limiting case.
OHS 4: Retention Region	Produces Ribbon ordered by draped ISMF. Does not require maintenance of ring-beam distribution. Reproduces observed ordering of ENA energies by heliographic latitude.	Includes only neutral SW but not ENAs from IHS source. Modeled Ribbon thus narrower than observed.
	Interface of Local Interstellar Cloud and Local Bubble	
ISM 1: LIC/LB Interaction	Calculates ENA intensity profiles at 1 keV for viewing geometries that produce circular emission feature. Intensities are consistent with observations.	Does not explain Ribbon's apparent ordering by ISMF or features reflecting solar wind structure and temporal behavior. Overestimates ENA survival probability, especially for lowest energies.

McComas et al. 2014

Ribbon – Secondary ENA Source

1. Interstellar neutral atoms travel inside heliosphere
2. Neutral atom charge-exchanges with solar wind ion
3. New "primary" ENA travels outside heliosphere
4. Primary ENA charge-exchanges with interstellar ion, creating pickup ion
5. Pickup ion charge-exchanges with interstellar neutral atom, creating "secondary" ENA
6. Secondary ENA travels back inside heliosphere
7. Secondary ENA may be detected by IBEX

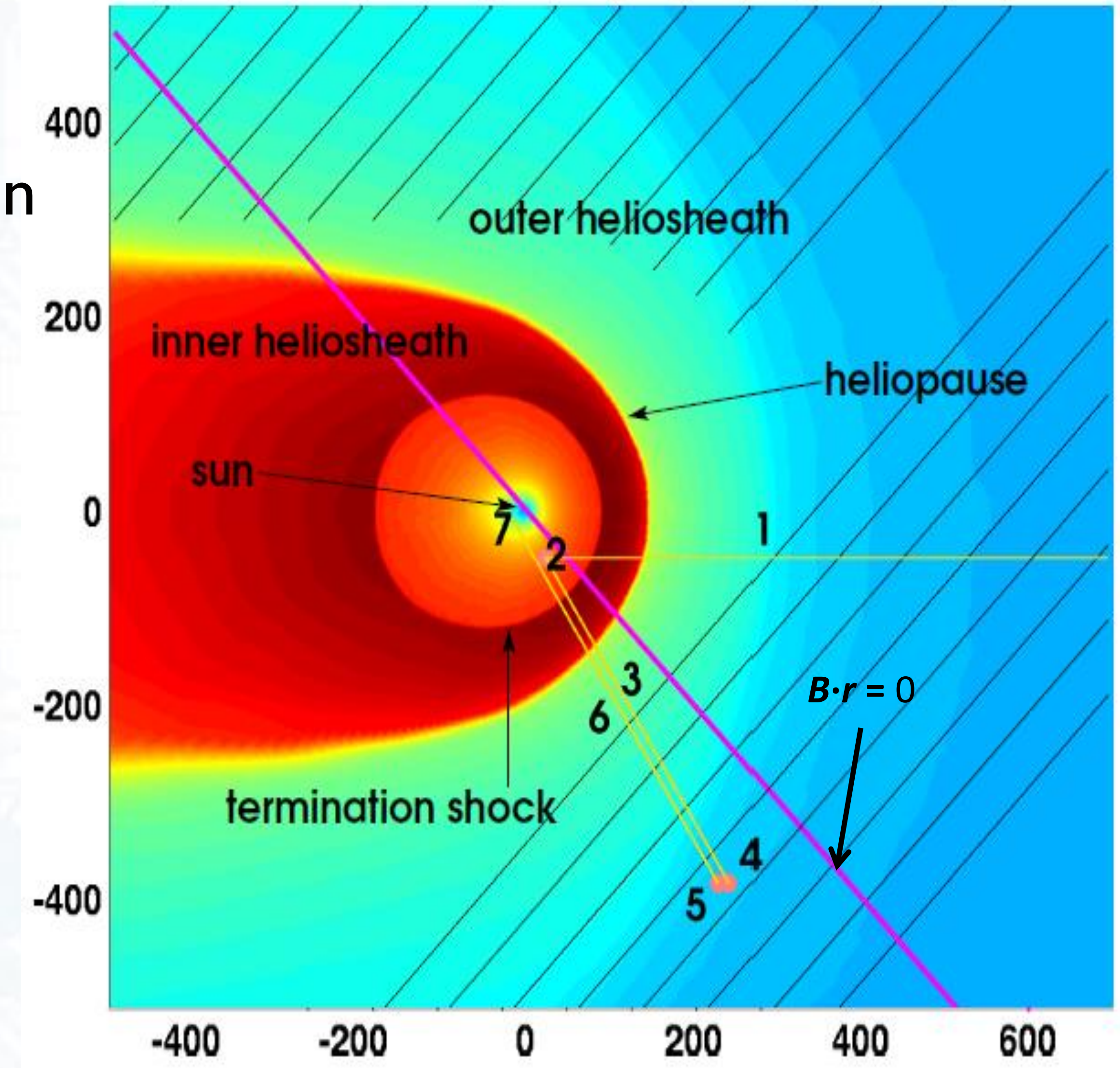

Ribbon – Secondary ENA Source

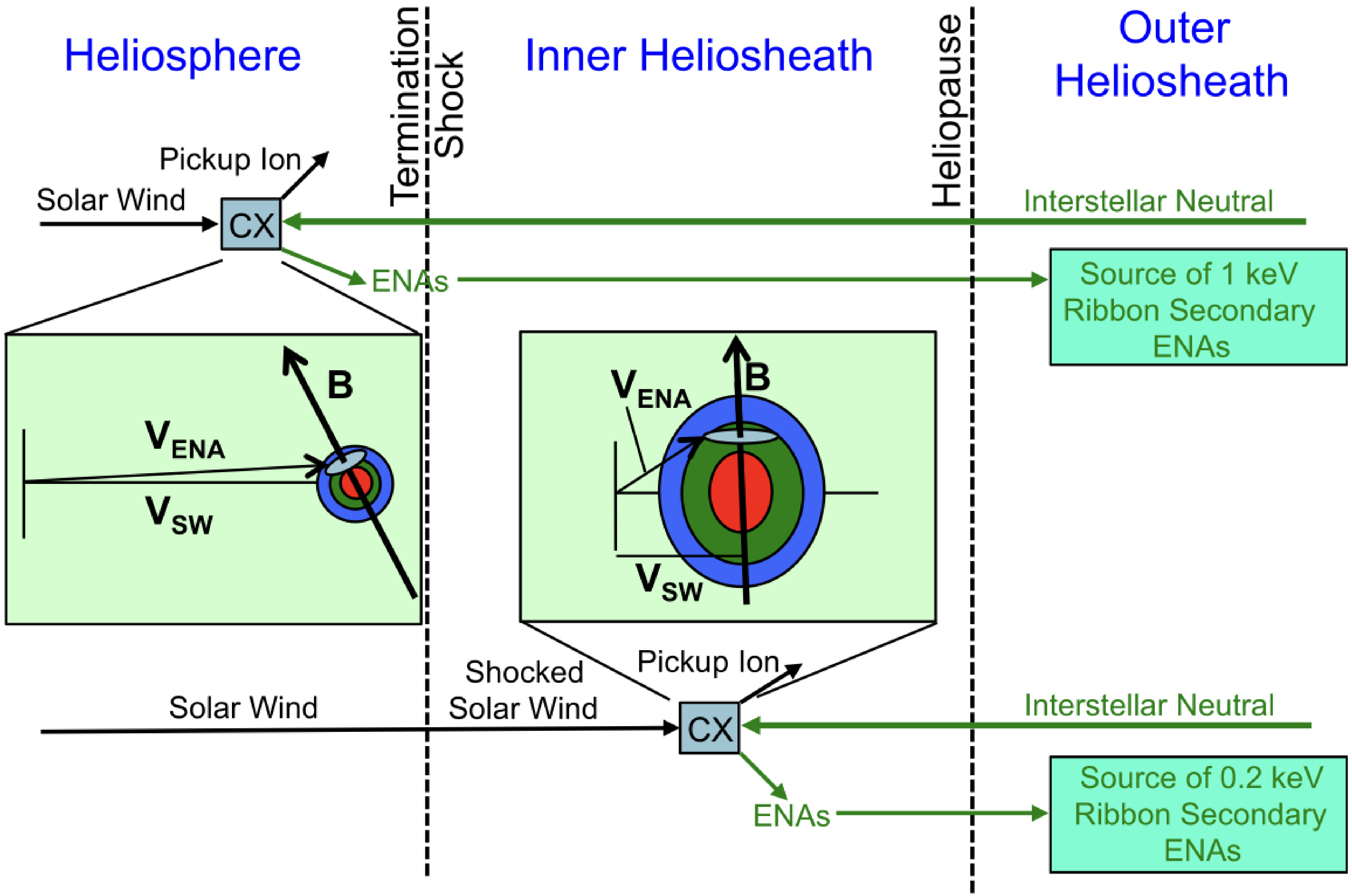

Fuselier et al. 2018

Ribbon – Secondary ENA Source

- neutral interstellar wind flows into the heliosphere, interstellar neutral atoms may charge-exchange with SW ions. The ionized neutral atoms are "picked up" by the SW. **"pickup ions from neutral interstellar wind," or PINI**

- Neutralized SW ions become ENAs that propagate radially away from the Sun and almost all escape the Heliosphere. And likely ionize outside the heliopause (OHS is ~50 times denser than IHS), becoming ions that gyrate around the ISMF. **"pickup ions from neutral solar wind," or PINS**

- Within a few years, these PINS will charge-exchange again with interstellar neutral atoms, creating secondary ENAs that may travel back toward Earth (IBEX) as the ribbon.

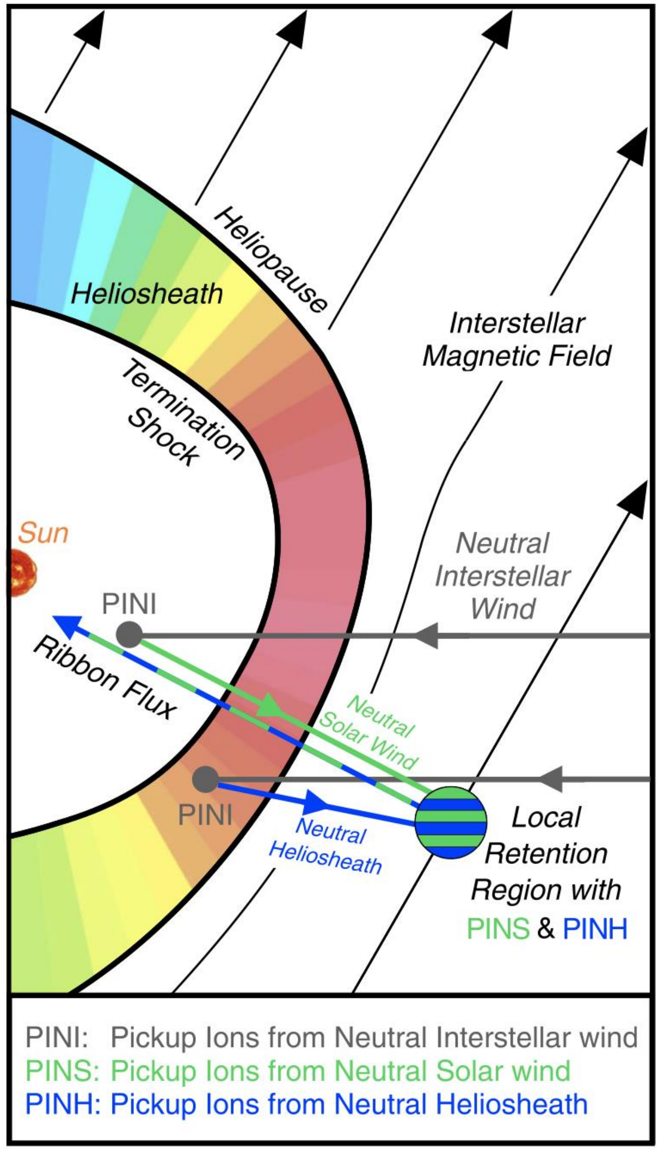

Zirnstein et al. 2019

Ribbon and B_{LISM}

- Draping of $\mathbf{B}_{LISM}$ around the heliosphere affects the source of the Ribbon in a unique way
- IBEX observations sample $\mathbf{B}_{LISM}$ over multiple ENA energies and distances from the heliopause
  - Can derive $\mathbf{B}_{LISM}$ using simulations and comparative analysis with data

Deriving the ISMF from the Ribbon

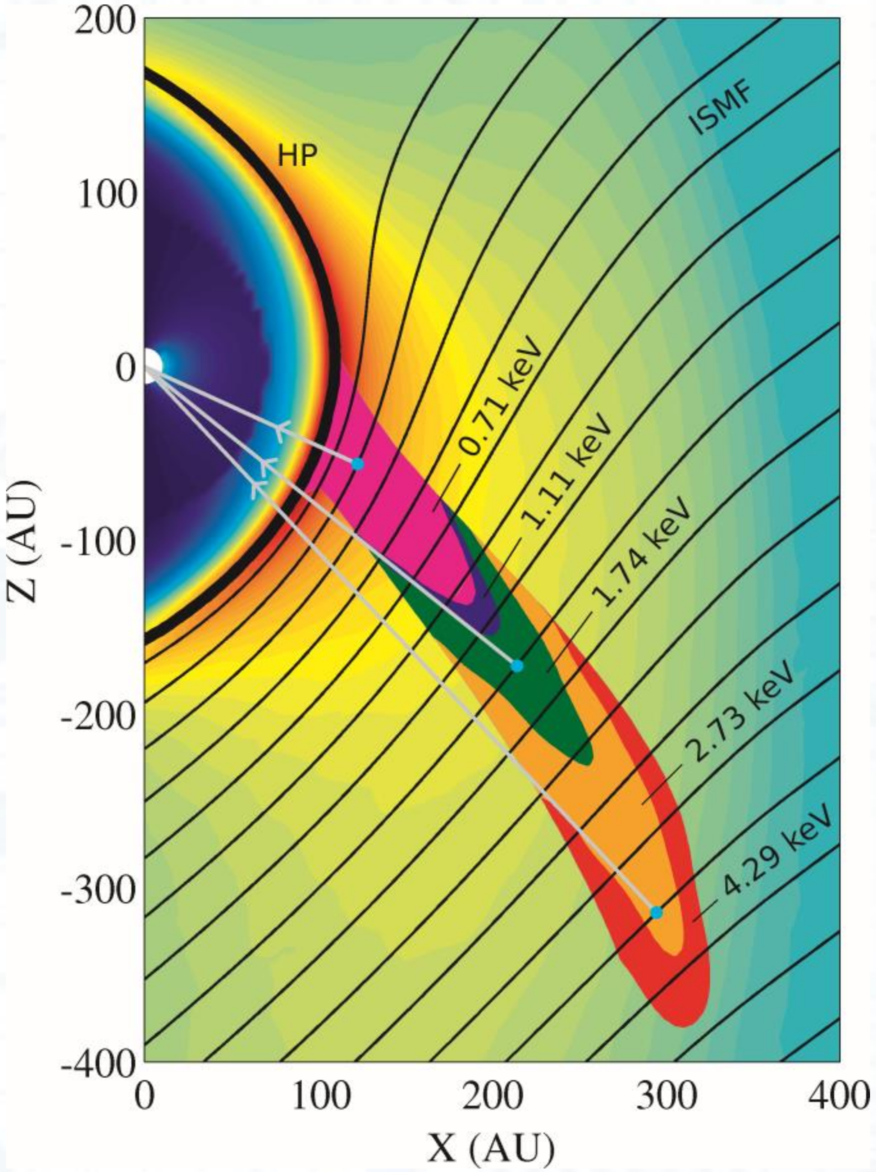

Ribbon in Different Configurations of B_{LISM}

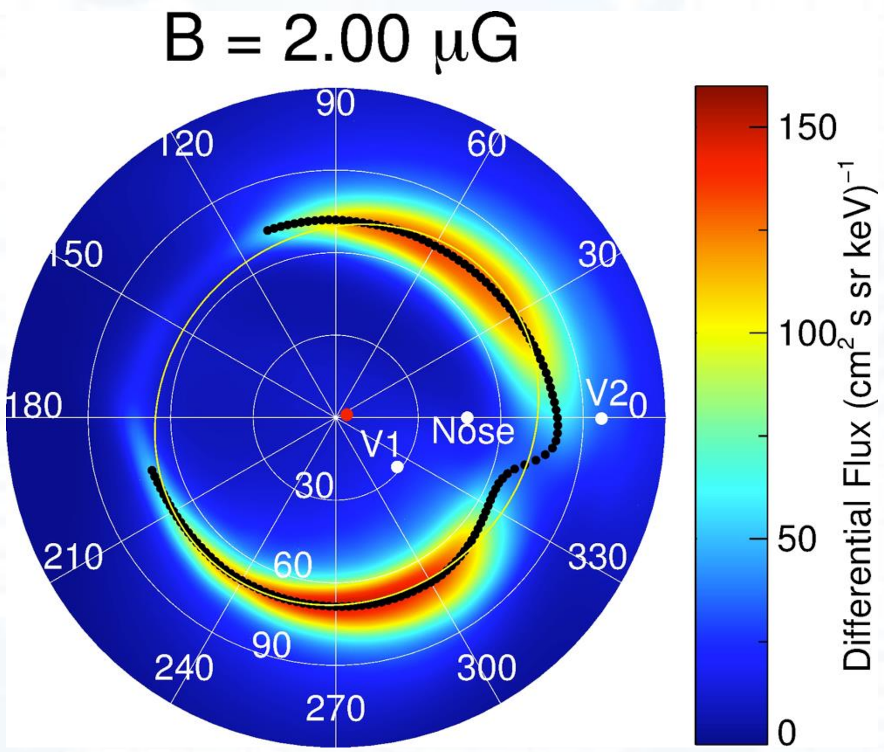

Zirnstein et al. (2016, ApJL)

Ribbon and Solar Cycle

Ribbon fluxes are latitude-dependent, a direct reflection of the latitudinal solar wind structure

McComas et al., *ApJ*, 2013

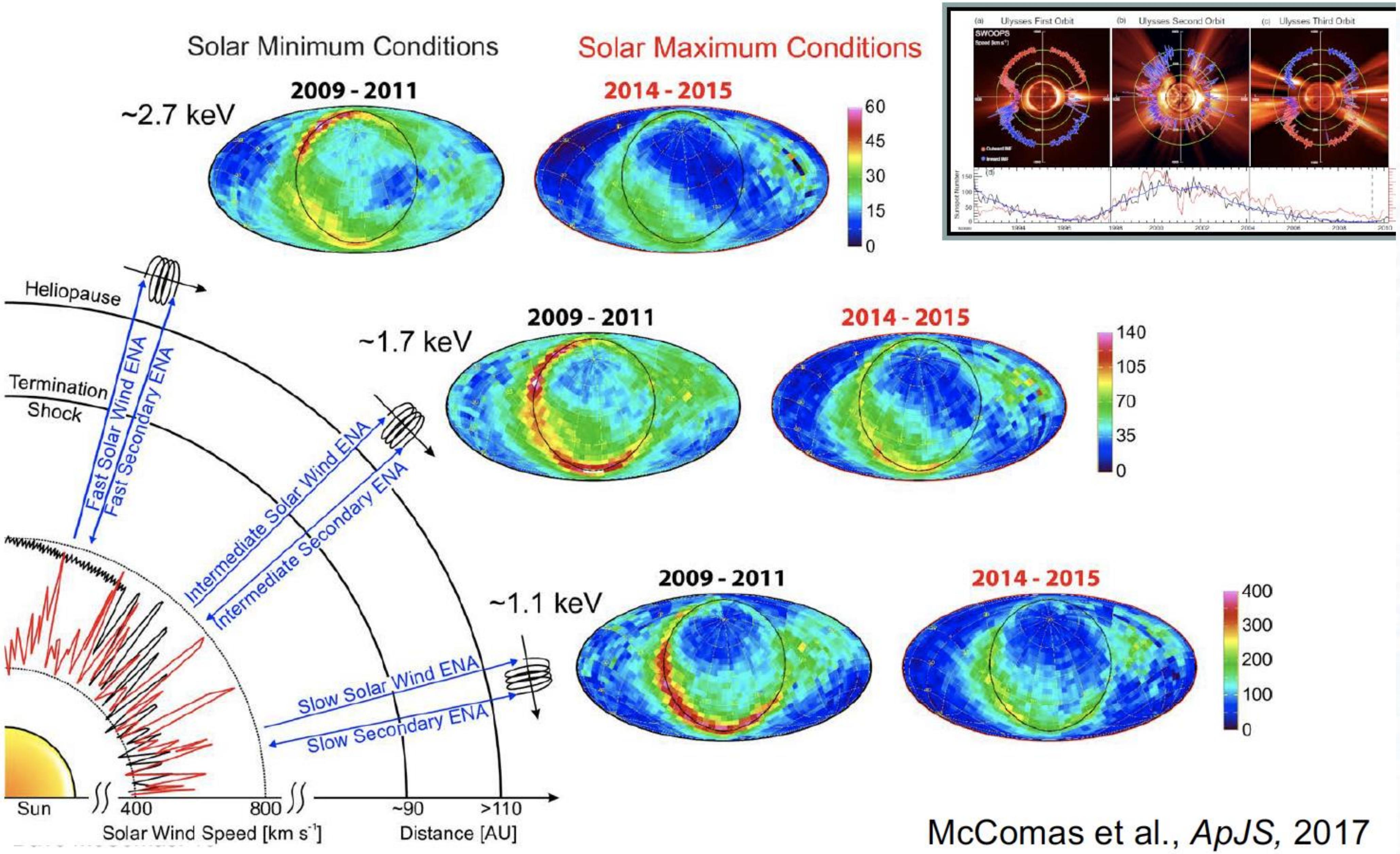

McComas et al., *ApJS*, 2017

Ribbon and Solar Cycle

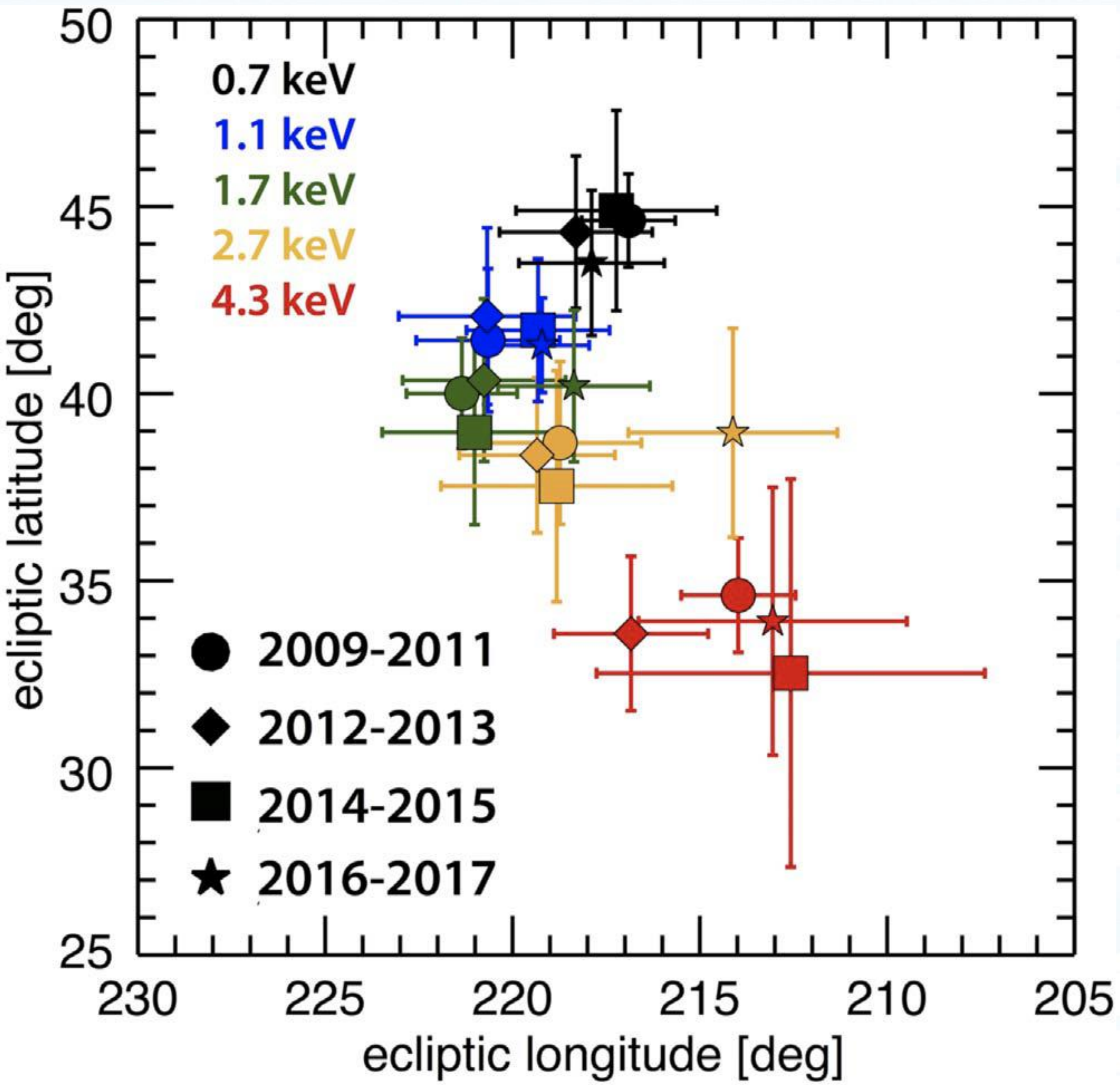

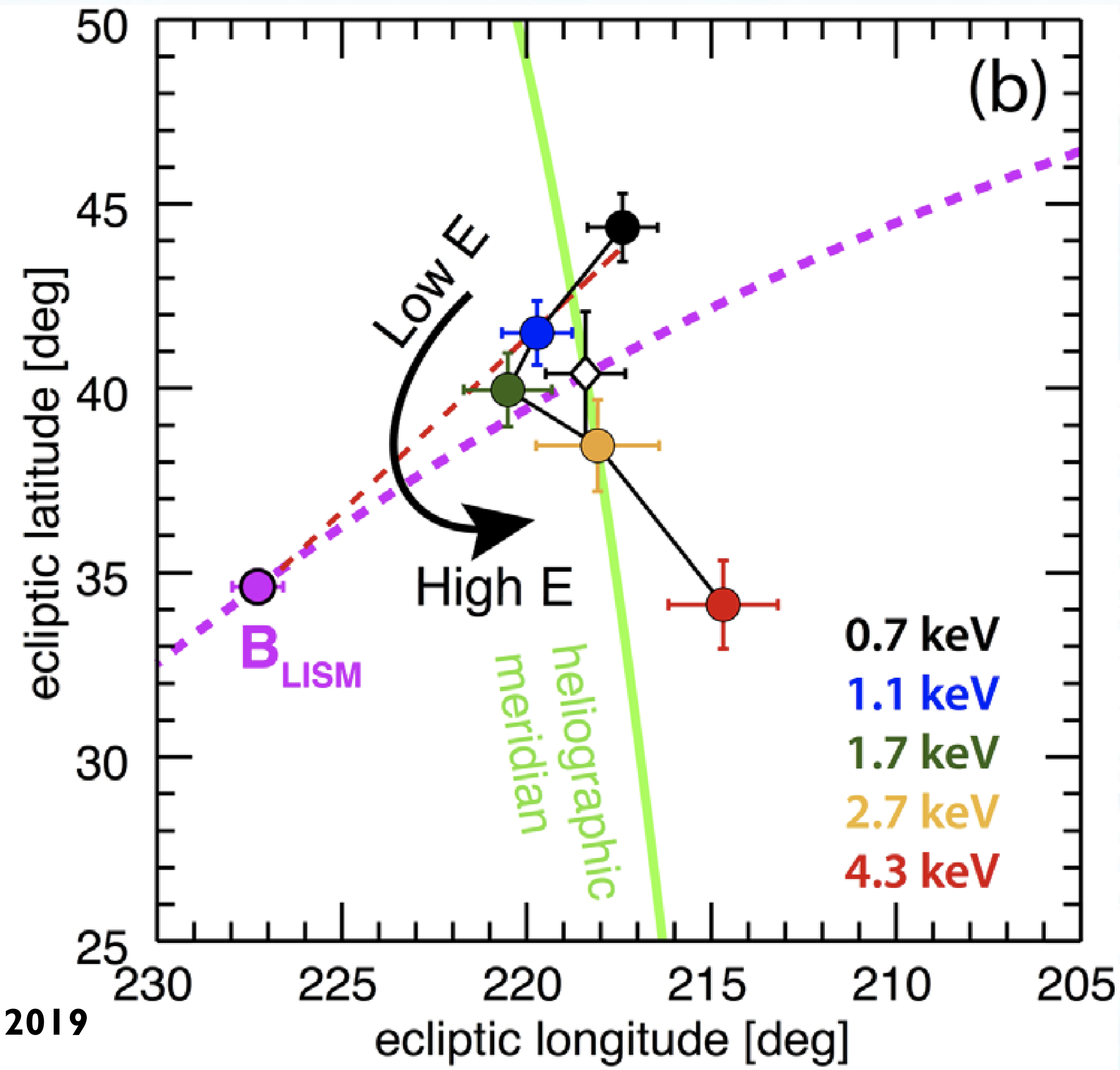

Dayeh et al. 2019

(1) the ribbon is stable over time, with distinct centers at each energy;
(2) ribbon location in the sky is driven by (i) the alignment of the ribbon centers along the B-V plane and (ii) the variable SW structure along the heliographic meridian

A full solar cycle of observations

Special Issue

10 studies

THE ASTROPHYSICAL JOURNAL
SUPPLEMENT SERIES

A Full Solar Cycle of Interstellar Boundary Explorer (IBEX) Observations

Editor: Gary Zank

PI: David McComas

The interaction of the solar wind with the local interstellar medium occurs over distances much larger than the size of our solar system (~hundreds to thousands of astronomical units), forming our heliosphere. NASA's Interstellar Boundary Explorer (IBEX) measures energetic neutral atoms (ENAs) created from this interaction, as well as directly observing the interstellar neutral gas that

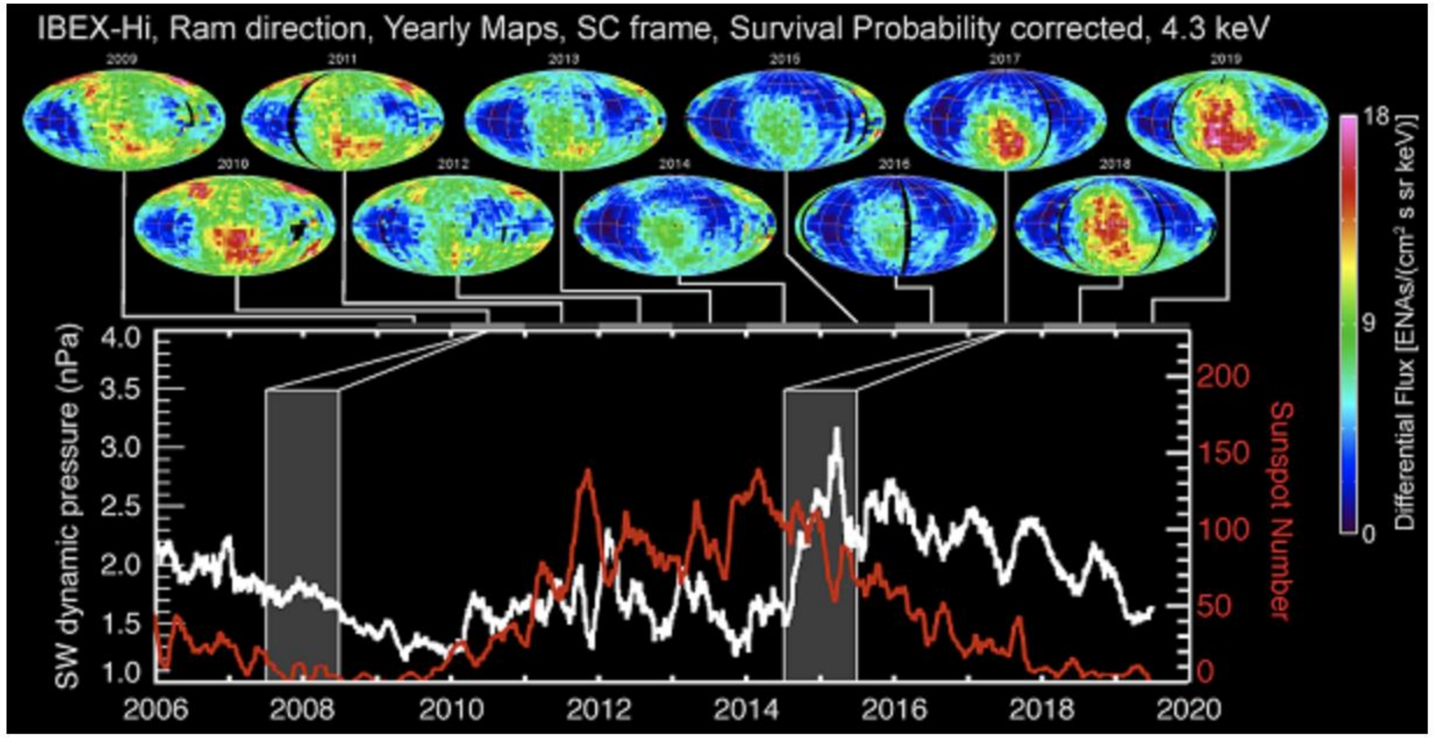

Heliotail - A full solar cycle of observations

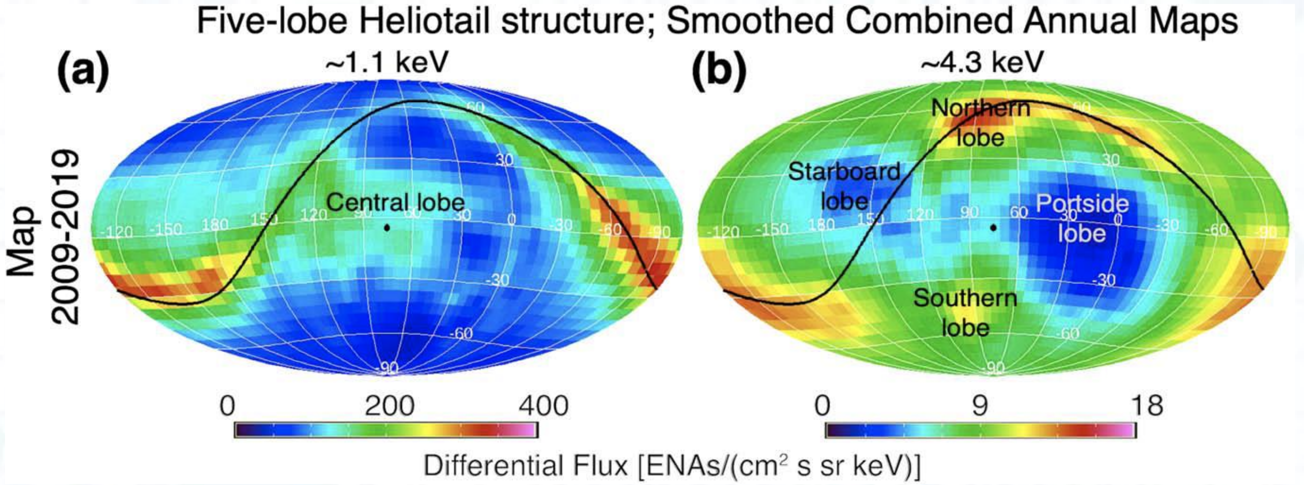

- Persistent 5-lobe structure

- Cyclic motion of low latitude centers → solar cycle
- North and South lobes motion → Fast & slow SW mixing
- Offset central lobe → ENA source effect?
- Port-starboard tilting → ISMF draping
- Tail transitioning → properties of the IHS plasma; i.e., when ENAs from fast SW exceed those of slow SW

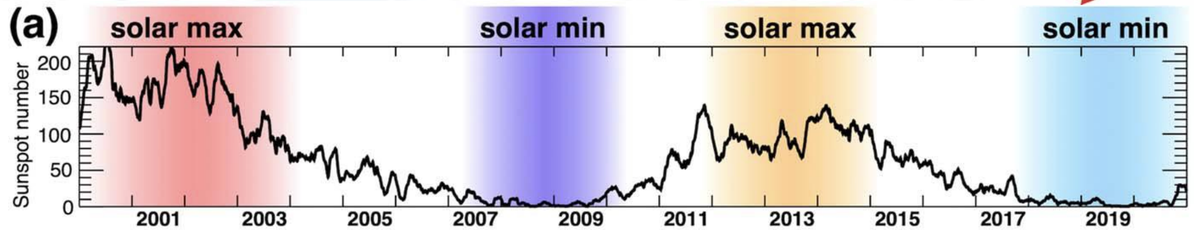

(b) SW progenitor conditions for all lobes, time delay simulated estimates from Zirnstein et al. 2021

C-lobe: > 7 year delay				
2002-2004	2005-2006	2007-2008	2009-2010	2010-2012
N-, S- lobes: ~5 year delay				
2004-2006	2007-2008	2009-2010	2011-2012	2013-2014
P-, SB- lobe: ~3 year delay				
2006-2008	2009-2010	2011-2012	2013-2014	2015-2016

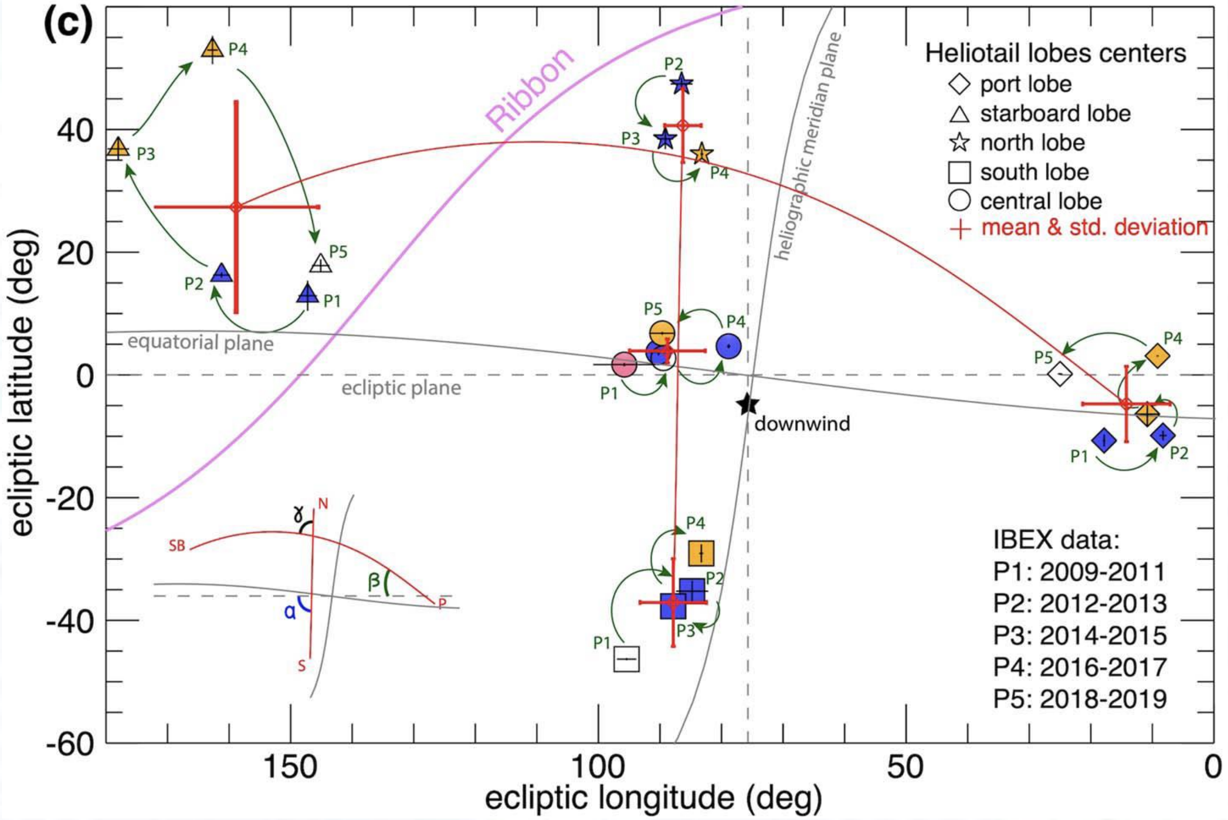

Dayeh et al. 2022

Heliospheric interface exhibit ripples

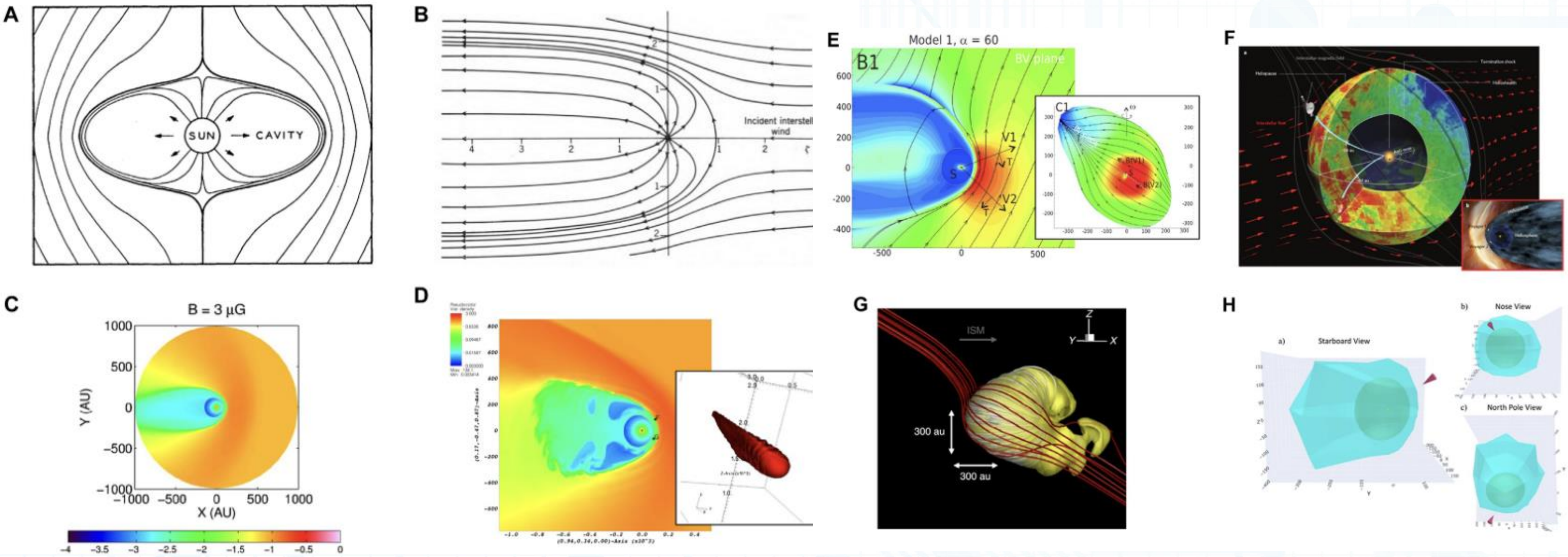

Spitzer et al. 2022

Heliospheric interface exhibit ripples

1. Heliosphere boundaries contain ~10 au - sized spatial variations

2. Comparisons with Voyager observations indicate substantial North-South asymmetries.

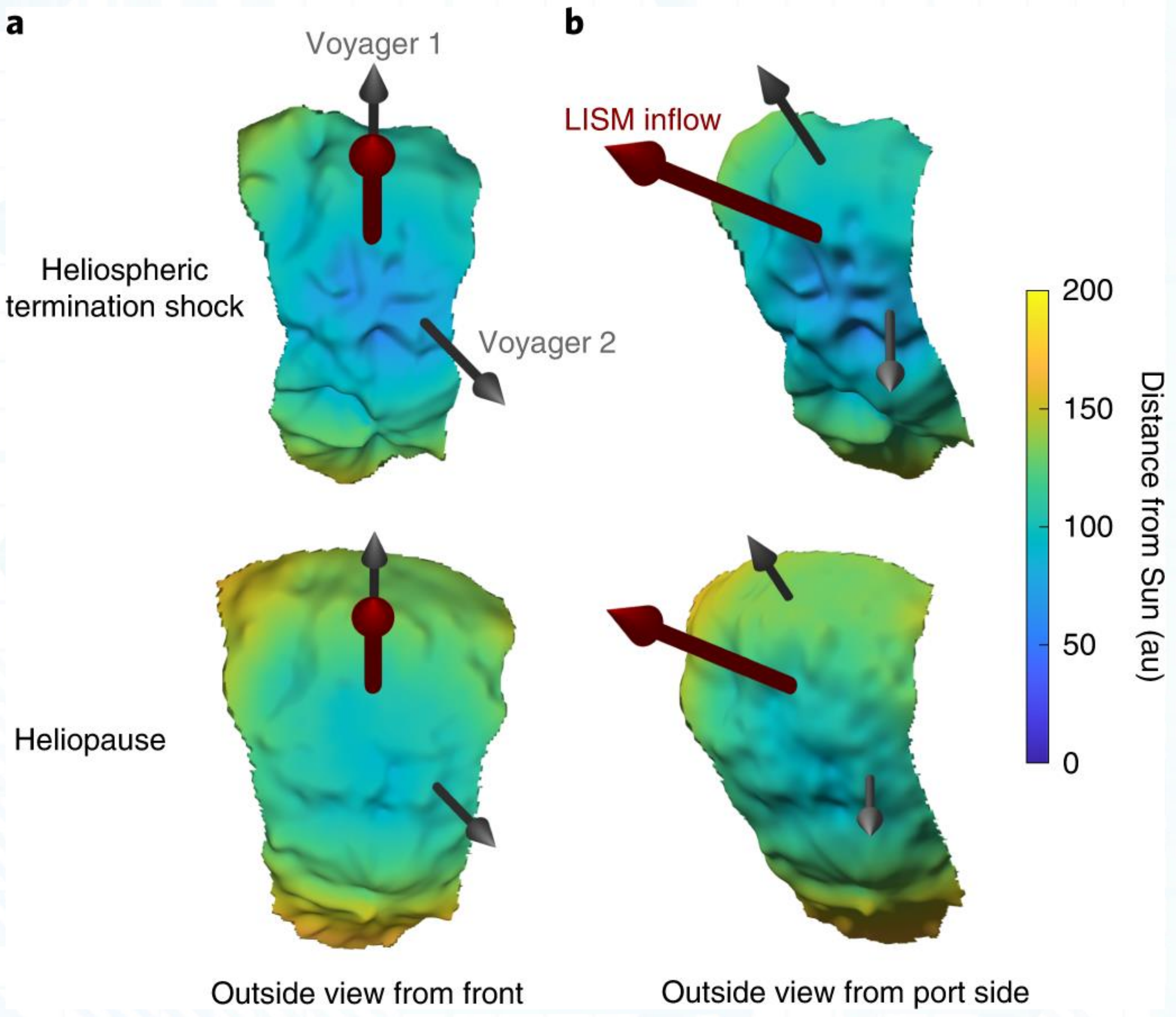

Zirnstein et al., Nature Astronomy, 2022

Heliospheric ENAs and Solar Cycle

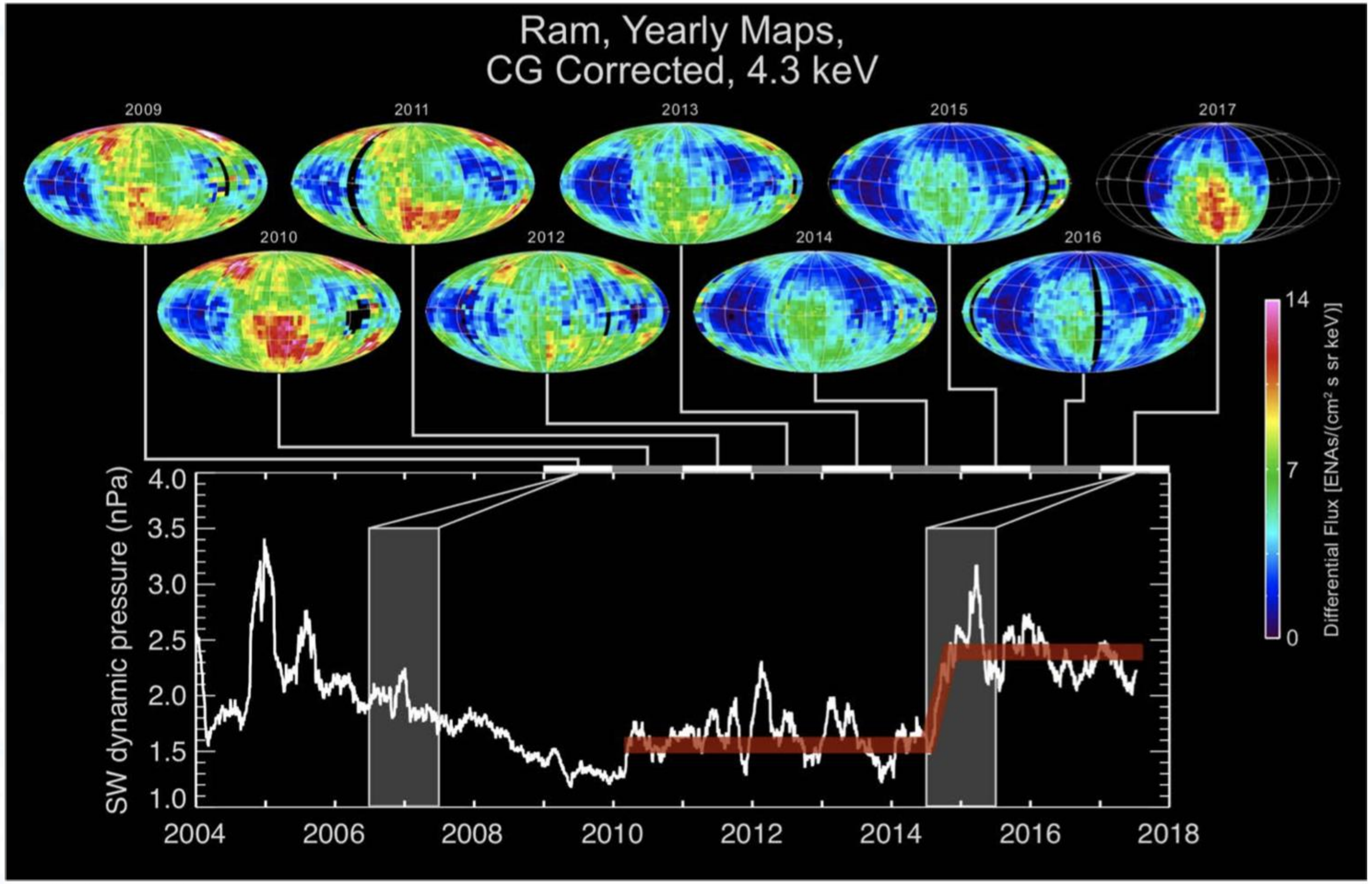

Observed response to a solar wind pressure pulse (predicted)

McComas et al. 2020

Heliospheric shape

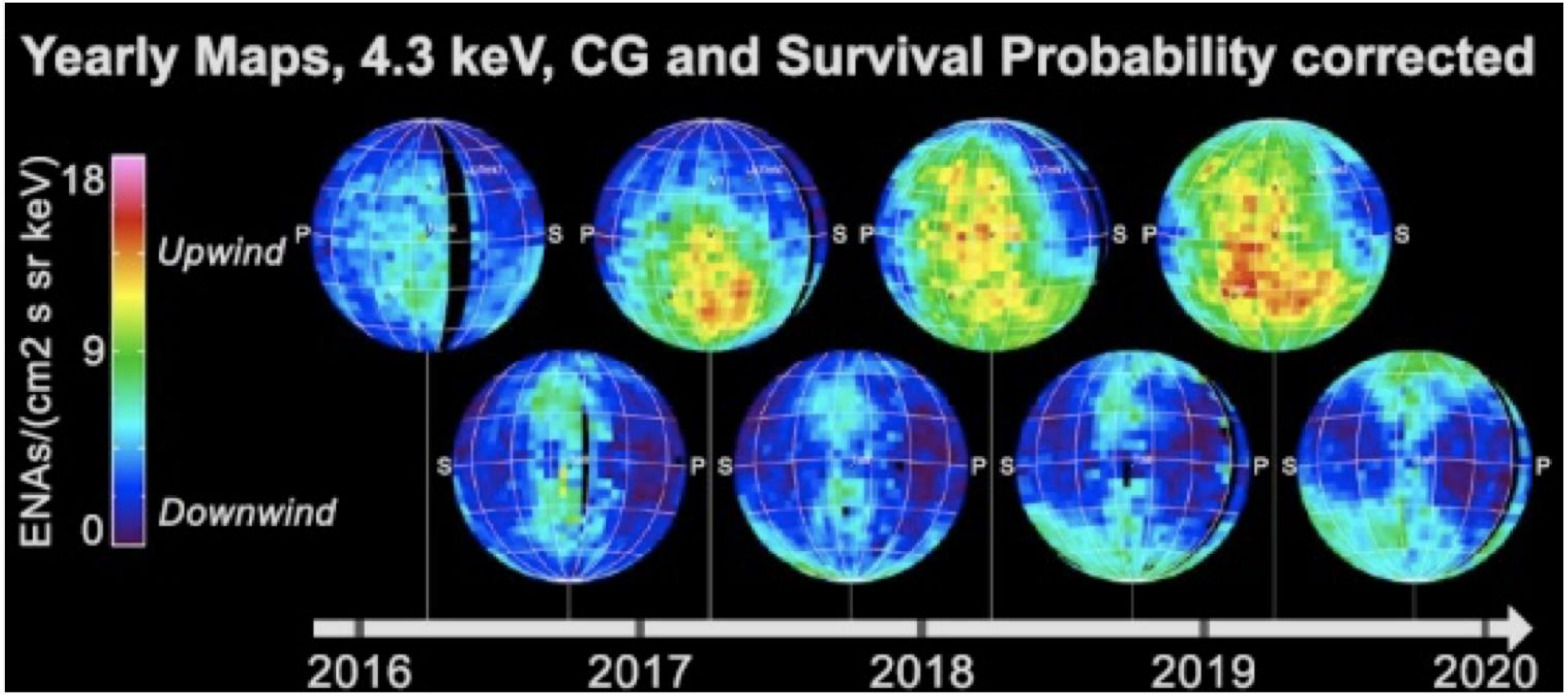

ENA response in the nose direction is > 2 years ahead of the tail.
Heliosphere is not symmetric, with nose closer to the Sun than the tail.

McComas et al. 2020

IMAP (2025)

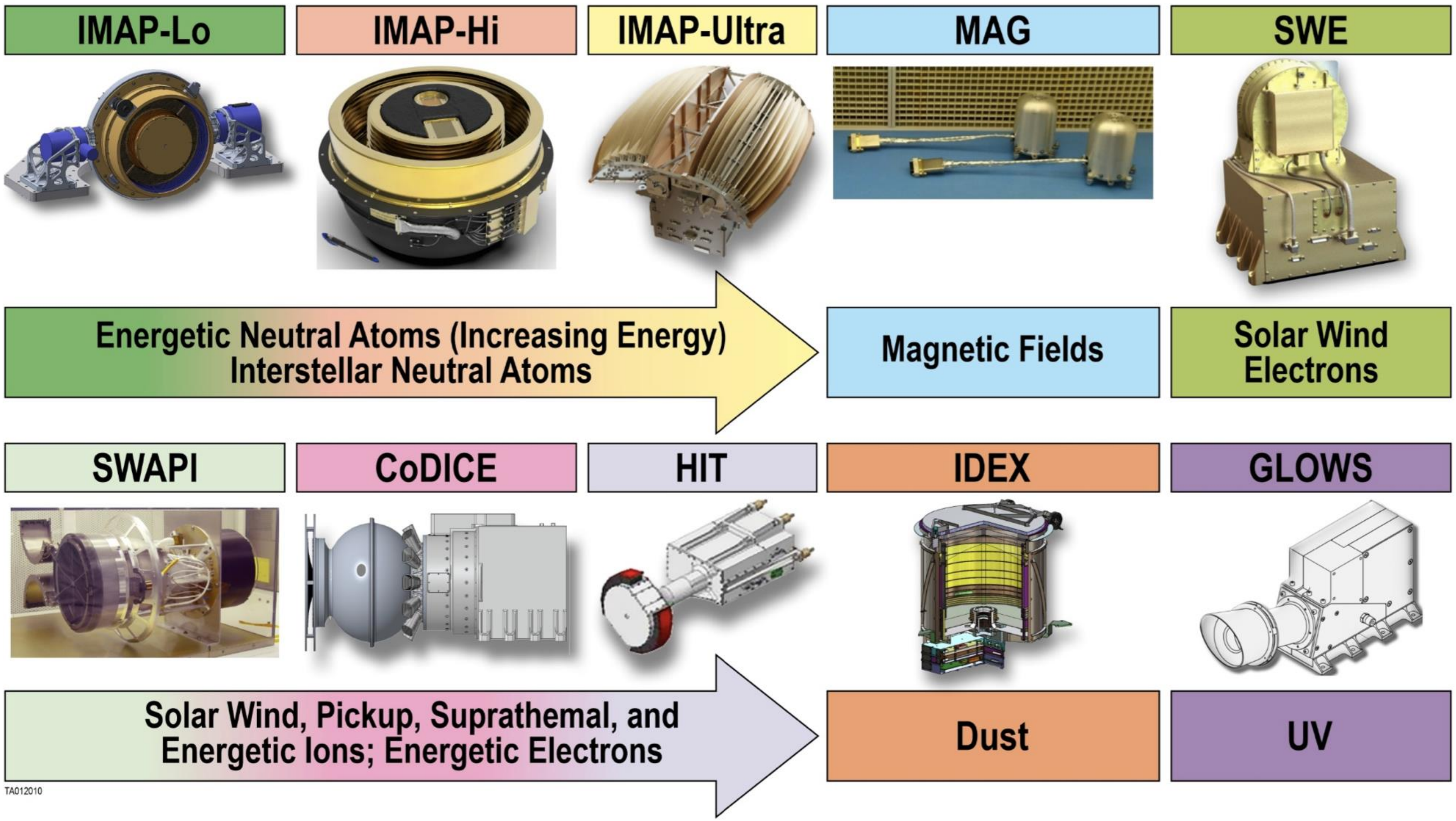

McComas et al. 2018

IMAP (2025)

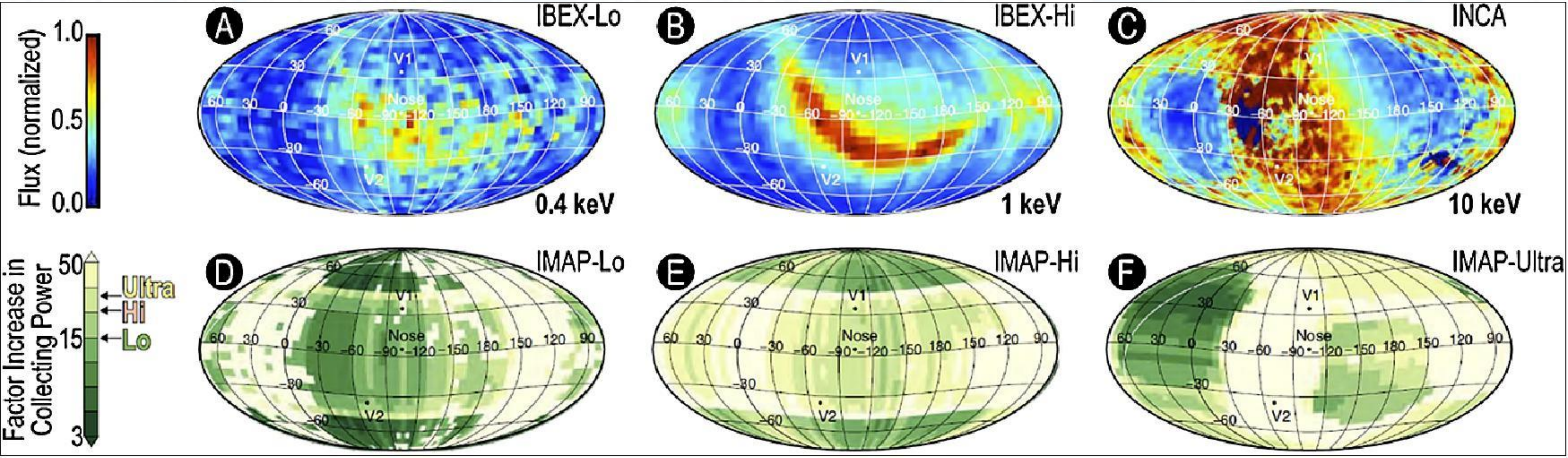

McComas et al. 2018

IBEX Magnetospheric ENAs

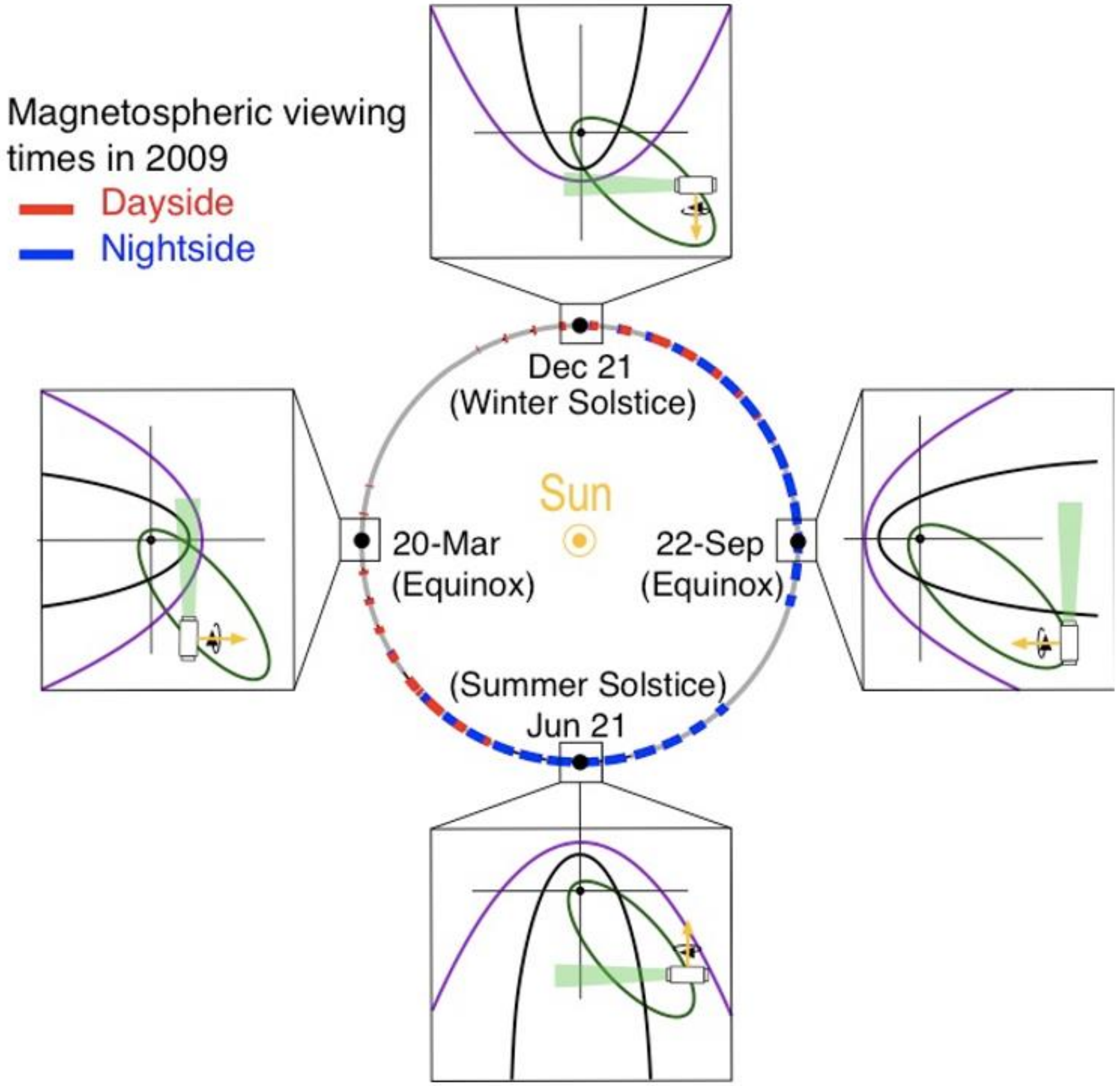

IBEX Magnetospheric ENAs

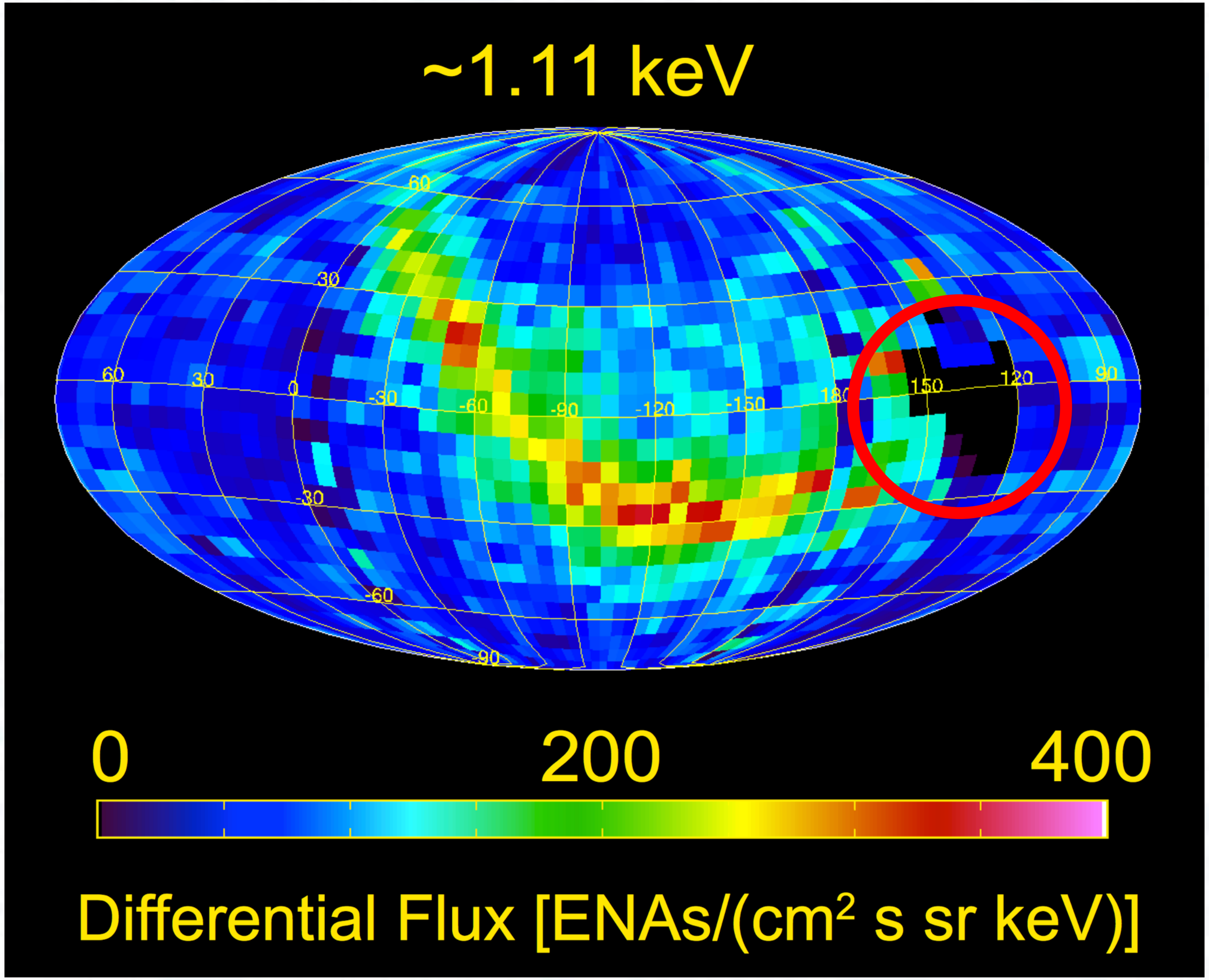

IBEX Magnetospheric ENAs

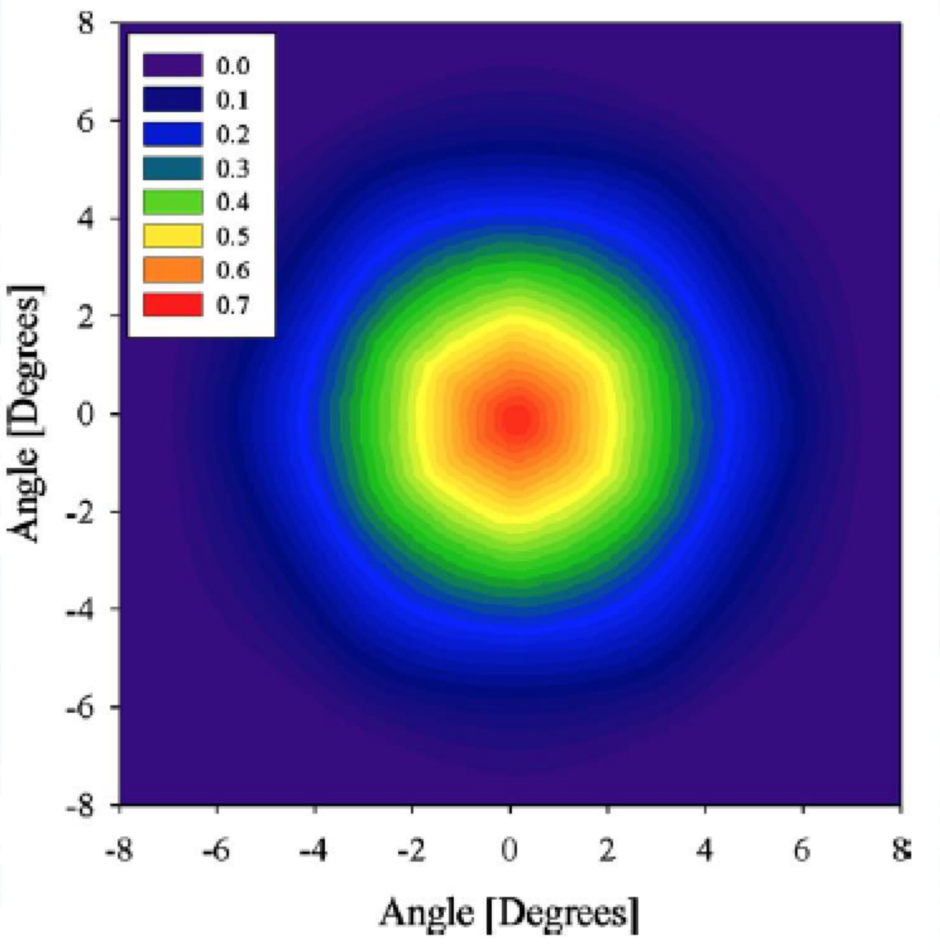

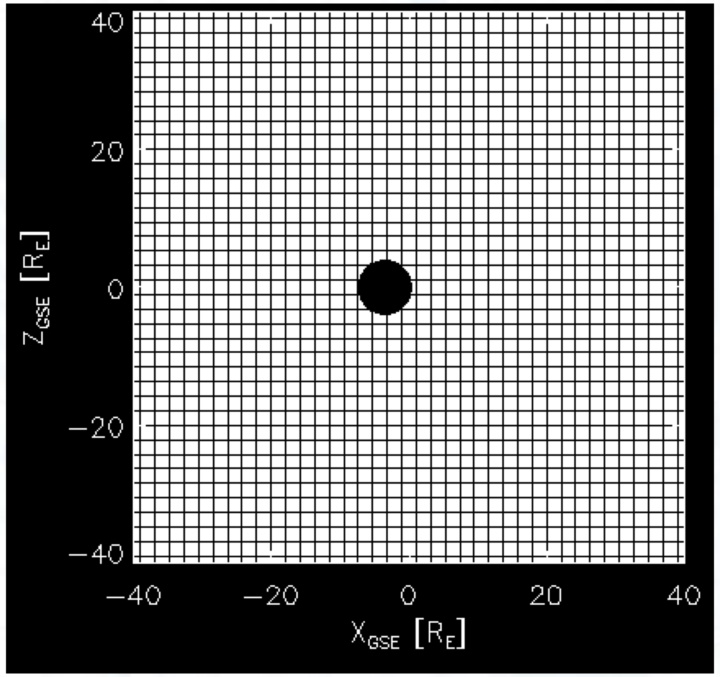

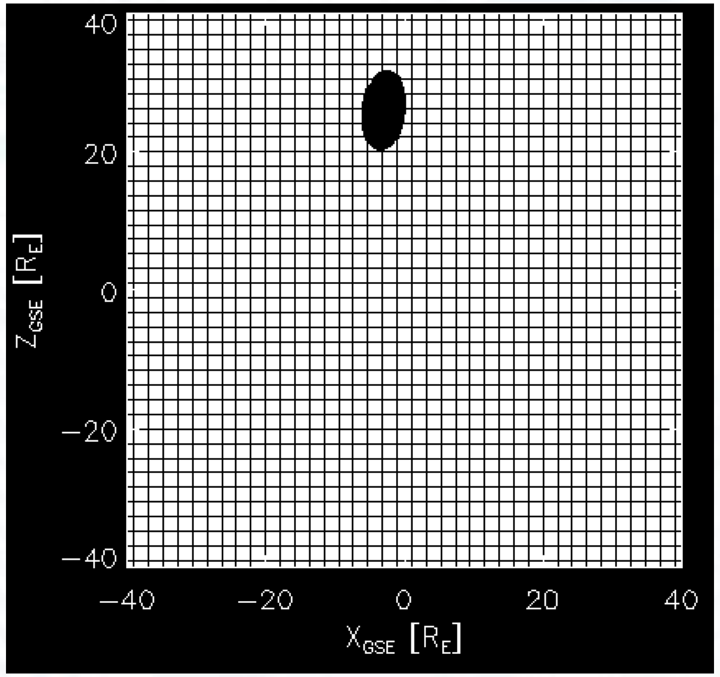

IBEX Magnetospheric ENAs

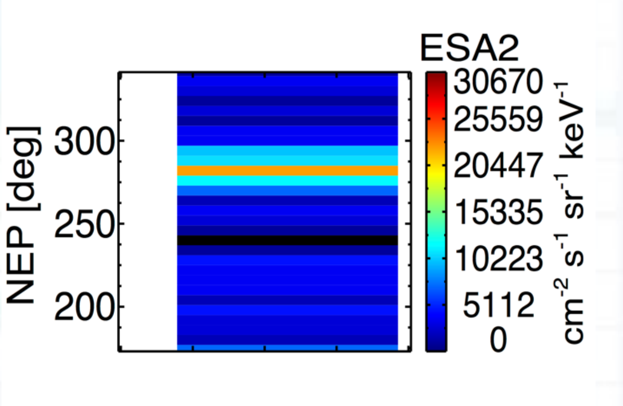

IBEX orbital configuration provides a unique opportunity to study magnetospheric, magnetotail and plasma sheet emissions, morphology, and dynamics from an external, side-viewing vantage point.

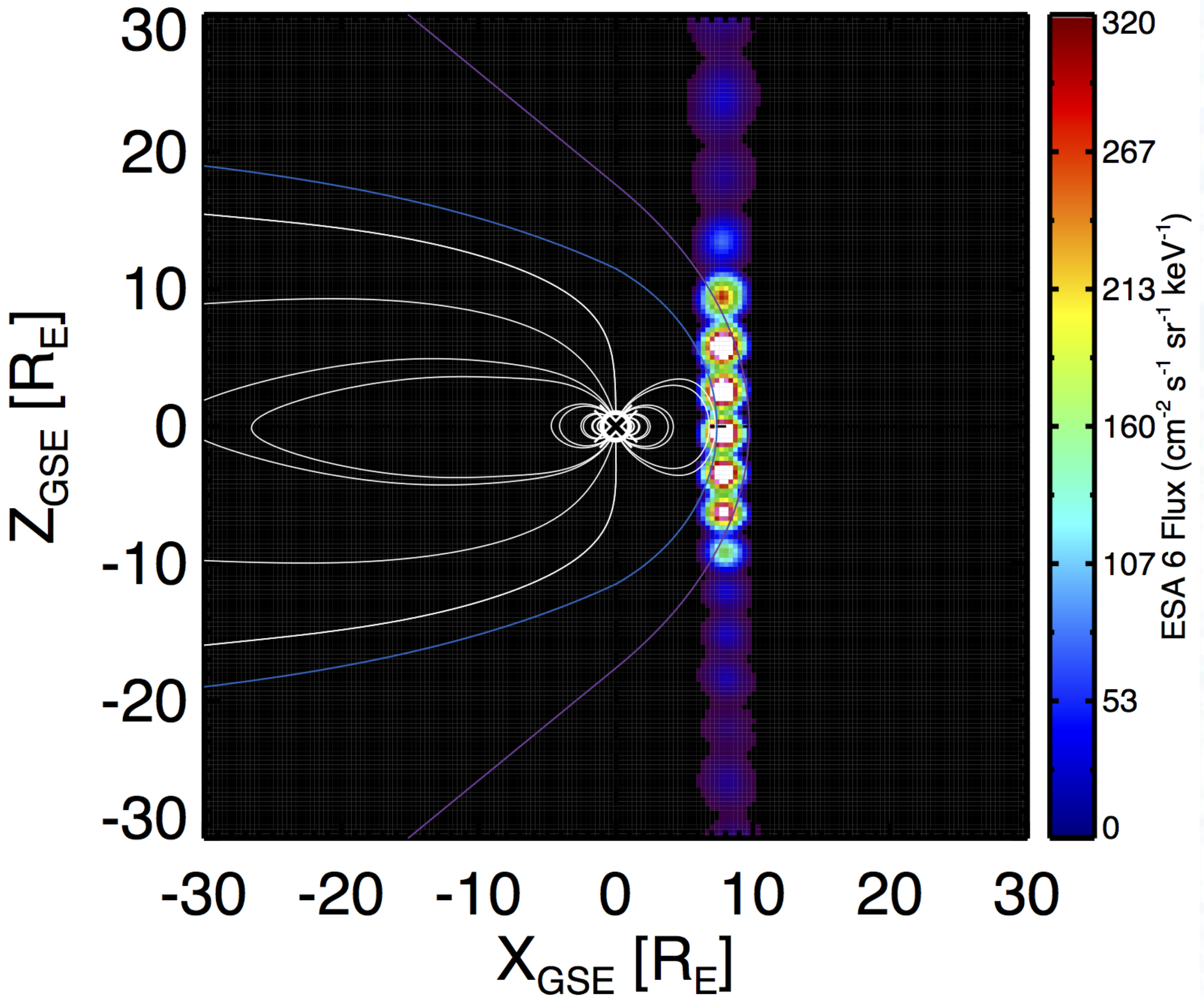

IBEX Magnetospheric ENAs

Dayeh et al. 2019

First remote-sensing global images of ion energization in the Earth's foreshock.

• Provided ion energization profile as a function of bow shock obliquity
• Quantified the difference of energization in magnetosheath and its magnetically connected counterpart in the upstream foreshock

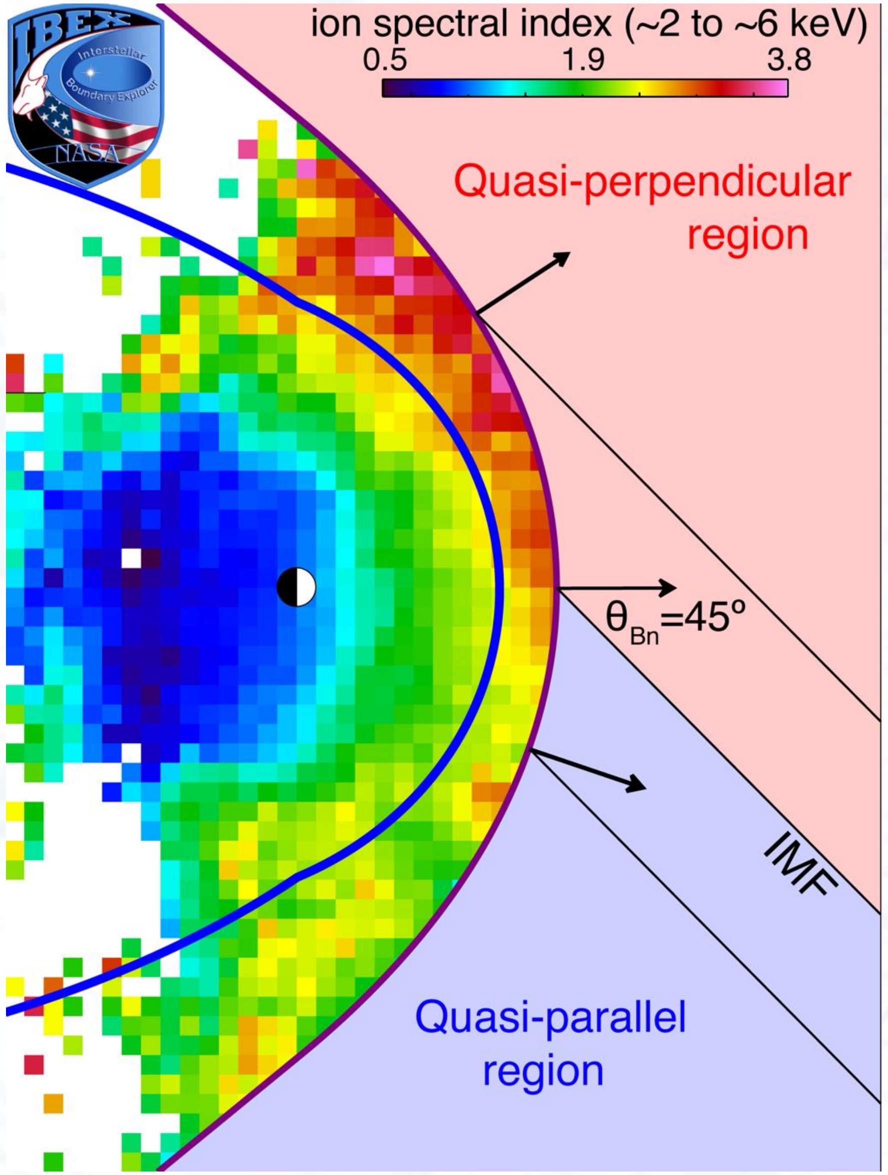

IBEX Magnetospheric ENAs

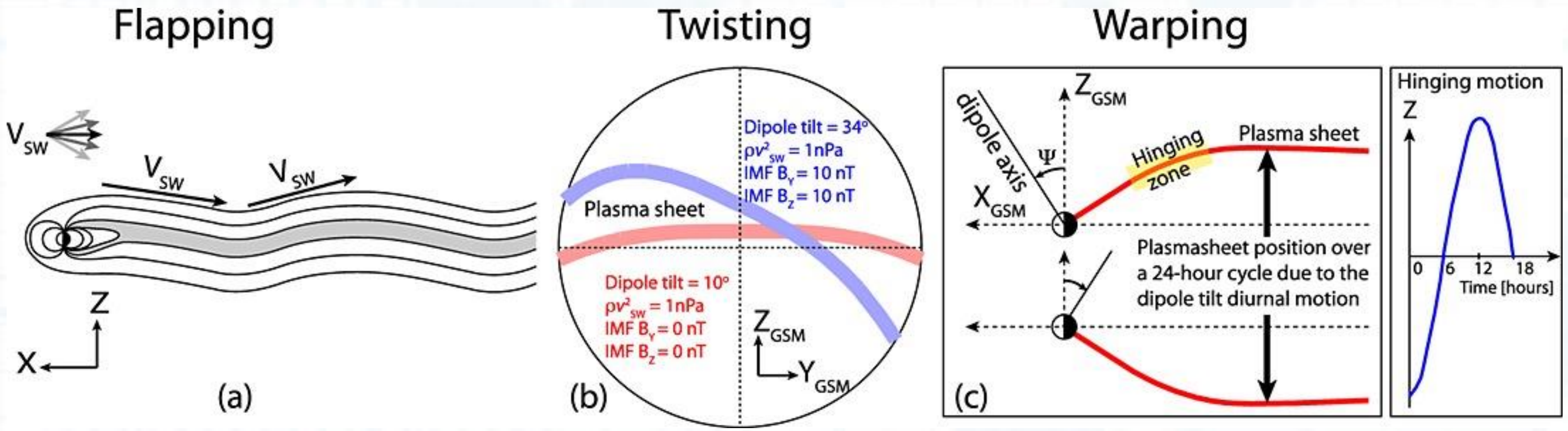

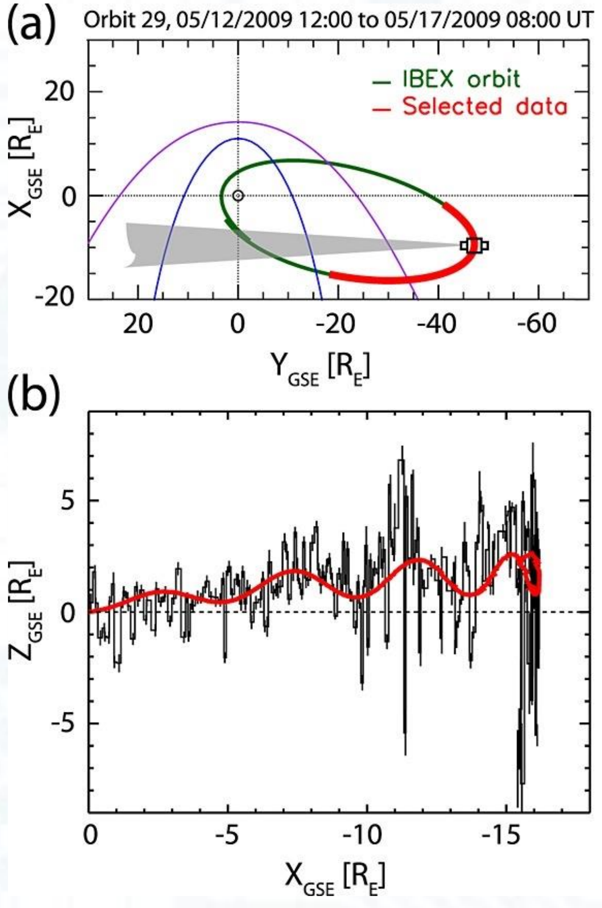

Dayeh et al. 2015

Seasonal and diurnal motions of the dipole tilt dominate the plasma sheet shape.

Superposed on the warped plasma sheet are short times, spatially-confined fluctuations.

Graduate Opportunities!

UTSA-SwRI Space Physics Graduate Program

https://grad.space.swri.edu

Graduate Opportunities

Thank you